LAB-ON-A-CHIP DEVICES FOR DRUG SCREENING

A Thesis Submitted to
The Graduate School of Engineering and Sciences of
İzmir Institute of Technology
in Partial Fulfillment of the Requirements for the Degree of

MASTER OF SCIENCE

in Biotechnology and Bioengineering

by
Begüm GÖKÇE

May 2019
İZMİR

We approve the thesis of **Begüm GÖKÇE**

Examining Committee Members:

Prof. Dr. Devrim PESEN OKVUR
Department of Molecular Biology and Genetic, İzmir Institute of Technology

Assist. Prof. Çiğdem TOSUN
Department of Molecular Biology and Genetic, İzmir Institute of Technology

Prof. Dr. Kadriye Arzum ERDEM GÜRSAN
Department of Faculty of Pharmacy, Ege University

31 May 2019

Prof. Dr. Devrim PESEN OKVUR
Supervisor, Department of Molecular Biology Genetic, Izmir Institute of Technology

Prof. Dr. Ali ÇAĞIR
Co-Supervisor, Department of Chemistry, Izmir Institute of Technology

Assoc. Prof. Dr. Engin ÖZÇİVİCİ
Head of the Department of Biotechnology And Bioengineering

Prof. Dr. Aysun SOFUOĞLU
Dean of the Graduated School of Engineering and Sciences

ACKNOWLEDGMENTS

I would like to express my deepest appreciation and thanks to supervisor Prof. Dr. Devrim PESEN OKVUR for her understanding, guidance, patience, encouragement and support throughout this study.

I am thankful to co-supervisor Prof. Dr. Ali ÇAĞIR for providing klavuzon novel molecule which is a generous gift and his support and suggestions.

I would like to thank also the members of my thesis defense committee Prof. Dr. K. Arzum ERDEM GÜRSAN and Asisst. Prof. Çiğdem TOSUN for helpful comments and giving suggestions.

As teamwork is essential, I am very thankful to the members of the Controlled *in vitro* Microenvironments (C*iv*M) laboratory for their team spirit and support.

I would like to thank to my friends and colleagues Ali YETGİN, Ali CAN for their support and help.

I would lke to thank to my teachers ad trainers for providing us to grow up depending on Atatürk's principles and reforms and knowledge I have gained throughout my education.

I would like to thank everyone who helped me win and live the Lindy Hop sprit.

I would like to express my sincere thanks to my dear friends who I met spontaneously in my life.

I would like to thank to my friend Gizem BATI AYAZ for guiding us in everything in laboratory and giving her support from the moment I first came to the lab.

I would like to express my gratitude and thanks to my dear friend and colleague Müge BİLGEN, whose support I felt in both my university and private life.

I would like to express my deepest appreciation and thanks to my friends Sevgi ÖNAL and Aslı ADAK for their support, help and friendship.

I would like to thank to also my dear friend Dr. Aslı KISIM whom I see to myself as a role model for her love, support, understanding, motivation, help for impossible situations and sophistication.

Finally, I would like to express my gratitude and love to my beloved mother Belgin GÖKÇE, my father Çetin GÖKÇE and my brother Mert GÖKÇE and all my esteemed family members who have been with me all the time during my life and have never avoided any sacrifice.

ABSTRACT

LAB-ON-A-CHIP DEVICES FOR DRUG SCREENING

Breast cancer is one of the cancers with the highest incidence and mortality rates in women in Turkey as well as in the world. Tumor micro environment comprises of cancer and normal cells, extracellular matrix, soluble biological and chemical factors. Research has shown that cell shape, adhesion, migration, response to growth factors and drugs are different in 2D and 3D culture. Today, only 8 out of 100 anti-cancer clinical trial gives effective results. 3D cell culture systems have shown to be a necessary step between *in vitro, in vivo* and clinical studies. Therefore, it is necessary to better understand the interactions of cancer cells with their micro environment, for which new cell culture setups are required. The most apparent disadvantage of widely used 3D cell culture setups is the lack of stromal cells. The systems to be developed should both provide a 3D environment and comprise multiple cell types. The drug screen in 3D tri-culture method with a lab-on-a-chip device, that will be developed in this study will be able to answer these needs. Cell lines that represent different breast cancer types alone or together with stromal cells were cultured in 3D in the to be developed lab-on-a-chip; by determining the effects of drugs with different targets on the viability and distribution of cells, a drug screening method is developed.

ÖZET

İLAÇ TARAMASI İÇİN YONGA-ÜSTÜ-LABORATUVAR AYGITLARI

Meme kanseri dünyada olduğu gibi dünyada ve Türkiye'de de kadınlarda en sık görülen ve ölüm oranı en yüksek olan kanser çeşitlerindendir. Tümör mikroçevresi, sağlıklı ve kanserli hücreleri, hücredışı matriksi, çözünür halde biyolojik faktörleri ve kimyasal etkenleri içerir. Araştırmalar hücre şekli, yapışması, hareketi, büyüme etkenlerine tepki ve ilaçlara karşı direncin, iki ve üç boyutlu düzeneklerde farklı olduğunu göstermiştir. Günümüzde kansere karşı yapılan 100 klinik deneyden sadece 8'i etkili sonuç vermektedir. 3B hücre kültürü sistemlerinin ise, tüpte, canlıda ve klinikte yapılan çalışmalar arasında çok gerekli bir adım oldukları gösterilmiştir. Bu yüzden, kanserin mikroçevresi ile olan etkileşiminin çok daha iyi anlaşılması, bunun için de yeni hücre kültürü düzenekleri gerekmektedir. Yaygın olarak kullanılan 3B düzeneklerin en belirgin eksik yönü, destek doku hücrelerinin kullanılmamasıdır. Geliştirilecek sistemler hem 3B ortam sağlamalı hem de birden fazla hücre çeşidi içermelidir. Bu çalışmada geliştirilen yonga-üstü-laboratuvar aygıtı ile 3B ve üçlü kültürde ilaç tarama yöntemi bu ihtiyaçlara cevap verebilecektir.

Farklı çeşitlerde meme kanserlerini temsil eden hücre hatları tek başlarına ve destek doku hücreleri ile beraber, geliştirilen yonga-üstü-laboratuvar aygıtında 3B kültürlenerek; farklı hedefleri olan ilaçların hücrelerin canlılıklarına ve dağılımlarına etkileri belirlenerek bir ilaç tarama yöntemi geliştirilmiştir.

To my family…

TABLE OF CONTENTS

LIST OF FIGURES

Figure **Page**

Figure **Page**

Figure **Page**

Figure **Page**

LIST OF TABLES

Table **Page**

CHAPTER 1

INTRODUCTION

1.1. Cancer

Cancer is composed of abnormal cells which dividing uncontrolled and spreading into other tissues[1]. In all types of cancer, some of the body's cells start dividing without stopping and spreading to surrounding tissues. Cancers of different origin show different characteristics. For each cancer type, cancer-causing factors are different. Cancer cells show an alteration in different ways than normal cells, which causes them to become out of control and invasive. The less specificity of cancer cells compared to normal cells is one of the most important differences[2].

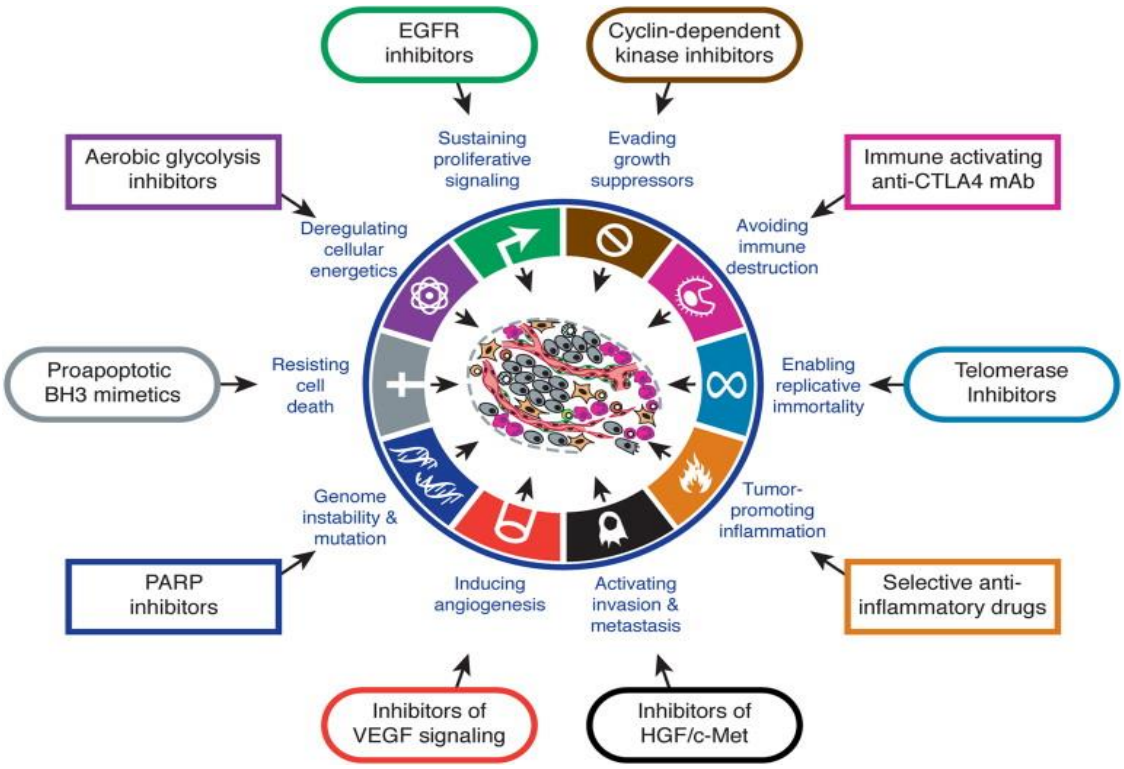

Figure 1.1. The hallmark of cancer[3] (Source: Hanahan et al., 2011).

In short, while normal cells mature into many different cell types with specific functions, cancer cells do not mature. This is because cancer cells continue to grow differently from normal cells. Also, cancer cells do not recognize signals which normal cells know stopping division signals or that start off programmed cell death or apoptosis processes. There are six main hallmarks of cancer. They are resisting cell death, sustaining proliferative signaling, evading growth suppressors, activating invasion and metastasis, enabling replicative immortality, inducing angiogenesis[3] (Figure 1.1).

1.1.1. Breast Cancer

Breast cancer starts with uncontrolled proliferation of cells that make up milk ducts or lobules and can end up in metastasis to in various parts of the body[4]. Breast cancer classification is based on three approaches. They are based on tissues, based on invasiveness, based on hormones and genes. Ductal cancer which arose by nozzle ducts is the most common type of breast cancer. Lobular cancers originating from milk-producing glands are also common. There are also rare types of medullary, tubular and mucinous originating from other tissues.

Breast cancer is one of the most common cancer type in all over the world. According to American Cancer Society's forecasts, approximately in women 268.600 new cases of invasive breast cancer will be diagnosed and 41.760 women will die from breast cancer in 2019[5]. Briefly breast cancer causes many deaths. Hence, early detection is important in order to prevent deaths.

1.2. High-Throughput Screening

Drug development and commercialization studies are quite complex and time consuming. Since the early 1990s, the transition from traditional drug discovery methods to highly efficient drug discovery methods has begun[6]. High-throughput screening (HTS) is the method for generally used in drug discovery. It is very useful for pharmaceutical application. It is intended to develop a rapid trial to test drugs and similar components[7]. HTS given rise to the excellent development in mechanization technology and

combinatorial chemistry, has been largely carried out drug breakthrough since the early 1990s and quickly changed one of the great information of drug samples. HTS is used to understand analyses of the drug effect on a large-scale[8].

1.3. Doxorubicin

Doxorubicin has been considered as one of the most effective agents against breast cancer since 1967 and has been used in clinical trials[9]. Doxorubicin is an important chemotherapeutic agent widely used for anti-tumor treatment[10]. Doxorubicin is also widely used in the treatment of various solid tumors, bladder cancer, lymphoma.

Doxorubicin is an anthracycline antibiotic derivative (Figure 1.2). It has extracted from *Streptomyces peucetius var. caesius*[11] . It is fluorescent molecule. Doxorubicin has two mechanisms on cancer cells. These are DNA intercalation and free radical formation. It interferes with DNA and prevents biosynthesis[12]. The progression of the topoisomerase enzyme is inhibited as a result of this intercalation. It inhibits DNA replication by stabilizing topoisomerase II enzyme which allowing the DNA helix to open during transcription[13]. In the treatment of breast cancer, doxorubicin causes DNA damage by entering the nucleus[14].

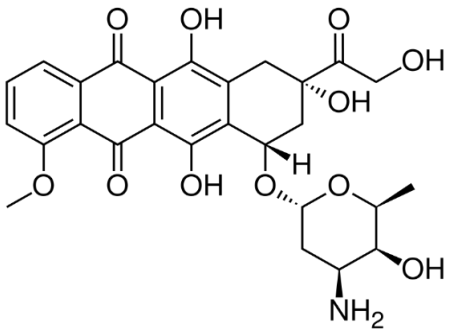

Figure 1.2. Molecular structure of Doxorubicin[15] (Source: Tewey et al., 1984).

1.4. Klavuzon

Goniothalamin is a component with cytotoxic properties which is isolated from *Goniothalamus macrophyllus* plant. Kasaplar et al. have found the klavuzon molecule by increasing the cytotoxic activity of this molecule a result of the change in the structure of this substance[16].

Klavuzon is a reagent which has topoisomerase-I inhibitor property[17]. The molecule derived from a naphthalen-1-yl substituted α, β-unsaturated β-lactone is klavuzon molecule (Figure 1.3). It has been shown in the studies that the klavuzon molecules have anti-proliferative effects to cancer cell lines[18].

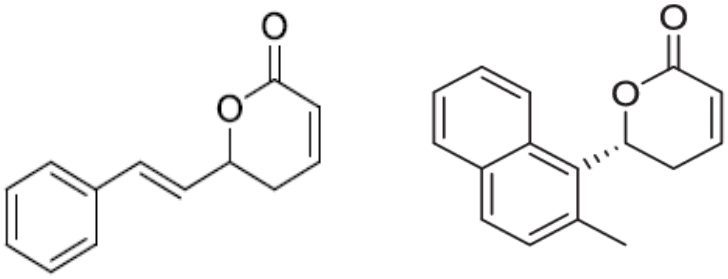

Figure 1.3. Molecular structure of Goniothalamin and Klavuzon[18]
(Source: Akçok et al.,2017).

1.5. Importance of 3D cell culture

The extracellular matrix is the key regulator of the normal homeostatis and tissue phenotype[19]. In two-dimensional cell cultures, cells may lose important signals. These vital micro environmental factors can be preserved in cells cultured in a three-dimensional environment containing the extracellular matrix[20]. Therefore, interest in three-dimensional cultures has gradually increased.

Nowadays, three-dimensional breast cancer tumor models play a valuable role in understanding breast cancer. 3D *in vitro* models allow the effect of the micro environment on cellular differentiation, proliferation, apoptosis and gene expression, as well as cell-cell and cell-cell extracellular matrix interactions. 3D cultures cope more effectively with cytotoxic agents than cells in 2D. For this reason, the importance of 3D culture in therapeutic studies is increasing[21].

The expression of many factors involved in drug metabolism has been shown to increase in 3D cultures compared to 2D cultures. It is also shown that the resistance to drug in 3D cultures is increased compared to that of 2D cultures[22]. Cells in 3D cultures are closer to *in vivo* conditions than 2D cultures. The most important feature of 3D culture is to reduce the gap between cell physiology and cell cultures. Two-dimensional (2D) cell cultures cannot fully mimic cell growth and differentiation *in vivo* as compared to original tissues. Therefore, the development of a drug test platform and the use of 3D cultures for drug screening systems give more realistic results[23].

Table 1.1. Differences in characteristics in 2D and 3D culture systems[21].

Cellular characteristics	2D	3D	Refs.
Morphology	Flat in monolayer	Natural shape	24, 25, 26
Proliferation	Generally faster proliferation rate	Variable proliferation rate	27
Exposure to medium/drugs	Equally exposed	Not fully exposed	24, 28
Drug sensivity	Drugs appear to be very effective	Cells are more resistant	29
Stage of cell cycle	Cells are usually same cell cycle	Cells are in different stage of cell cycle	30, 24, 31
Gene expression	Display different gene expression compared to *in vivo*	Display more similar gene expression level to *in vivo*	32, 29

2D cell culture models are preferred because of their easy applicability to test the pharmacological properties of the drugs. These 2D models reflect only the direct effects of the drugs and ignore the effects of the physiological 3D micro environment. Therefore, the use of 2D *in vitro* models may lead to poor predictive outcomes regarding the efficacy of the drug[33]. In contrast to 2D cultures in 3D cultures, higher cellular organization and resistance to anticancer drugs are provided.

3D cultures are more advantageous because they consider the relationships of receptors with the environment in addition to the organization of cell surface receptors. In addition to differences in physical and physiological characteristics, gene, protein and cell receptor expression were found to differ according to 2D cultures in 3D cultures [34]. Cells cultured in 3D compared to cultured in 2D exhibit different gene or protein

expression than those in 2D because they behave differently in processes such as drug sensitivity, morphology, cell proliferation and cell growth. Although cells lost most of their natural i*n vivo* properties after being removed from the primary tumor and cultured in a 2D system, the cells improved most of their lost function when returned to *in vivo* environment. This observation suggests that the 3D environment is important for cell adaptation and makes the cells more likely to behave as they are in their own natural environment [21].

In order to obtain reliable results in the drug testing, the test platform must be constructed in a similar manner *in vivo*. Cells in 3D culture compared to cells in 2D were found to respond closer to *in vivo* in drug therapies[35]. The reason for increased drug resistance is that drugs gradually lose their activity in 3D cultures.

3D cultures reflect the patient profile better than 2D cell cultures. For this reason, with 3D cell cultures more realistic results can be obtained for toxicity and drug screening tests and they used for therapeutic purposes[36].

3D cell culture models provide more effective conditions for drug discovery by reducing failure by eliminating the use of animals in experiments[37].

1.6. Importance of Co-, Tri-Culture

Cancer micro environment is composed of cancer cells with many different cells and tissue types. In 1889, Paget stated that cancer metastasis depends on the interaction between the target organ micro environment and carcinoma cells[38]. Tumor micro environment is responsible for metastasis and drug resistance [39].

The primary culture of cancer tissues obtained by surgery provides important information for understanding of the cancer microenvironment, but also includes technical difficulties. Therefore these difficulties, co-cultures comprising the combination of at least two different cell types have been formed in order to mimic cell-cell interaction in the cancer micro environment[40].

Breast cancer tissue consists of stromal cells containing different cell types. These cells include fibroblasts, adipocytes, lymphocytes, macrophages, pericytes, and endothelial cells. Communication between these cells has been shown to play important role in the development and spread of cancer. Co-culture systems have advantages in terms of evaluation of cell-cell interaction around the cancer micro environment[40]. Cell-

cell contact is known to play a role in the mechanism of cancer invasion by adhesion molecules[41].

In drug research, co-cultures are very important because they provide a more realistic tissue model for monitoring drug effects [36].

1.7. Lab-on-a-chip Devices

Microfluidic devices having high sensitivity in controlling micro environment in small scales are becoming increasingly important[42]. Depending on this microfluidic technology new notions such as lab-on-a chip, organ-on-a chip have emerged. Lab-on-a-chip (LOC) devices are miniature platforms which includes process from collection of samples to analysis[43]. Recently, LOC devices have been widely used due to their many advantages, such as saving time, requiring small sample volume, making rapid analysis, being low cost, being disposable, mimicking the *in vivo* micro environment and providing high-efficiency analysis[44]. LOC systems minimize the risk of contamination due to closed systems.

Most LOC devices are manufactured using photolithography and soft lithography methods. As a result of the production of PDMS microfluidic devices, cheap and easy LOC devices have been produced[45]. LOC devices are closely associated with microfluidic devices which allow the flow of fluids in the channels[46].

Direct accessibility is one of the advantages of microfluidics to cell culture. Many conditions can be tested on a single platform simultaneously or separately in a small area without cost[47]. Therefore, it offers a great advantage for high-throughput screening.

LOC research provides innovations for global health development. Microfluidic devices are used for drug testing, symptomatic process, screening and detection studies[48].

Microfluidic devices are suitable for various stage of drug discovery and are also important for applications of cancer detection. For this reason, they can take an important place in the early detection, diagnosis and treatment of patients with cancer[49].

More than 90% of the drug candidates who are screened fail after clinical trials. Traditional drug screening studies are costly and time-consuming[50]. Therefore, LOC devices will be useful approach to reduce sample volume and time.

CHAPTER 2

MATERIALS AND METHODS

2.1. Cell Culture

Cell culture is a process in which cells are grown under controlled conditions with unnatural environment containing nutrients, ideal pH, humidity, temperature and gas conditions[51].

Cell culture is an important technique since it provides optimal conditions for observing the physiology and biochemistry of cells[52].

2.1.1. Cell Lines And Features

MDA-MB-231 cell line was isolated from Caucasian woman aged 51 years. It is estrogen negative, a quite tumorogenic, adenocarcinoma-derived breast cancer cell line.

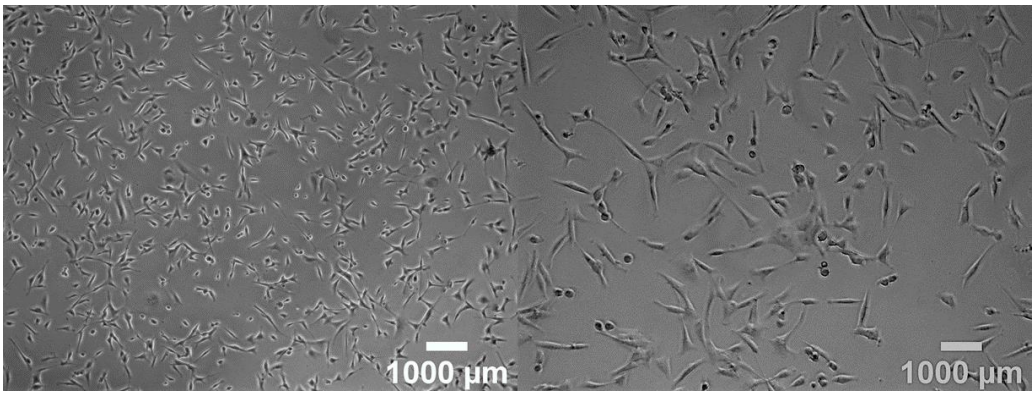

Figure 2.1. MDA-MB-231 cell line.

MCF-10A cell line was isolated from Caucasian woman aged 36 years. It is a non-tumorigenic epithelial cell line.

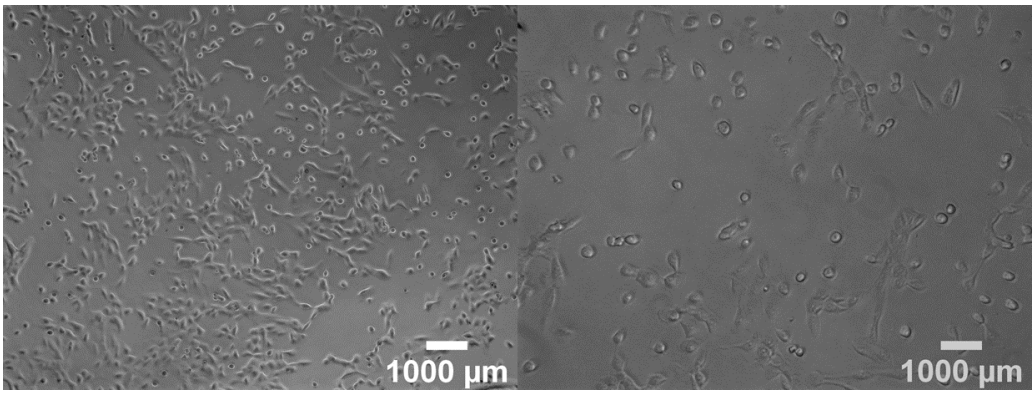

Figure 2.2. MCF-10A cell line.

RAW 264.7 cell line is adherent, macrophage cell line. It was derived from tumor induced by Abelson murine leukemia virüs. It is required biosafety level 2 conditions.

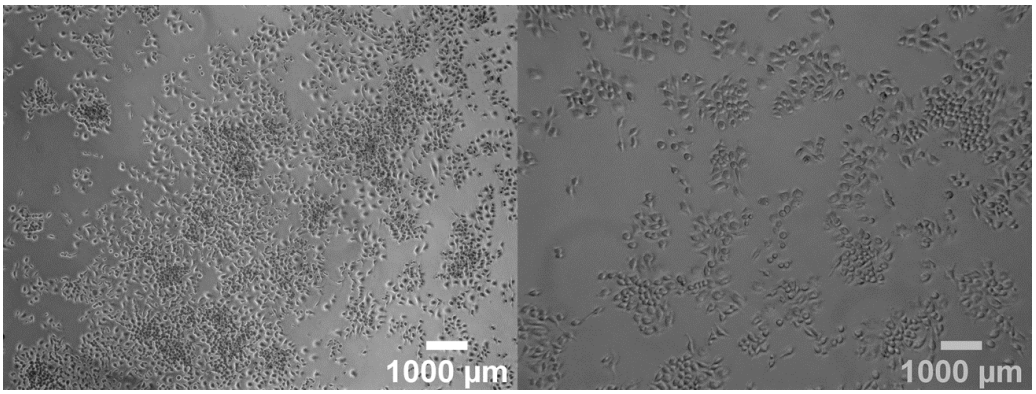

Figure 2.3. RAW 264.7 cell line.

2.1.2 MDA-MB-231 Cell Line Medium Preparation

A day ahead of preparation, 5 ml Pen-streptomycin (Pen-Strep) (Biological Industries-03-031-1B), 5 ml L-glutamine (Biological Industries-03-020-1B) and 50 ml fetal bovine serum (FBS) (Biological Industries-04-001-1A) aliquotes were taken from +4°C to -20°C. 450 ml DMEM High Glucose (Biological Industries-01-055-1A) and 50 ml FBS was mixed. Then 5 ml Pen-Strep and 5 ml L-glutamine were added to this solution. The bottle was thoroughly mixed and filtered with polyethersulfone (PES) membrane filter system (Milipore). The preparation process was occurred in a laminar

cabinet (Thermo Scientific MSC1.2 and Nüve MN120). Medium was stored at +4°C except for usage.

2.1.3. MCF-10A Cell Line Medium Preparation

A day ahead of preparation, 5 ml Pen-strep, 5 ml L-glutamine and 50 ml donor horse serum (Biological Industries-04-004-1A) aliquotes were taken from +4°C to -20°C. First before the mixture was added to DMEM F-12 serum-free (Biological Industries-01-170-1A) culture medium, 25 ml donor horse serum, 5 ml Pen-strep, 5 mlL-glutamine and approximately 10-12 ml DMEM F-12 were mixed in 50 ml falcon. 500 microliters insulin (Sigma-I1882-100MG) (stored at -20°C), 250 microliters hydrocortisone (Sigma -H0888-1G) (stored at -20°C) and 50 microliters choleratoxin (Sigma-C8052-1MG) (stored at +4°C) were added to falcon. Ultimately, 100 microliters epidermal growth factor (EGF) (Sigma-E96442 MG) (stored at -80°C) was added to falcon. Then, mixture in this falcon was transferred to 500 milliliters bottle. The bottle was thoroughly mixed and filtered with polyethersulfone (PES) membrane filter system. The preparation process was occurred in a laminar cabinet. Medium was stored at +4°C except for usage.

2.1.4. RAW 264.7 Cell Line Medium Preparation

A day ahead of preparation, 5 ml Pen-step, 5 ml L-glutamine and 50 ml fetal bovine serum (FBS) aliquotes were taken from +4°C to -20°C. 450 ml RPMI1640 (Biological Industries-01-104-1A) and 50 ml FBS was mixed. Then 5 ml Pen-Strep and 5 ml L-glutamine were added to this solution. The bottle was thoroughly mixed and filtered with polyethersulfone (PES) membrane filter system. The preparation process was occurred in a laminar cabinet. Medium was stored at +4°C except for usage.

2.1.5. Thawing Out Cells

Cells should be frozen at -196°C (Thermo Scientific Locator JR Plus) with appropriate techniques using liquid nitrogen so that they can be stored for extended periods of time without damaging the genome, cellular metabolic activities and essential

physiological properties. The cells were removed from the liquid nitrogen tank are melted in a water bath (Nüve bath nb2) at 37 ° C and transferred into the medium. The cells were homogenously dispersed by pipetting the cells with the suspension. After thawing cells suspension were transferred to falcon tube (Corning) and centrifuged at 1000 rpm for 5 minutes (Nüve bench top centrifuge NF 400R). Then the supernatant was removed and pellet was dissolved with 1 ml complete medium. Cells was added to 100 mm^2 petri dish (Corning 100 mm TC-Treated culture dish). Petri dish was moved in the form of eight signs for homogeneous distribution. Observation of the densities and morphological structures of the seeded cells were performed by looking at their appearance on the microscope (Olympus CKX41). Then petri was incubated at 37°C, 5 % CO_2 in incubator (Binder ve ThermoScientific 3404).

2.1.6. Passage of MDA-MB-231 Cells

Cells reaching a certain density in the petri dish were passaged. Before the passage laminar cabinet were sterilized with 70% ethanol. Prior to passage procedure, trypsin-EDTA solution and the complete medium were taken from +4°C to room temperature. Petri dish was taken to laminar cabinet. Then the medium of the cells was aspirated. 2 ml trypsin-EDTA solution was added for washing step. This solution was aspirated. Afterwards, for the purpose of detaching the cells from the surface, 4 ml trypsin-EDTA solution (Biological Industires-03-053-1B) was added to petri dish. It was placed to incubator for 3 minutes. After the required time has passed, cells were checked under the microscope to observe whether the cells were detached. Then, petri dish was taken to laminar cabinet. 1 ml complete medium was added to cells in order to inactive the trypsin-EDTA solution effects. This 5 ml complete medium and trypsin-EDTA solution mixture was transferred to 15 ml falcon tube. And 5 ml complete medium was added to petri dish to wash and collect cells then medium was transferred to falcon. After that, falcon was centrifugated at 1000 rpm for 5 minutes. Supernatant was aspirated with vacuum. Pellet was dissolved fresh complete medium. Then cells were counted. The cells in desired ratio were added to petri dish which contained 10 ml complete medium. Petri dish was placed into incubator. Passage procedure was performed each 2-3 days.

2.1.7. Passage of MCF-10A Cells

The whole procedure was the same passage procedure of MDA-MB-231 cells except for the waiting times in the trypsin-EDTA solution. It was placed to incubator for 17 minutes for MCF-10A cells. The remained procedure of passage was done by same way.

2.1.8. Passage of RAW 264.7 Cells

First, 8 ml fresh medium was added to the new petri dish (Corning 100 mm NTC-Non-treated culture dish). In the petri dish to be taken the passage, medium was withdrawn as 1 ml medium. The petri was scraped slowly with the scraper. Petri was washed slowly and collected cells to falcon tube. Then cells were centrifugated at 400 rcf for 5 minutes. After centrifuge, 2.5 ml supernatant was taken for petri dish. 1 ml supernatant was left for dissolved the pellet. And the remaining supernatant was discard. The cells in desired ratio were added to petri dish which contained 10 ml complete medium. Petri dish was placed into incubator.

2.1.9. Cell Counting

Passage is carried out as described above. After centrifugation step, according to the cell pellet complete medium was added to pellet. Then pipetting was done. 10 µl of sample was mixed with 10 µl of dye and cells were counted in EVE ™ Automatic Cell Counter.

2.1.10. Cell Freezing

Cells reaching a certain density were passage. After centrifugation step as described above, supernatant was removed, pellet was dissolved 1 ml complete medium. Quantity of DMSO was calculated seven and half percent of (total volumex2). Required

volume of DMSO was mixed complete medium. Then, DMSO solution was added to cells gradually. Cells were divided to 2 cryotubes. The they were placed at -80°C. After one day, cells were taken to liquid nitrogen tank.

2.2. Chip Preparation

The chip preparation process started with uv lithography and ended with the sterilization with the sterilization process required for the chips to be ready for use.

2.2.1. UV Lithography

UV lithography procedure was continued three days. First day, the process was consisted of pouring SU-8 (Microchem) to the silicon wafer (Universal wafer), spin coating and soft baking. Silicon wafer was placed on hot plate at 65 ºC for 5 minutes.

SU-8 was poured onto the silicon wafer at the appropriate amount and spread. Wafer was placed on spinner at 500 rpm. It was placed on bench for 5 minutes. Then it was placed on hot plate at 65 ºC for 5 minutes. Later, hot plate was adjusted 125 ºC. And wafer was placed on hot plate for 1 hour. After 1 hour, wafer was placed on the bench at room temperature until second day. On the second day, the wrinkle test was done. Hot plate was adjusted to 125 ºC. Then wafer was placed on hot plate for 5 minutes to see/not see the wrinkle. If there was no wrinkle, wafer was waited on the bench for 5 minutes for cooling. Mask design was put on wafer then wafer was put on mask aligner. Wafer was exposed UV light for 30 seconds. After expose, wafer was put on the bench. Hot plate was set to 65ºC. Wafer was placed on hot plate for 5 minutes. Then the heater was adjusted 125 ºC. Wafer was placed on for 10 minutes. After post baking, hot plate was turn off. Wafer was left until the next day. On the third day, wafer was waited in SU-8 developer (Microchem) for 5 minutes without shaking. Then, in this solution wafer was shaked for 5 minutes. Wafer was tested with isopropanol. IPA was dripped to wafer. When the white color was seen, development process was continued. When white color was not seen, process was completed. And the wafer was dried with dust free wipes. The wafer was checked under the microscope.

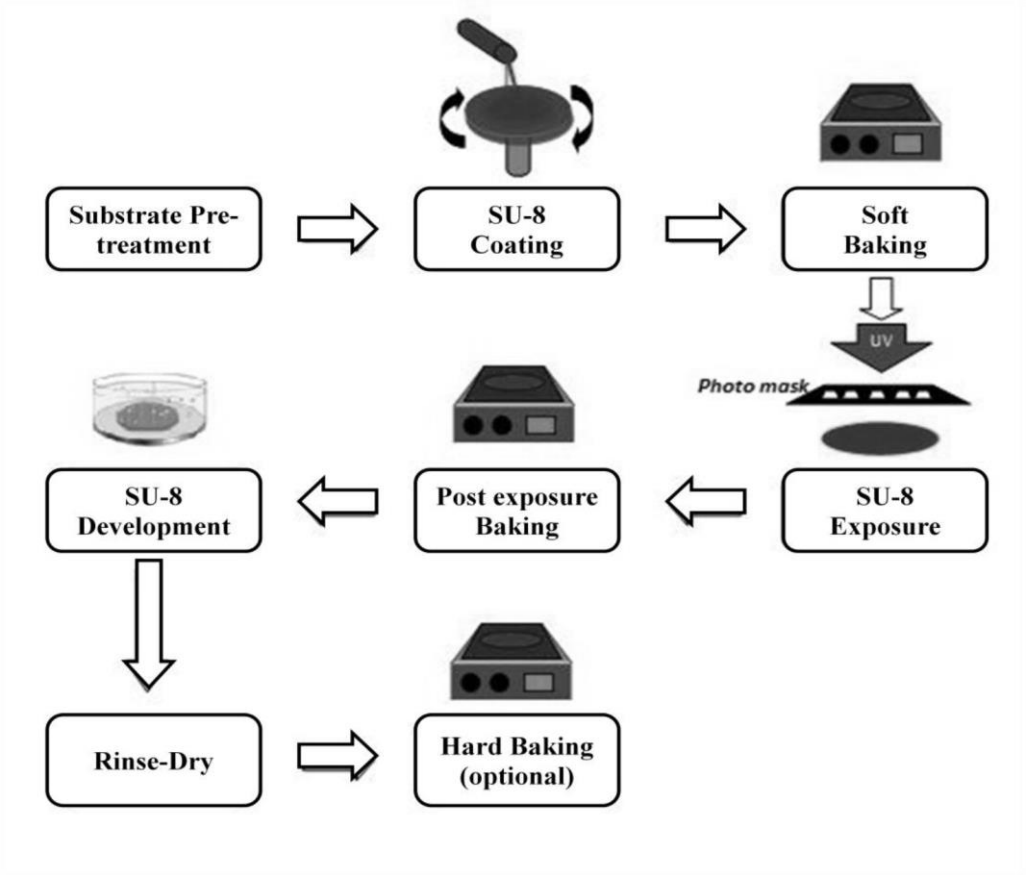

Figure 2.4. UV lithography technique[53] (Source: Murat Sağlam, 2014).

2.2.2. PDMS Molding

PDMS molds were made of mixing PDMS elastomer base and curing agent (SYLGARD® Dow Corning) at 10:1 ratio by weight. The mixture was taken to dessicator to remove bubbles and degassed. The wafers were washed respectively with water, alcohol, water and wet with demolding agent. The mixture was poured these wafers. And they were kept at room temperature, two days on a flat surface. After the polymerization was complete, the PDMS was removed from the wafers by the aid of ethanol. Then PDMS was cut by scissors. Holes were opened with punchers suitable for the hole size to be formed.

2.2.3. PDMS Molds Cleaning and Sterilization

PDMS molds were passed through a cleaning stage prior to use. PDMS molds were washed with ultra pure water and treated with 70% ethanol. To resolve the ethanol residues, they were cleaned with ultra pure water. After this first cleaning step, the molds placed the containers sequentially in ethanol and ultra pure water and kept into sonicator. Removal of any substances from PDMS molds was provided with sonication. Then, the molds were allowed to dry at room temperature for 2 days.

2.2.4. PDMS Cleaning

Firstly, the dust on top of PDMS molds were removed with scotch tape. Then these steps were occured. First molds were placed in the petri dish with their patterns facing up. They were rinsed with respectively UpH_2O, EtOH, UpH_2O. They were sonicated in UpH_2O for ten minutes. Then they were rinsed 5 times with UpH_2O. They were sonicated in EtOH for five minutes. They were rinsed 3 times with EtOH. Then they were waited in EtOH for five minutes. After this step, they were rinsed with UpH_2O 1 time. Finally, they were dried with the dessicator. They were placed on disinfector for one night.

2.2.5. Chip Bonding and Sterilization

Before the bonding steps, PDMS molds were cleaned with scotch tape. Clean molds and glass slides were placed in the UV/Ozone device. PDMS was placed in the device with their patterns facing up. They were treated with UV light and ozone gas for five minutes. Then PDMS and glass were assembled. They were placed on the hot plate for ten minutes at 100ºC. Then they were exposed UV light in the laminar flow cabinet for 30 minutes.

2.2.6. Experimental Design

Cells were studied as mono-culture and tri-culture. MDA-MB-231 cells were cultured in DMEM 10% FBS medium, RAW 264.7 cells in RPMI 1640 10% FBS medium, MCF-10A cells in DMEM / F12 + additional chemistry environment. Additional chemicals for MCF-10A cells were: 5% horse serum, 20 ng/ml EGF, 0.5 ug/ml hydrocortisone, 100 ng/ml cholera toxin and 10 ug/ml insulin. Tri-culture was performed at 1:1:1 culture environment conditions. Cells were loaded three-dimensionally in the matrigel to LOC devices. Matrigel was diluted with DMEM medium. Cells were mixed with matrigel at a 1:1 volume ratio. The process was carried out on ice cubes until the loading process. Final cell density was selected to be over $6x10^6$ million. One ratio was studied for the ratio of cell numbers in tri-culture 1:1:1 for cancer cells: normal cells: macrophages. In this way, early cancer stage was tried to be mimicked. In mono-culture, cancer cells were marked with green-emitting cell-tracing dyes (Thermo Fisher Scientific) before being loaded onto the LOC devices. The second day drug administration was performed. Lyophilised doxorubicin (Sigma- D1515) (10 mg) was dissolved in water. The drug was prepared such that the concentration was 100 µM. Doxorubicin was diluted with DMEM medium as 10 µM final concentration. Klavuzon (A generous gift from Dr. Ali ÇAĞIR) (2.2 mg) was dissolved in DMSO (Dimethyl sulfoxide). Stock solution concentration was 10 M. Then klavuzon was diluted with DMEM medium as 100 µM final concentration.

On the third day, cells were visualized in 3D and their counts and viabilities were determined on a confocal fluorescence microscope. Dead cells were identified with NucRed Dead 647 (Thermo Fisher scientific) which only dyed dead cells and emitted far-red. NucRed Dead647 reagent which is non-permeant stain bound to DNA. This reagent that is used to detect cell viability is effective in cells with impaired cell membrane integrity. It was preferred because it is suitable for 3D environment and doesn't require any steps such as washing step.

In tri-cultures, two different colors (blue and green) (Thermo Fisher Scientific) were used for fluorescence tracking for three different cells. 3D (z-stack) images were taken on at least three different sites in LOC devices for viability determinations, live and dead cell counts and percentages were determined for all cells stained. Numerical studies of the cells were performed with ImageJ / Fiji software.

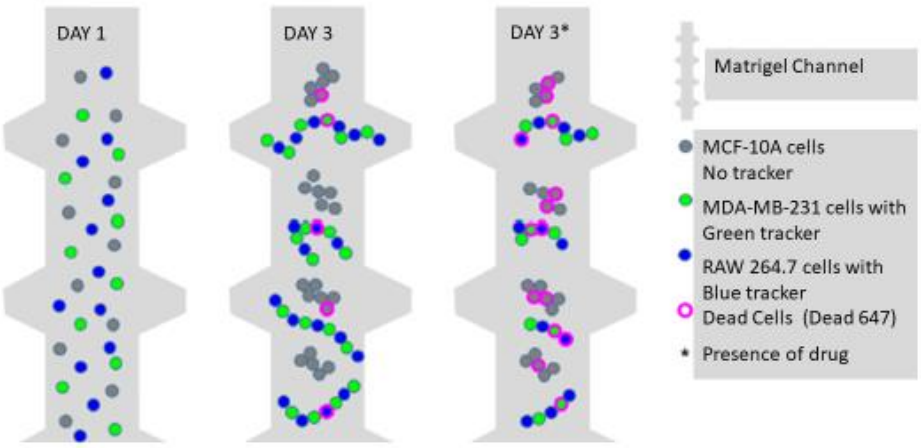

Figure 2.5. Distribution of cells in LOC devices according to days for tri-culture.

Cells showed a random homogeneous distribution within the LOC device. Until the third day, distribution of cells has changed and number of cells has increased because of cell proliferation and migration. More cell death was observed in the presence of drug and drug candidate.

CHAPTER 3

RESULTS AND DISCUSSION

3.1. LOC Fabrication for 3D Experiments with UV Lithography Method

SU-8 molds were prepared by UV lithography for LOC production. These molds were used for the fabrication of PDMS structures. By bonding PDMS structures with glass surfaces, LOC fabrication was completed. The LOC device has three parallel channels.

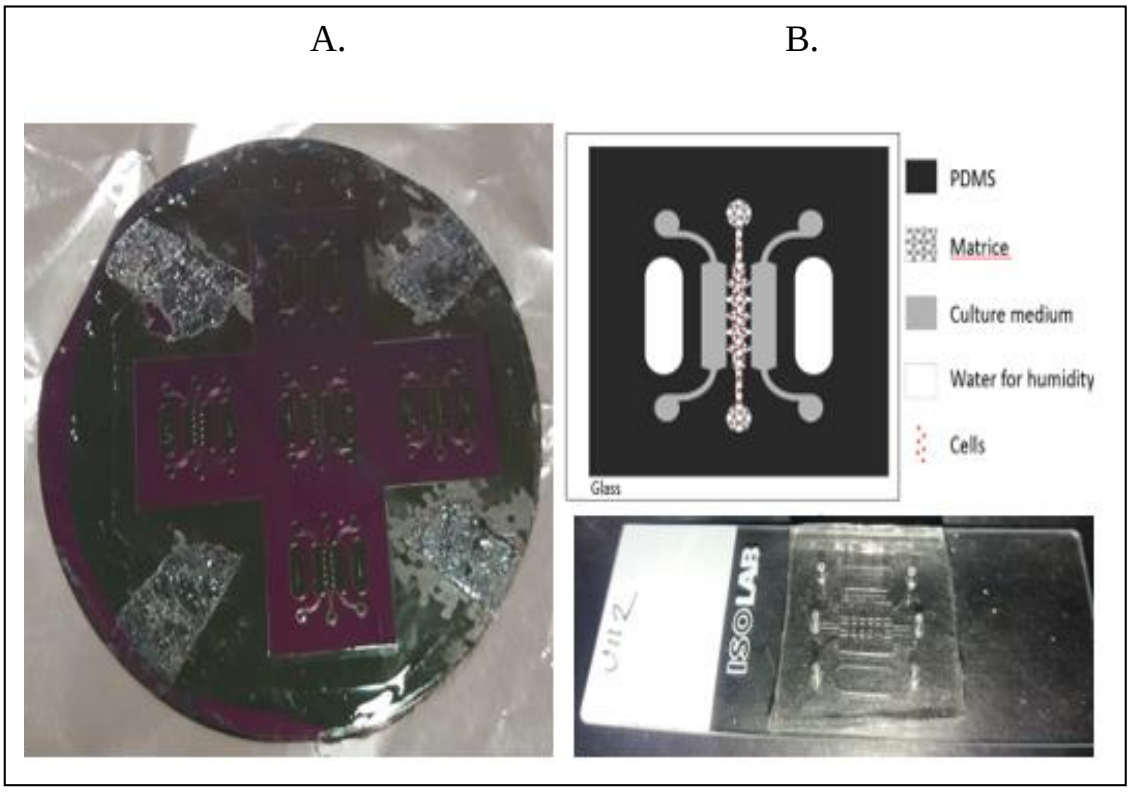

Figure 3.1. SU-8 mold. B. Design of LOC devices.

3.2. Optimize drug screen parameters

3.2.1. Determination of viability and distribution of cells in 3D mono and tri-culture in the LOC

Since the tumor micro environment is a critical component of cancer biology and is responsible for metastasis and drug resistance, mimicking this micro environment is important in drug studies[39]. It is well known that the interaction between macrophages and breast carcinoma cells plays an important role in carcinogenesis[54]. Literature search was made for the selection of cell lines in "Pubmed" and "Web of Science" sites. As a result of scans, MDA-MB-231, MCF-10A and RAW 264.7 cell lines were selected as examples of different cell phenotypes. The cell lines to be used are MDA-MB-231 triple-negative (ER-PR-HER2-) metastatic breast cancer cells, MCF-10A normal mammary epithelial cells and RAW264.7 macrophages. Normal breast epithelial cells and macrophage cells that are important cells of the immune system have been preferred as supporting tissue cells. In this way, the side effects of drugs to normal cells other than cancer cells were also investigated.

The culture medium conditions and the density of the cell number are important for optimizing the drug screening parameters.

Cells were grown in three different culture media in order to determine culture conditions required to create tri-culture. DMEM medium was selected to use for tri-culture experiments because of providing optimal culture conditions. MDA-MB-231 and MCF-10A cells can be used culture medium in 1: 1 ratio in co-cultures[55, 56]. Based on this data, cells were used 1: 1:1 volume ratio in tri-culture. By means of this ratio, early cancer stage was attempted to be mimicked[57].

Then, different cell densities were tested to determine optimal cell density. For this purpose, $10x10^6$, $6x10^6$, $5x10^6$, $3x10^6$, $2x10^6$, $1x10^6$, $0.5x10^6$ cells/ml final densities were used. $10x10^6$ cells/ml final density was chosen as the ideal cell density for our experiments. According to the our results $10x10^6$ cells/ml final density is also suitable for studies in the literature[58].

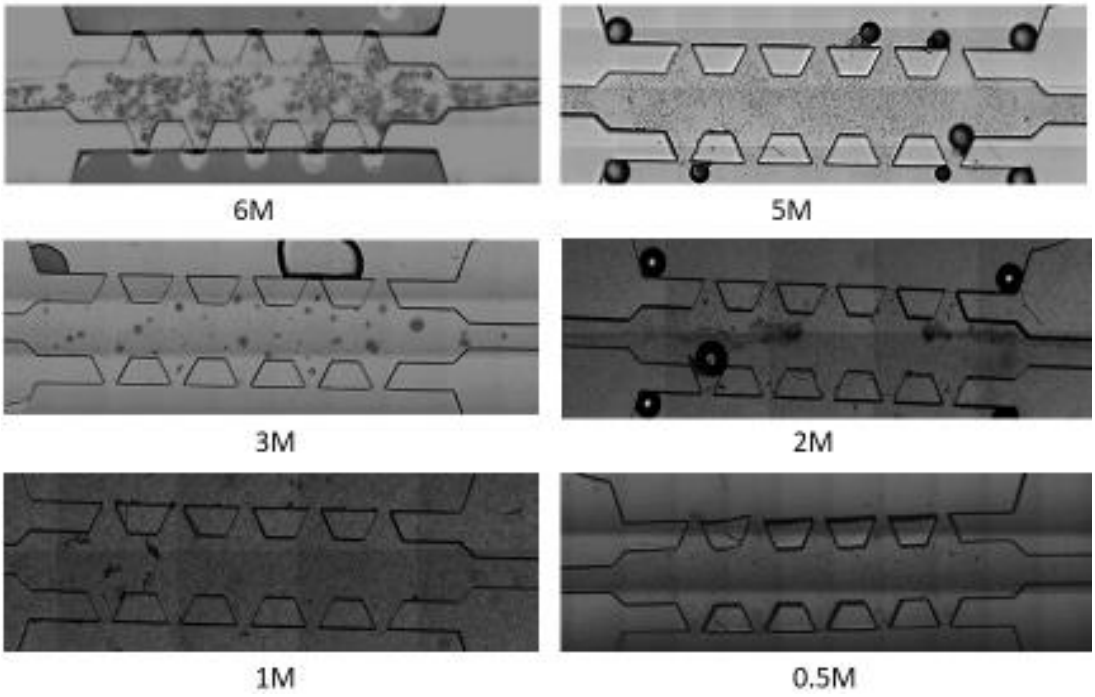

Figure 3.2. Microscope images of cells at different cell densities. Images were taken with confocal microscope by using 10x objective.

Optimization of cell number was important for comprising of the 3D micro environment. When there was insufficient number of cells, there were gaps between the posts in LOC device. If the cells don't spread homogenously, the exact result will not be reflected. In the case of excessive density of cells, precipitation occurred in the 3D micro environment. The optimal number of cells has been used to ensure that 3D environment was appropriately created.

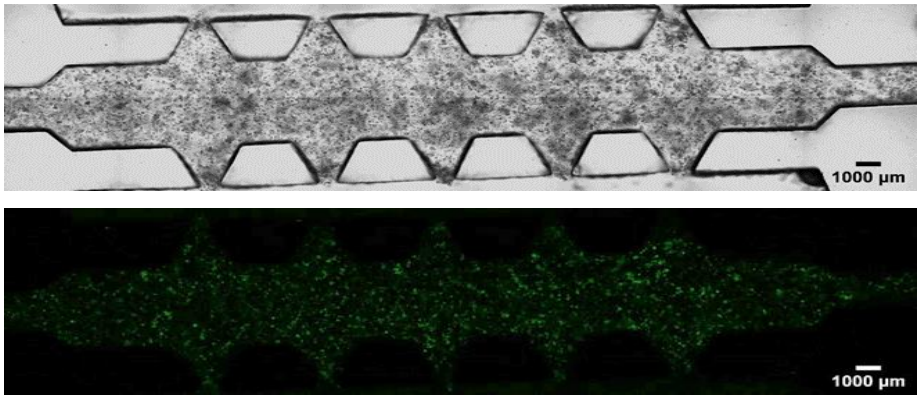

Figure 3.3. 20x106 cells were mixed with matrigel at a 1:1 volume ratio and they were loaded into LOC device.

3.2.2. Determination of dosage of drugs

As a result of literature research for the selection of cancer drugs, doxorubicin, which is an anti-tumor growth agent, was preferred because of its widespread use. A scan of the words " doxorubicin AND cancer " resulted in 56184 publications (June 2019). In addition, klavuzon was preferred because it is known to be an inhibitor of topoisomerase-I and its anti-proliferative effect.

In order to determine the dosage of drugs, the selected dose range from the literature were confirmed at 24, 48 hours by Alamar blue assay[59]. Alamar blue assay which is widely used in literature, is a test of metabolic function. It is a redox indicator. Resazurin which is a component of Alamar blue reagent, is reduced after entering living cells. Changes in cell viability can be detected with measurement of absorbance[60]. We chose this assay for cell viability testing as it can be used in 3D cultures.

$10x10^4$ cells were mixed with matrigel at a 1:1 volume ratio. And they were loaded as drop on 96-well plate surface. After polymerization, DMEM medium was added to petri dish. The following day, in the dose range 0-100 µM doxorubicin and 0-100 µM klavuzon were administered for 24-48 hours. Then, 10 µM Alamar blue reagent was applied and after 4 hours, plates were measured at a wavelength of 570-600 nm. Three independent assays were occurred using three wells for each assay.

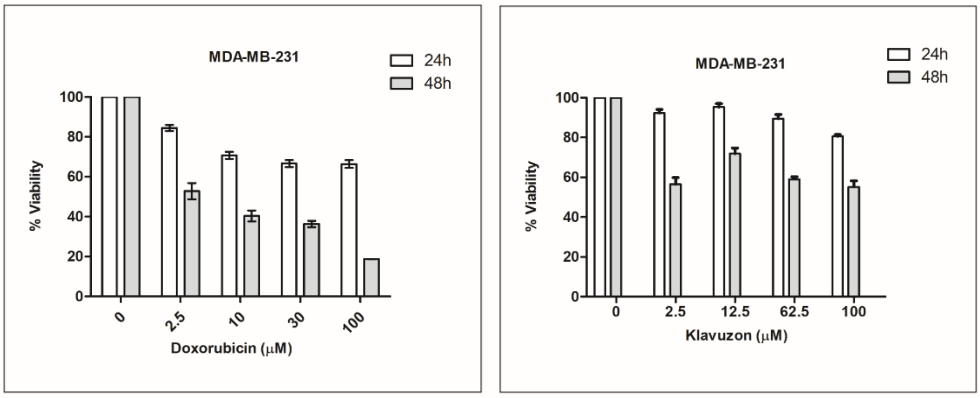

Figure 3.4. Demonstration of the effect of dose and time-dependent drug administration on relative viability in MDA-MB-231 breast cancer cells by Alamar blue testing. Concentration-dependent cell viability for 24 and 48 hours was shown.

According to two-way ANOVA test rsults, there were no significant differences between doses of both drugs for 24 hours ($p>0.0001$). Therefore, the appropriate duration

of administration in both drugs was determined as 48 hours. In studies in the literature, doses were determined 30-40% higher doses than in selected doses for 3D environment to predict doses in the chip environment[61]. Based on the percentage of cell viability in the results of dose trial studies performed as 3D environment in well plate layer, we tried to determine the appropriate doses for 3D cell culture systems within the microchips. In the literature studies, the IC50 of doxorubicin was found to be 10 uM for MDA-MB-231 cells[62].

The appropriate dose was determined for doxorubicin as 10 µM and 100 µM for klavuzon.

3.2.3. Determination of the effect of drugs on viability and distribution of cells in 3D mono and tri-culture in LOC

Dextran is a complex branched anhydrous glucan polymer[63]. Diffusion of dextran has provided preliminary information for many studies[64, 65].

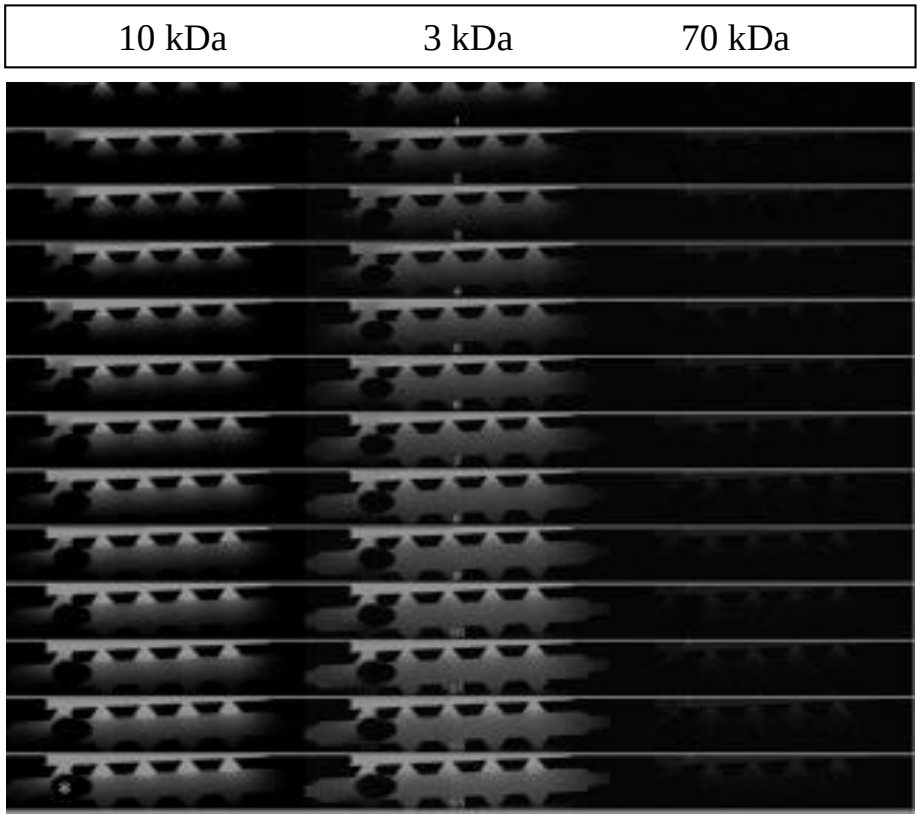

Figure 3.5. Distribution of dextran molecules. Images were taken with confocal microscope with 10x magnification.

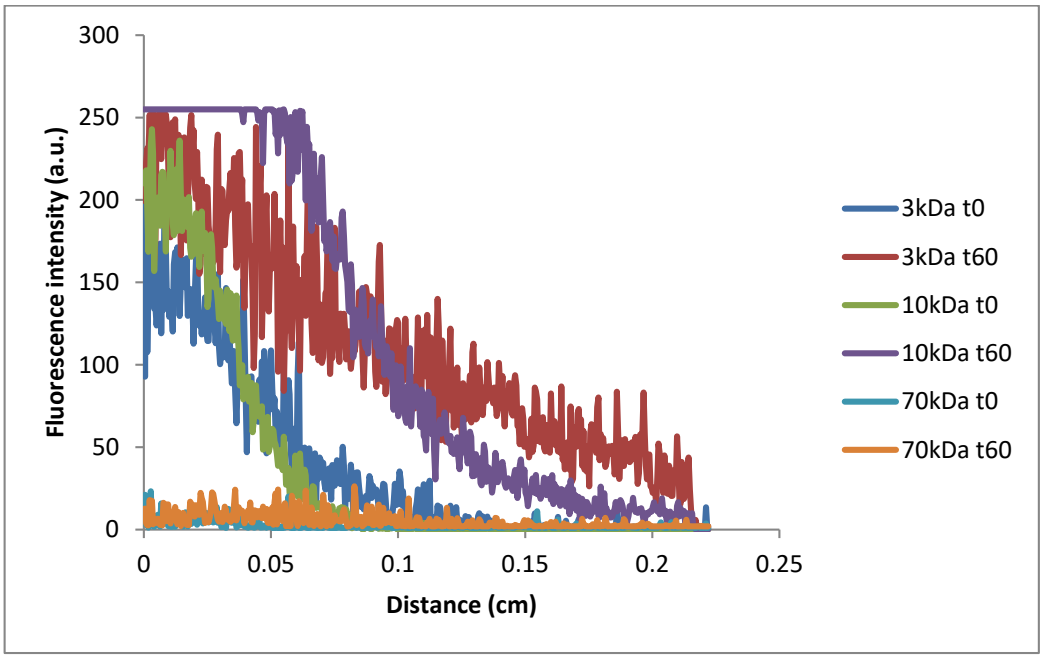

Figure 3.6. Time-dependent distribution of dextran molecules.

Fluorescent 3,10,70 kDa dextran molecules were charged to the culture media wells to predict the distribution of drugs and other molecules by diffusion. In order to predict diffusion distribution, 3,10,70 kDa dextran molecule was loaded into the chip. Images were taken at five minute intervals for 65 minutes. It was shown that the fastest diffusion distribution with inversely proportional to molecular weight was in the 3 kDa dextran molecule at 10x magnification with confocal microscopy.

As a result of the dextran assay, it was predicted that the diffusion of drugs and other molecules could occur within the LOC devices.

The fact that even the 70 kDa dextran molecule was diffused over time predicted that diffusion of various chemicals and drugs might be occured in LOC devices.

Cells were loaded with matrigel in the middle channel to create a 3D micro environment. Side channels were used for loading culture medium. MDA-MB-231 cancer cells, MCF-10A normal mammary epithelial cells and macrophages were used for tri-culture. As a control MDA-MB-231 cells were used as mono-culture.

Cells were labeled with fluorescent trackers and cell density was optimized to be at least $6x10^6$ cells/ml. Then cells were treated with doxorubicin and klavuzon and viability was determined after 48 hours.

As is in literature studies, NucRed™ Dead 647 ReadyProbes™ reagent (Invitrogen™) was used to measure the cell viability[58, 66]. Dead647 signals were observed in the live control groups, less than treated groups. All images were taken with confocal microscope at 10x magnification as 3D.

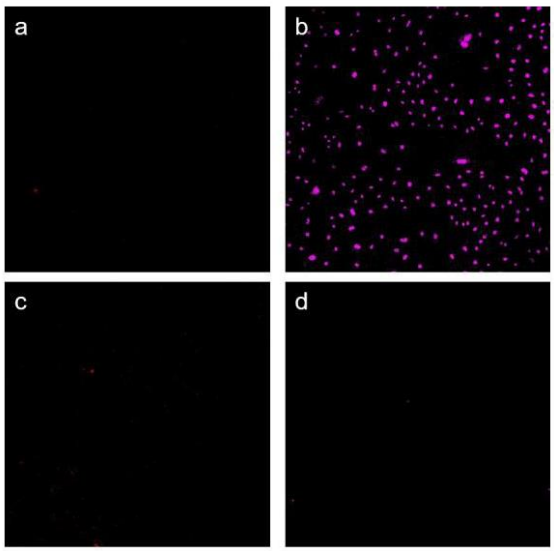

Figure 3.7. Testing NucRed Dead 647.a. Red emission image of cells exposed to ethyl alcohol and stained with Dead647 b. Remote red emission image of the same area (a). c. Red emission image of cells live and stained Dead6 47. d. Remote red emission image of the same area (c).

NucRed Dead 647 which only dyed dead cells and emitted far-red. As expected, Dead647 only stained dead cells and did not give any signal to the red channel. Thus, doxorubicin drug spontaneous red fluorescent signal did not affect the determination of dead cells.

MDA-MB-231 cells were stained green tracker and were in 3D environment as shown is Figure 3.8. Cells had homogeneous distribution due to slides. All cells stained with green tracker. Cells were mixed with matrigel in a 1:1 ratio and loaded into the chip and then kept at the PDMS side for 15 minutes, after on the glass side for 15 minutes. Depending on slides, there were more cells on the PDMS side. In figure, some cells appeared to in groups among themselves such as minor clusturing. Not all cells were the same size. A narrow distribution was exhibited. Differences were observed when we looked at all cells from the same angle. These differences may be due to the fact that different phases occured in cell cycle and cells have different positions.

Individual z-stack images for 3D images in Figure 3.8 were shown each section of 3D images detailed view in independent at z-position. As expected, Dead 647 signal was not observed in the untreated control group cells.

Figure 3.9 shows individual z-stack images for MDA-MB-231 cells. Figure 3.10 shows individual z-stack images for dead cells which stain NucRed Dead 647 reagent**.** Since the control group cells were not treated, no cell death was observed compared to the treated groups.

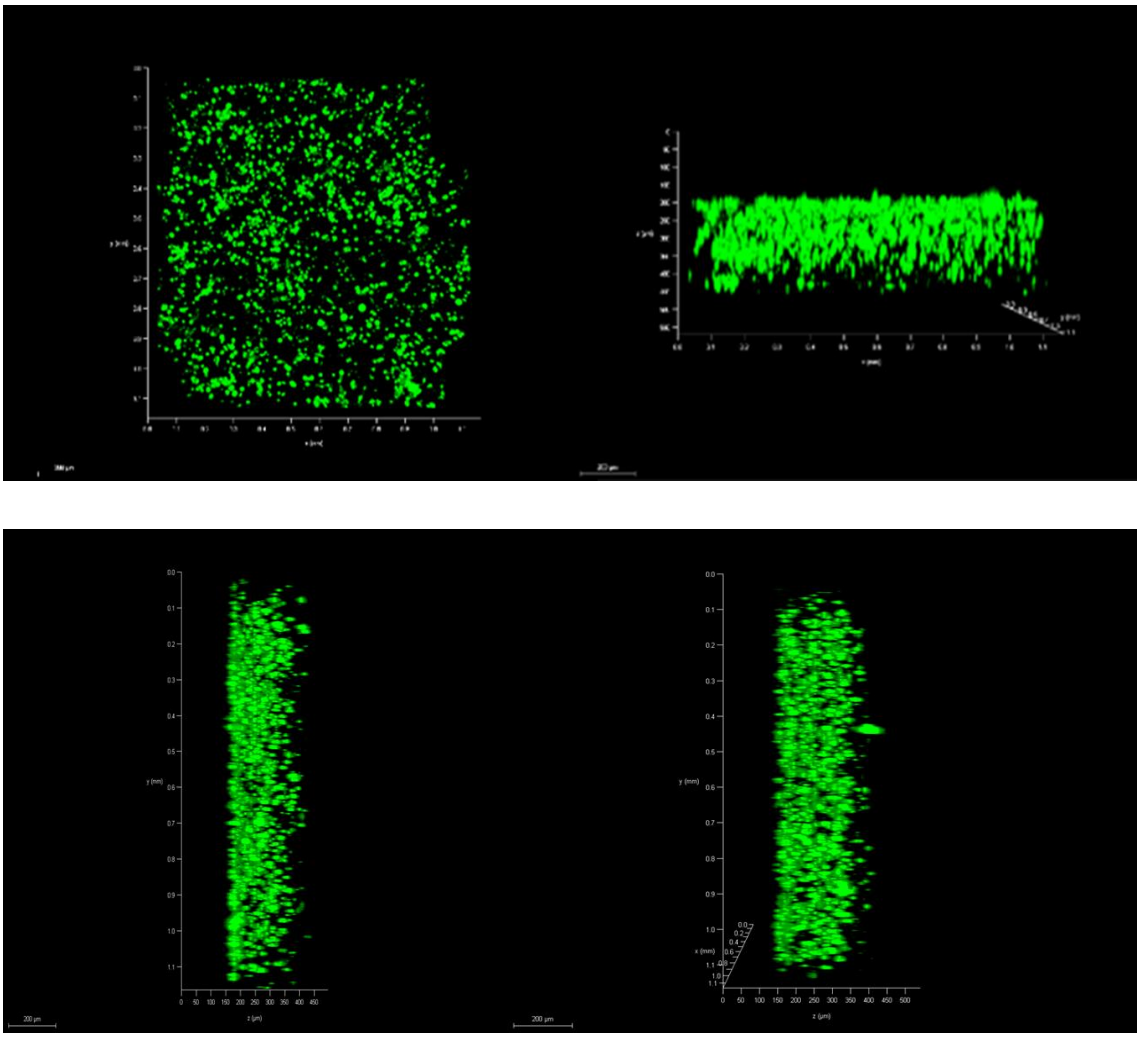

Figure 3.8. Mono-culture. MDA-MB-231 cells (green) were stained with green tracker as a control group. MDA-MB-231 cells were mixed with matrigel at a 1:1 volume ratio. Top and side view were illustrated.

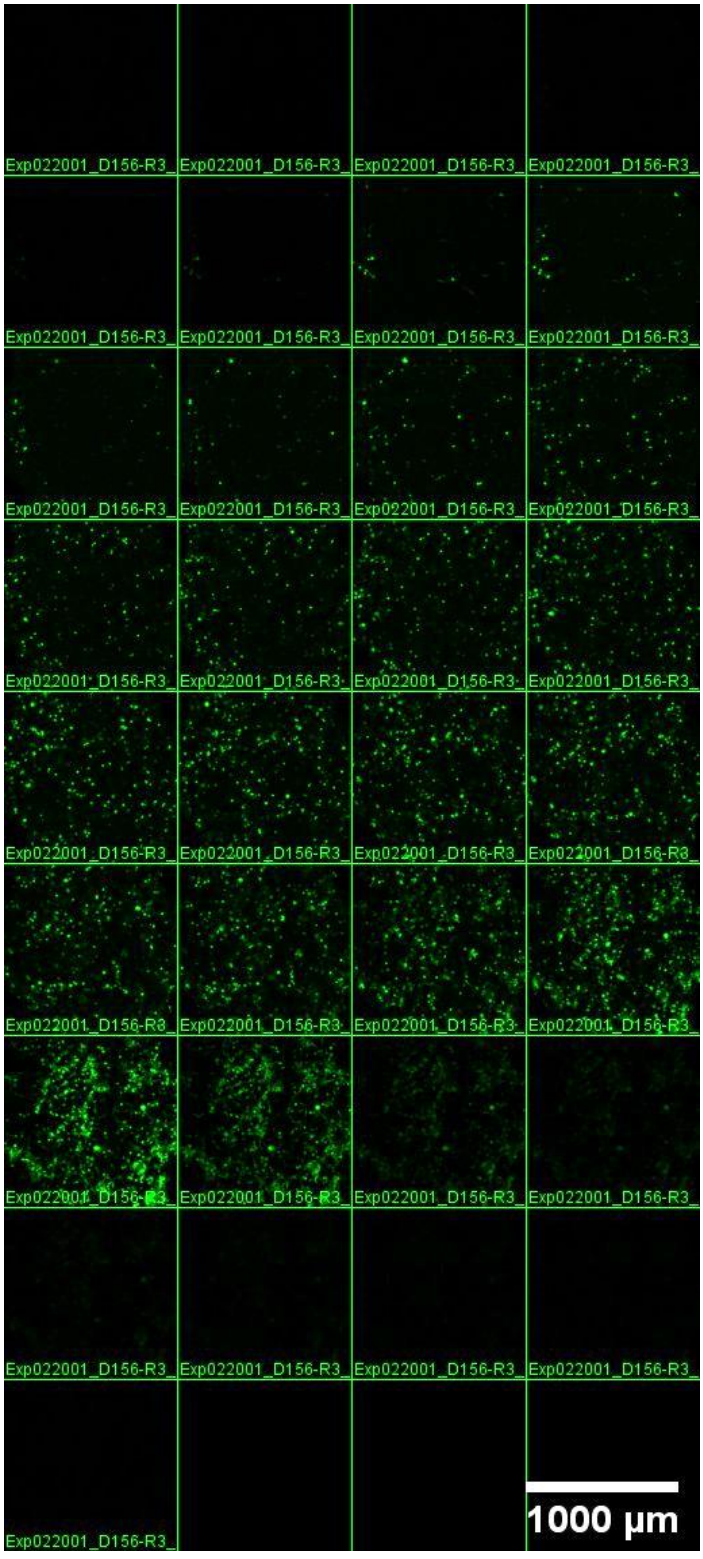

Figure 3.9. Individual z-stack images for MDA-MB-231 cells.

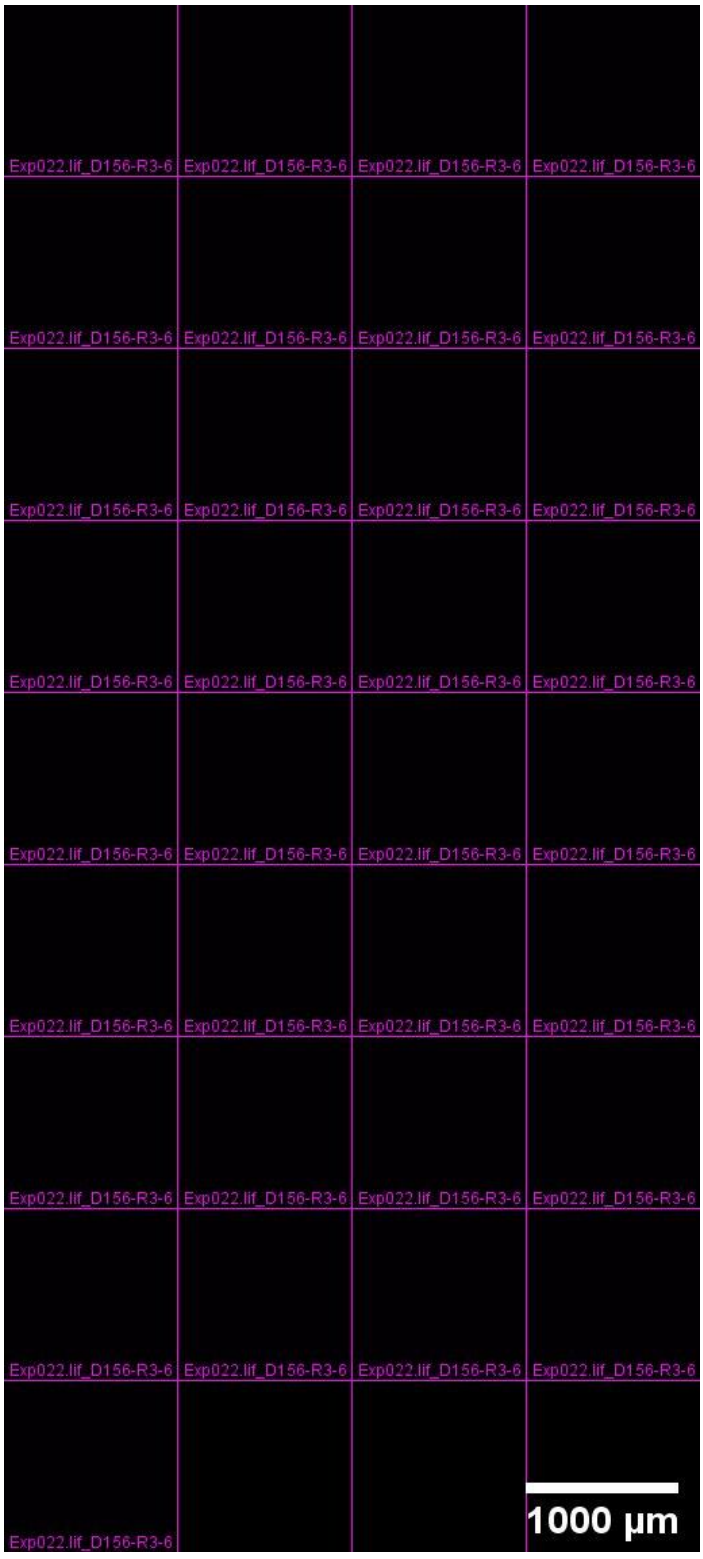

Figure 3.10. Individual z-stack images for dead cells which stain NucRed Dead 647 reagent (Not observed dead cell).

DMSO was used internal control since drug candidate klavuzon was solved in DMSO solution. MDA-MB-231 cells were stained green tracker and were in 3D environment as illustrated in Figure 3.11. DMSO was applied to cells for 48 hours. Dead 647 signal was not observed in the DMSO-treated internal control group cells.

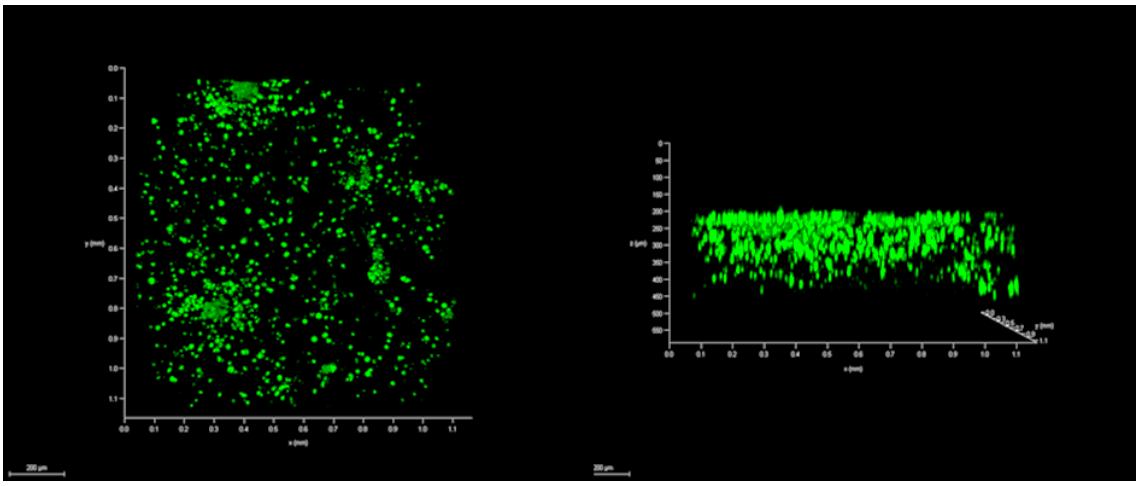

Figure 3.11. MDA-MB-231 cells (green) were treated with 100 uM DMSO as positive control group at 48 hours.

Figure 3.12-3.13 show MDA-MB-231 cells stained with green tracker and treated with doxorubicin which is red fluorescent. More clustering was observed between cells. As in the control group cells, not all cells were in the same size and distribution. Although the cells were appeared stacked to PDMS side depending on the viewpoint, the 3D structure was formed.

Doxorubicin channel, MDA-MB-231 cells channel, Dead647 channel were shown in figure 3.14-3.16. Before adding Dead 647, no signal was observed in the channel 647. Doxorubicin was administered to the cells, but not every cell received doxorubicin. Where doxorubicin signal was observed but cells were not stained green, all cells may not be labeled at 24 hours.

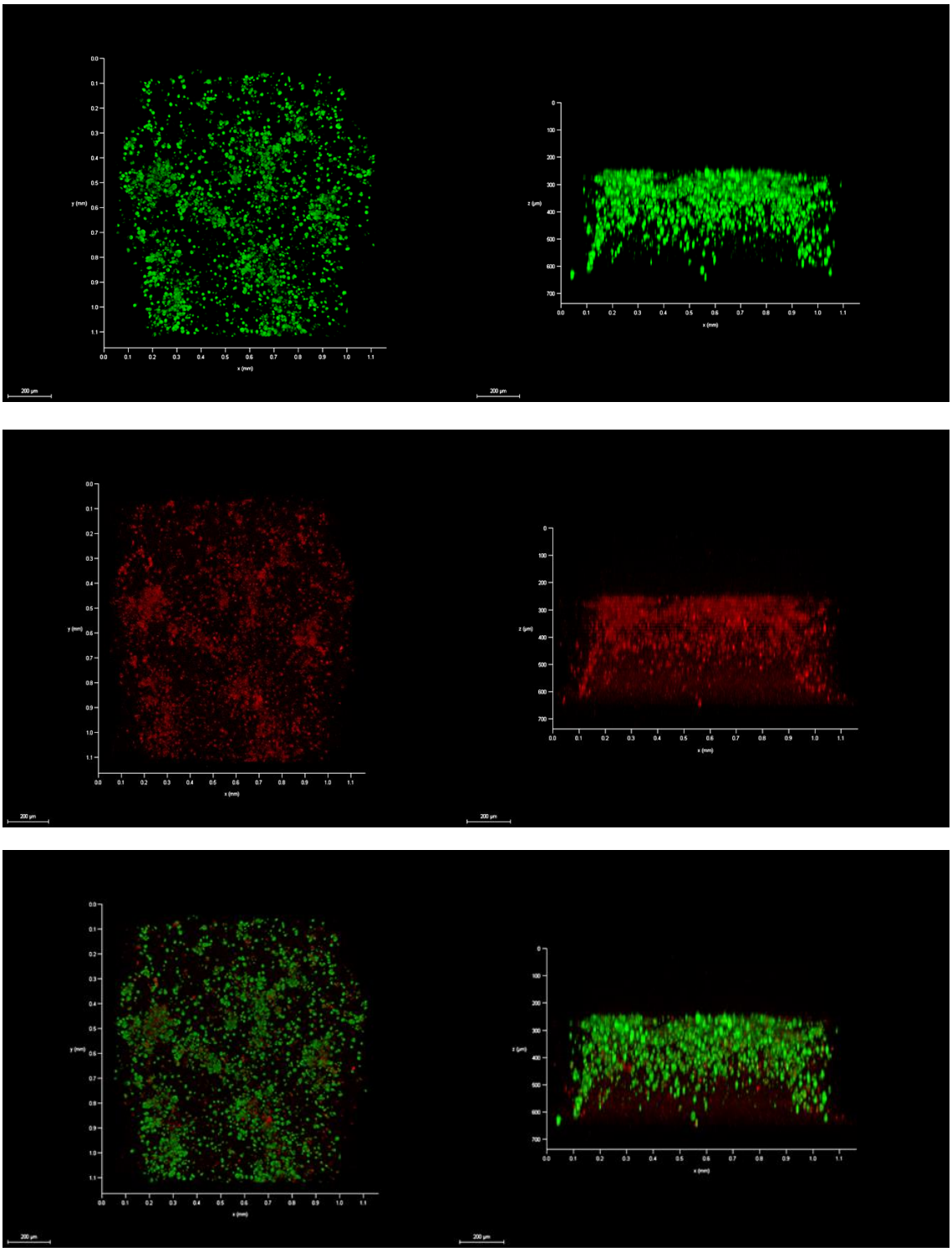

Figure 3.12. MDA-MB-231 cells (green) were treated with 10 uM Doxorubicin (red) at 48 hours (Doxorubicin has already red fluorescence property).

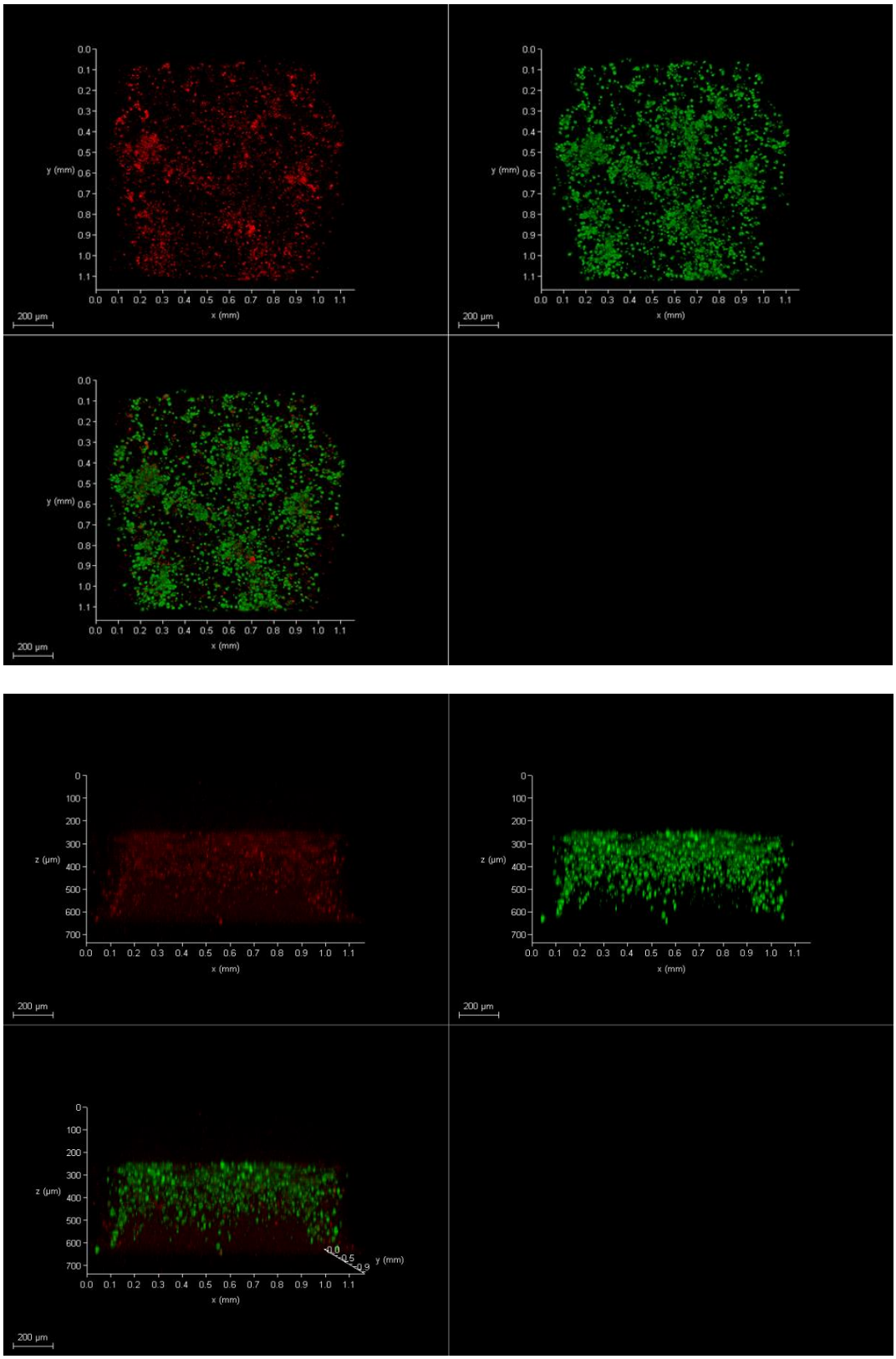

Figure 3.13. MDA-MB-231 cells (green) were treated with 10 uM Doxorubicin (red) at 48 hours (Doxorubicin has already red fluorescence property).

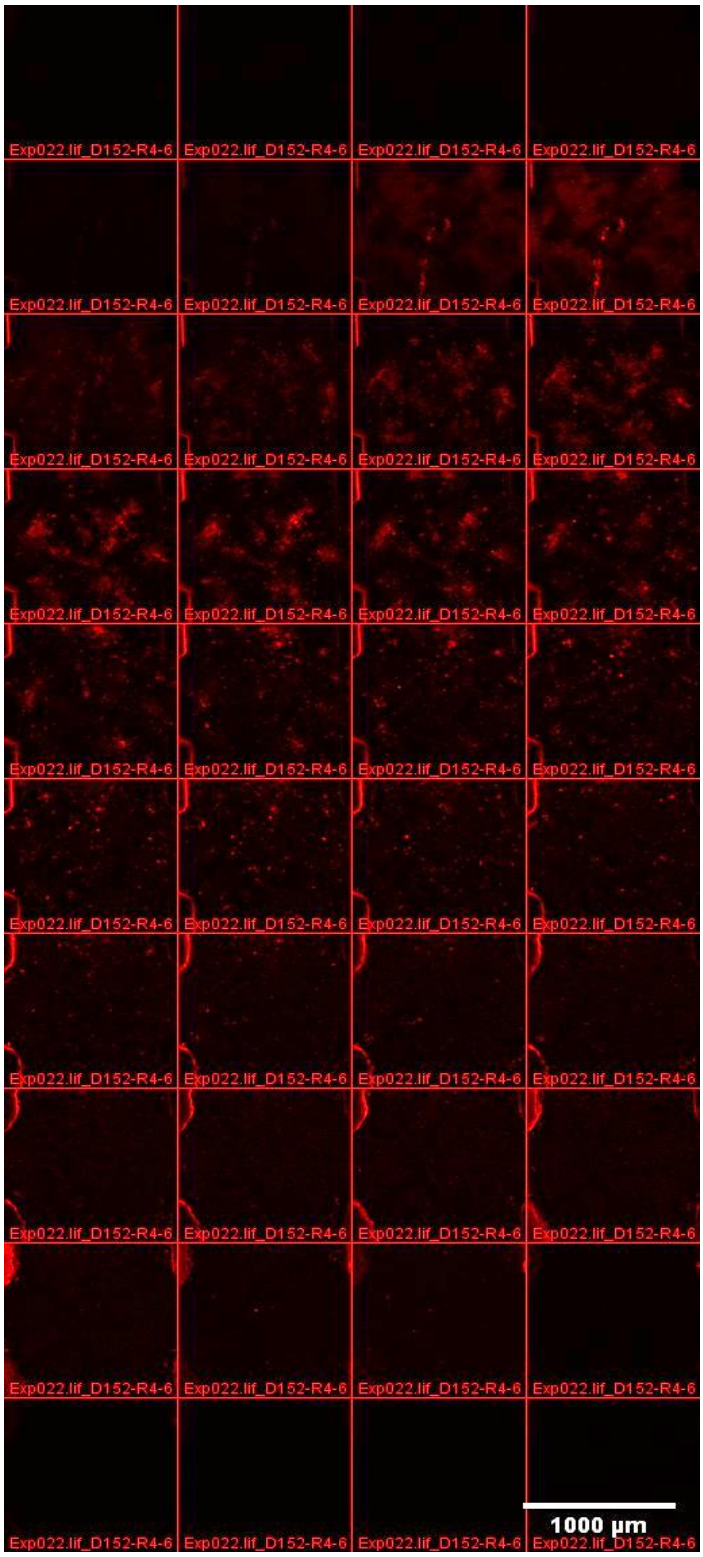

Figure 3.14. Individual z-stack images for cells which uptake doxorubicin.

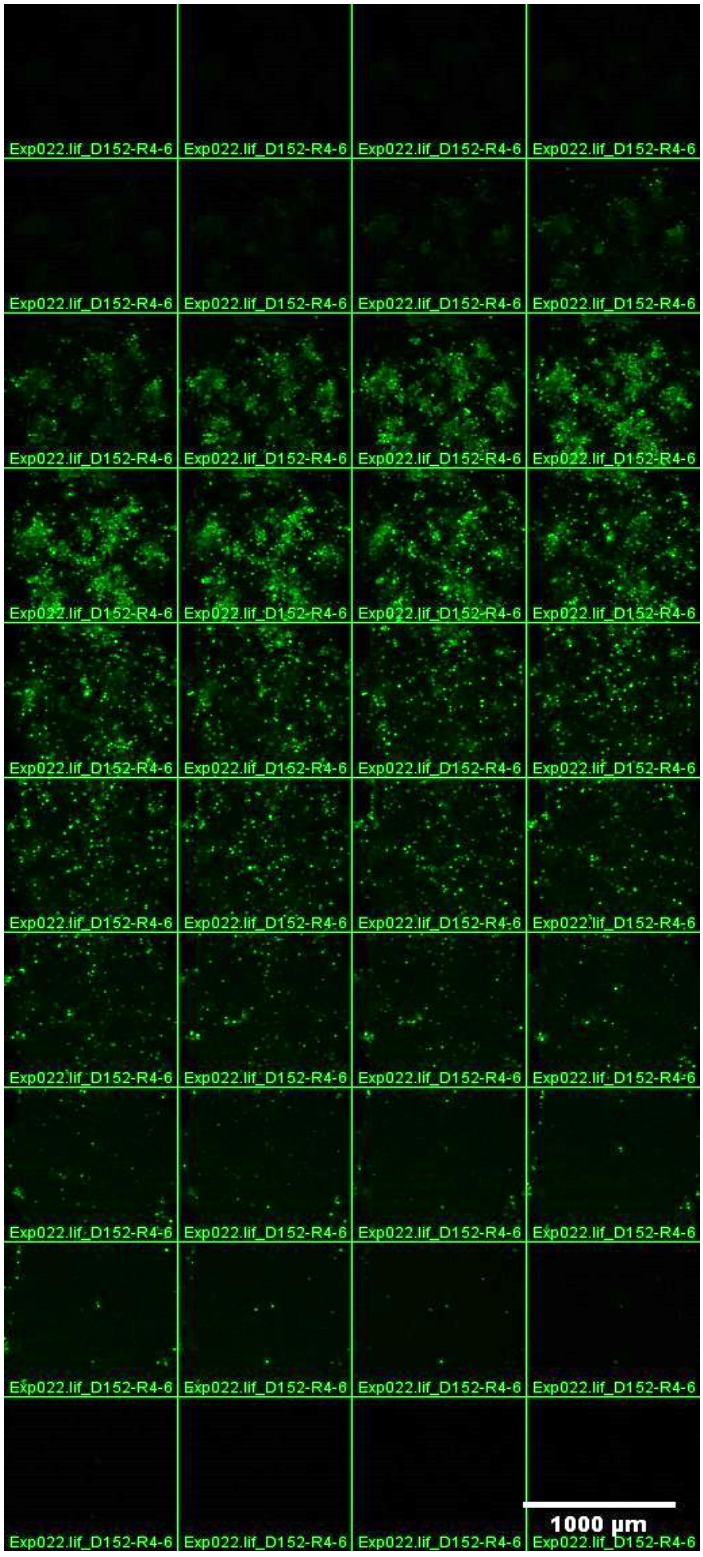

Figure 3.15. Individual z-stack images for MDA-MB-231 cells.

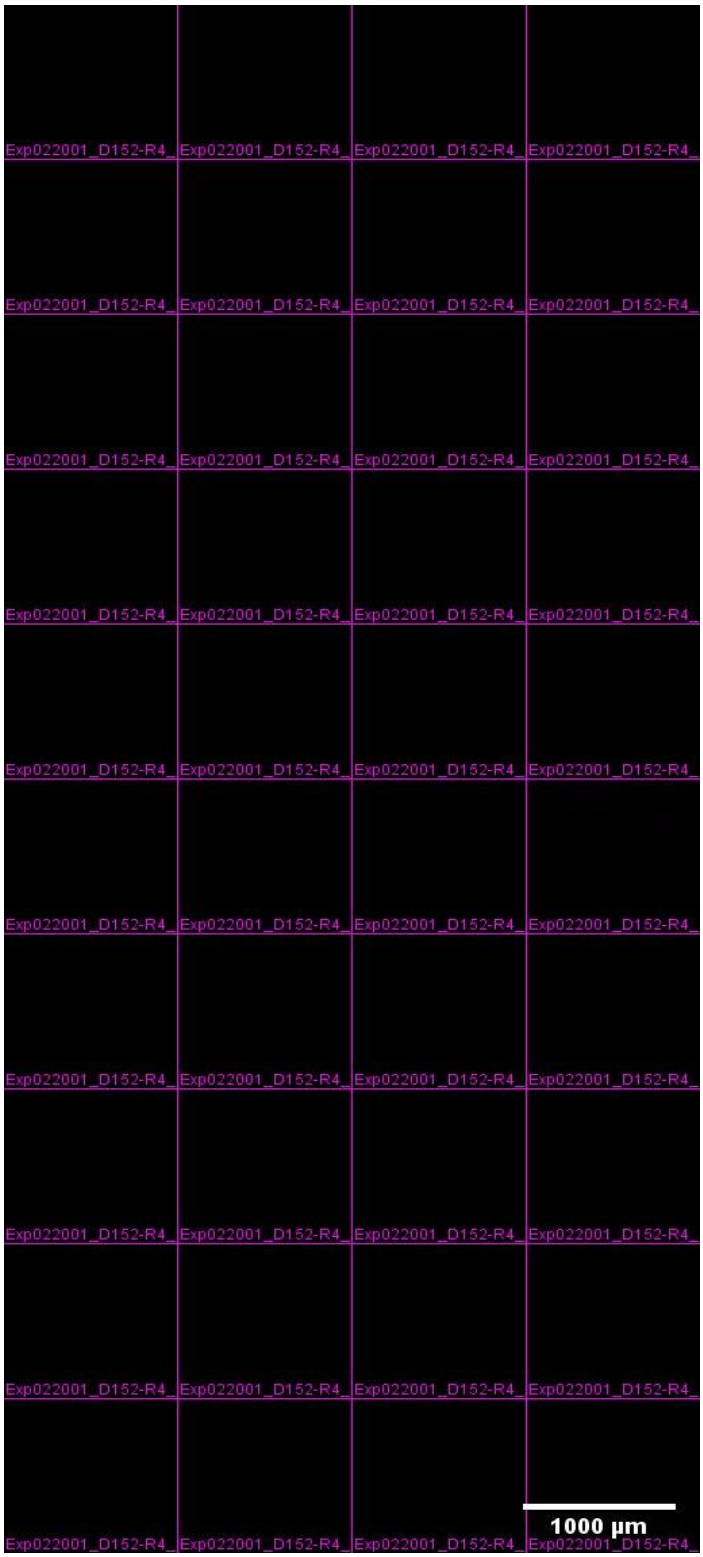

Figure 3.16. Individual z-stack images for dead cells which stain NucRed Dead 647 reagent (Not observed dead cell).

Figure 3.17-3.19 show a 3D confocal microscope image of MDA-MB-231 cells treated with doxorubicin and applied Dead647 reagent to detect dead cells.

Doxorubicin is a hydrophobic molecule and has no absorbance at PDMS side. Due to Dead647, an absorbance in PDMS was observed. Dead cells were stained with Dead647.

Doxorubicin channel, MDA-MB-231 cells channel, Dead647 channel were shown in Figure 3.20-3.22 respectively. Dead 647 signals were observed in doxorubicin-treated cells. Signal was observed in cell channel, drug channel and dead 647 channel. When Dead647 signals were taken into consideration, it was observed that not every cells receiving doxorubicin died. Reasons for this condition may be that some cells were resistant to doxorubicin or they are unable to enter nucleus of those cells for 48 hours.

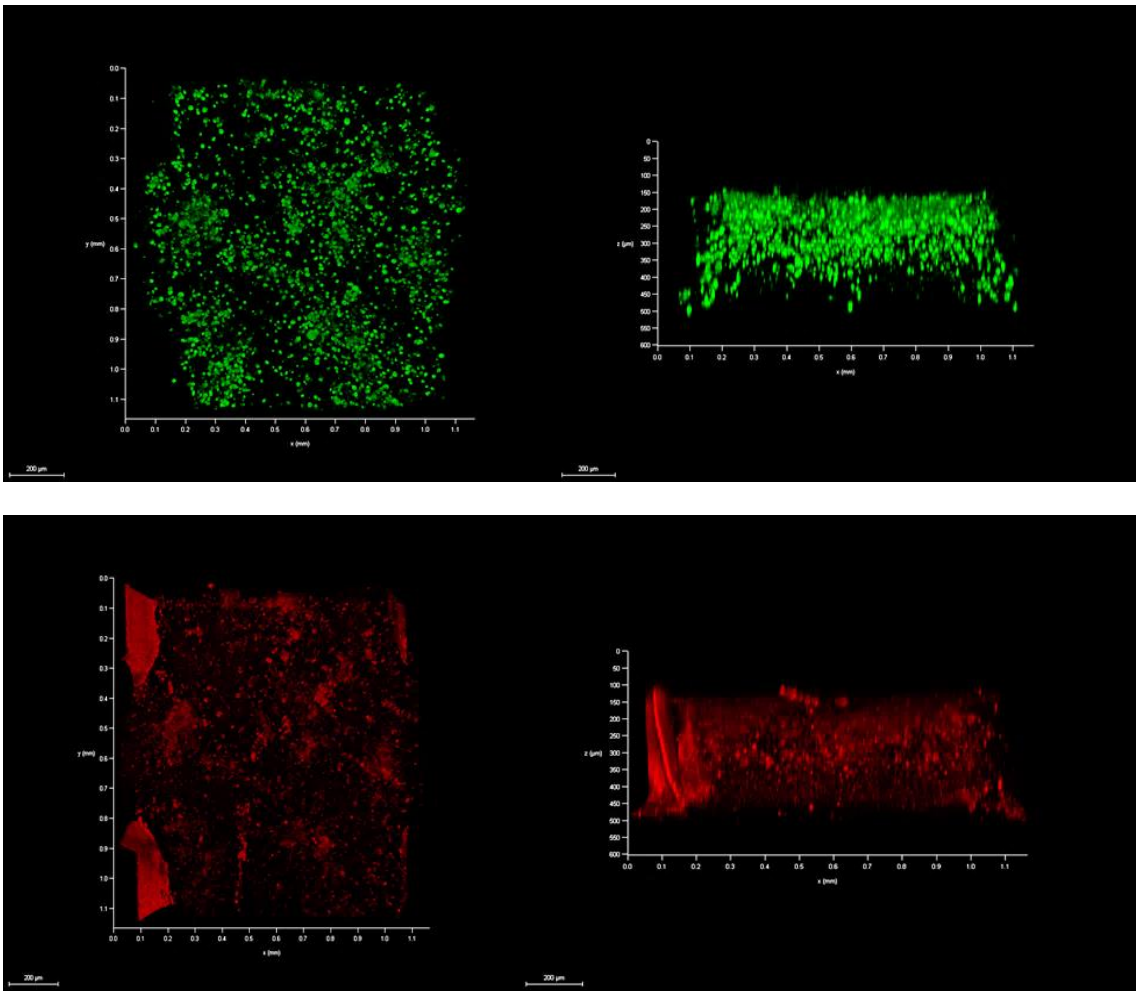

Figure 3.17. After 48 hours, NucRed Dead 647 dye (magenta) was used to measure cell viability.

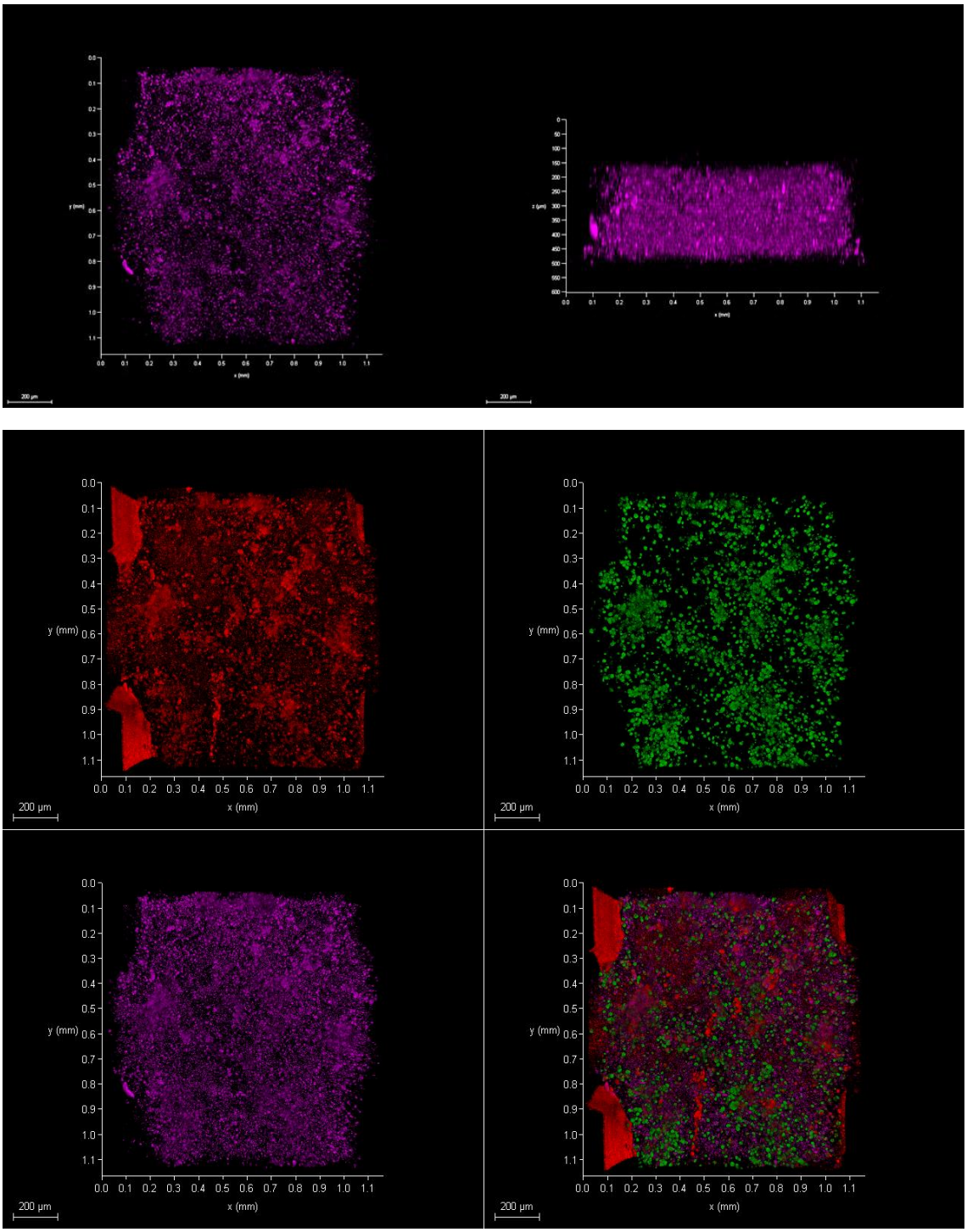

Figure 3.18. After 48 hours, NucRed Dead 647 dye (magenta) was used to measure cell viability.

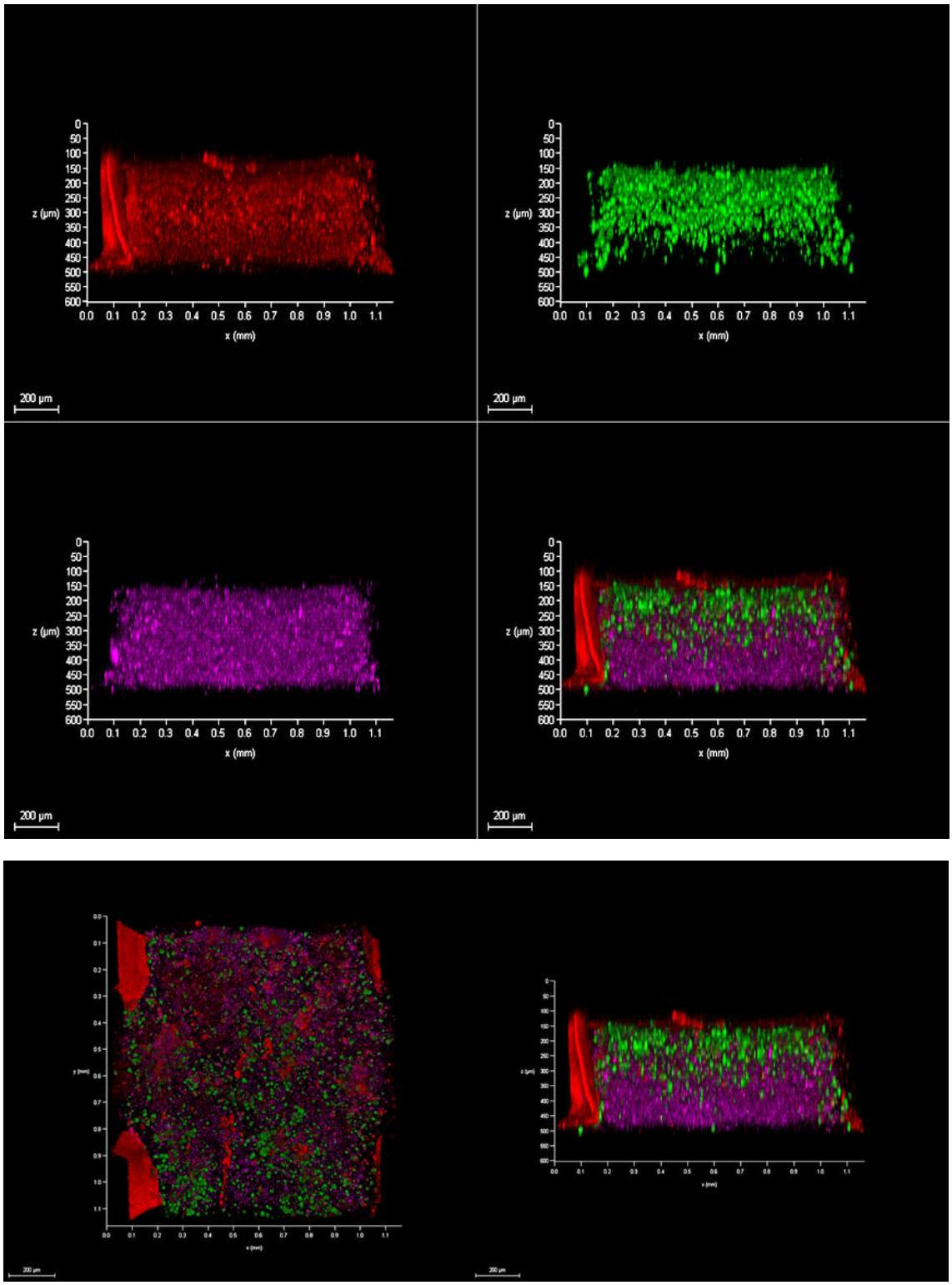

Figure 3.19. After 48 hours, NucRed Dead 647 dye (magenta) was used to measure cell viability.

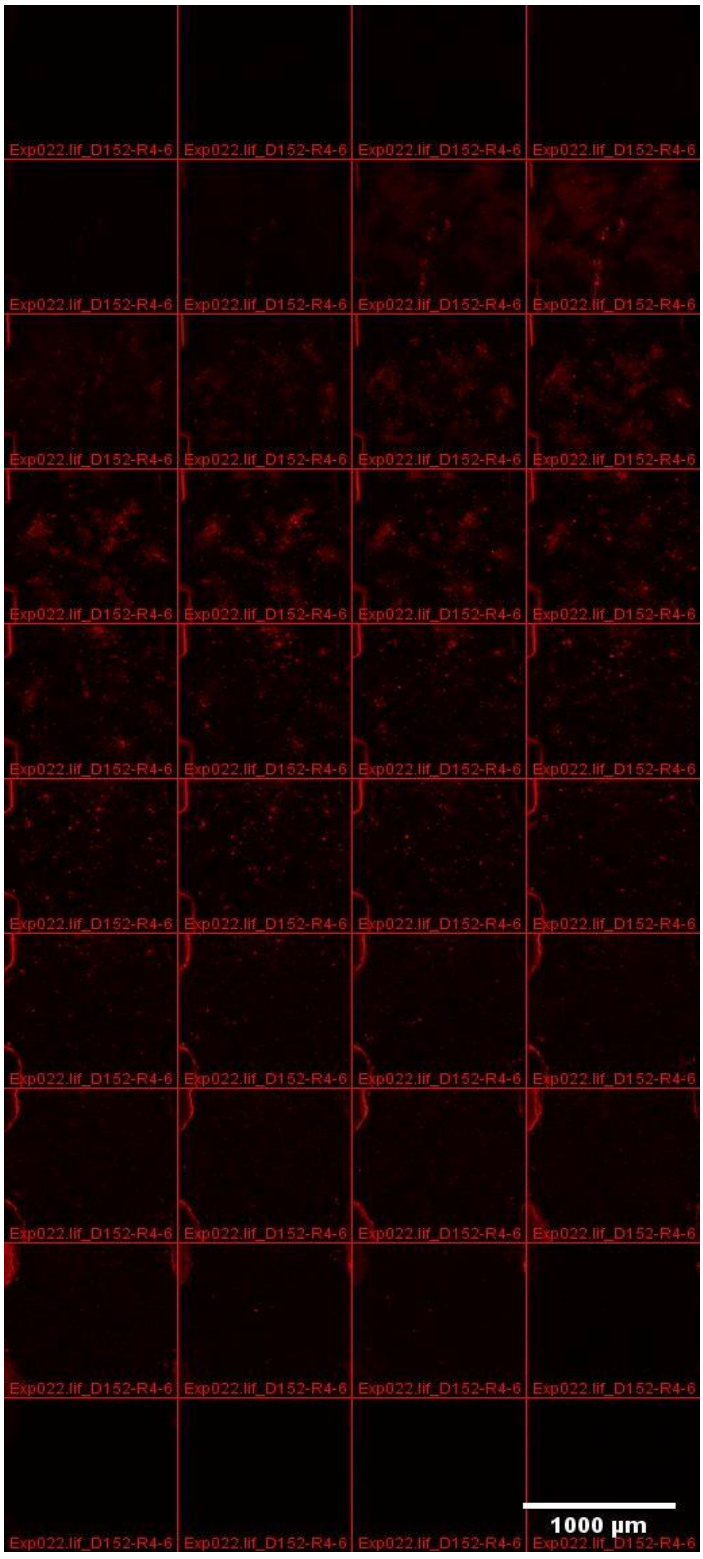

Figure 3.20. Individual z-stack images for cells which uptake doxorubicin.

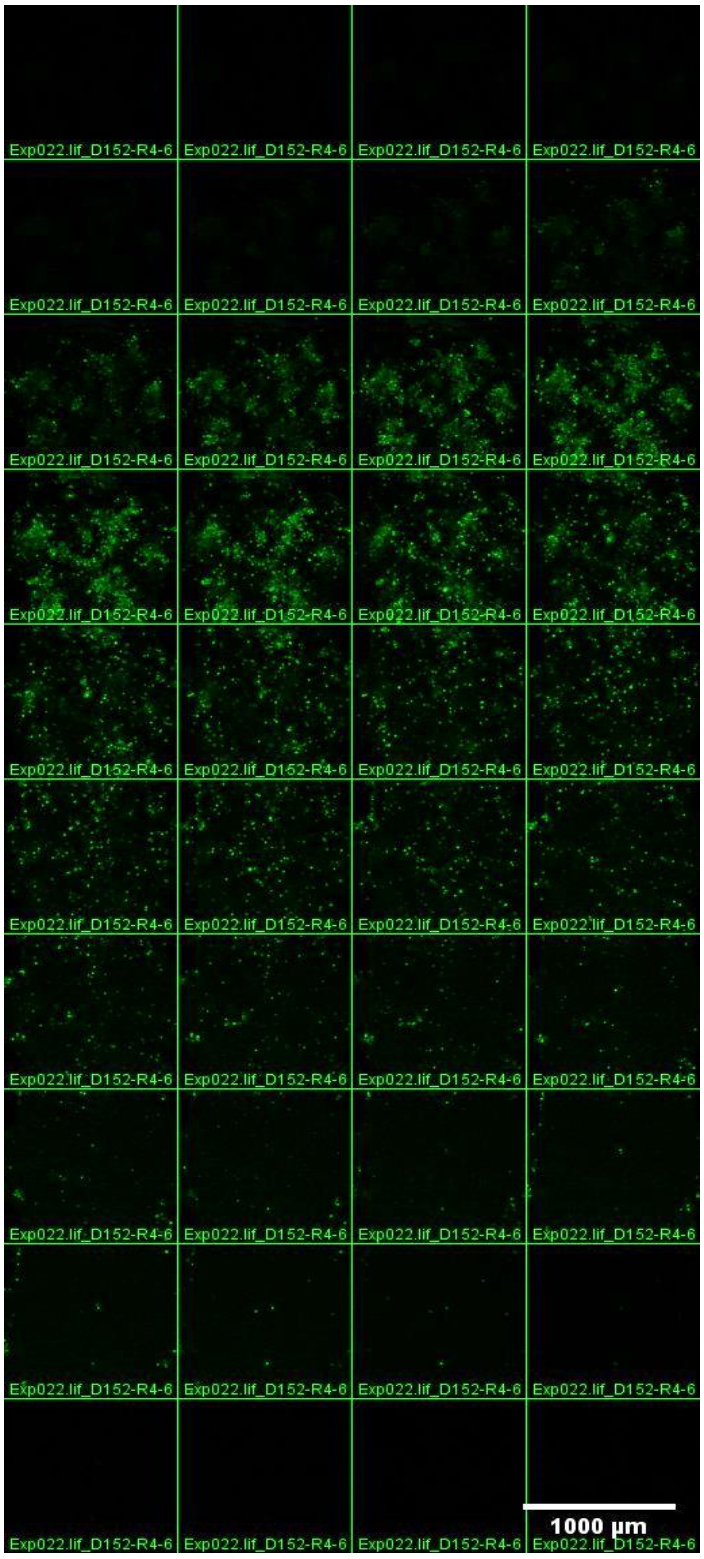

Figure 3.21. Individual z-stack images for MDA-MB-231 cells.

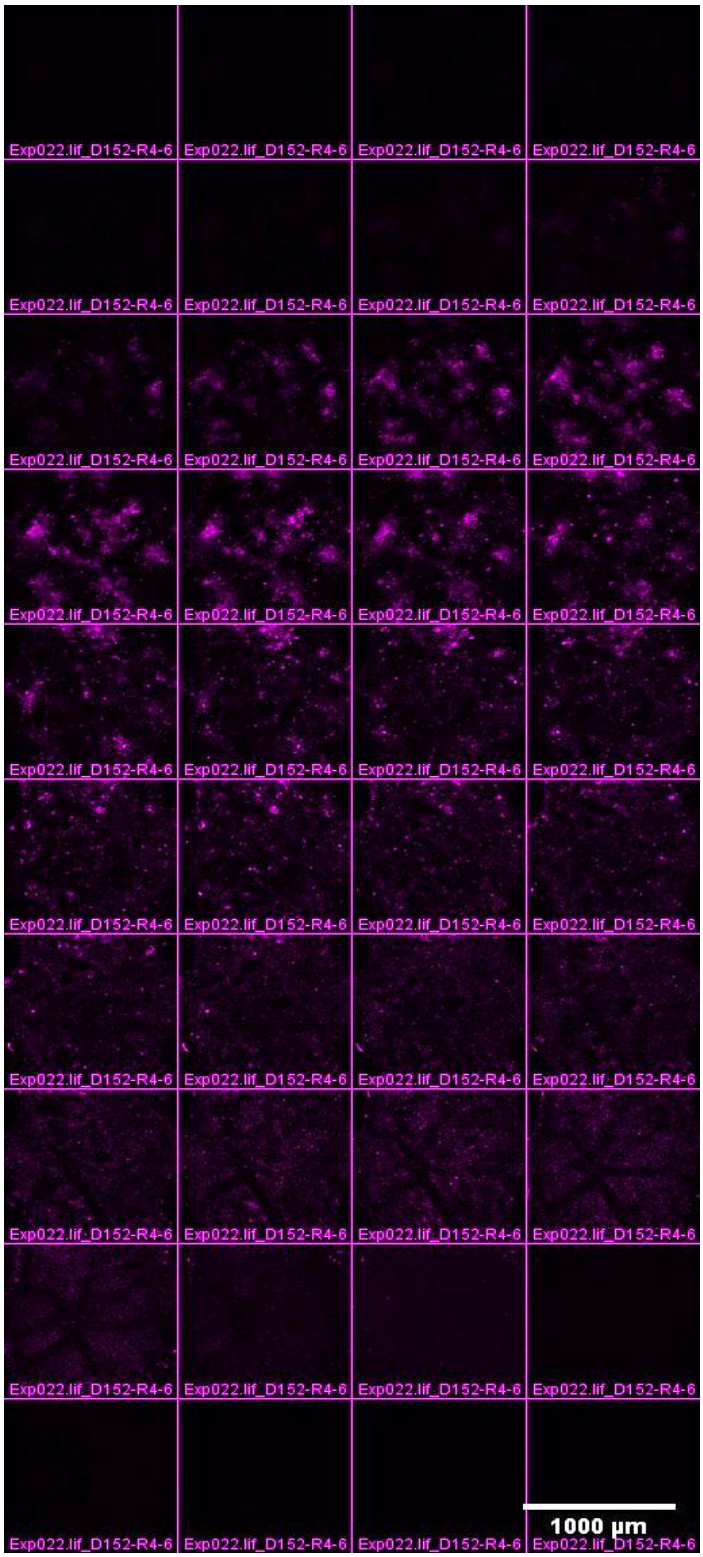

Figure 3.22. Individual z-stack images for dead cells which stain NucRed Dead 647 reagent.

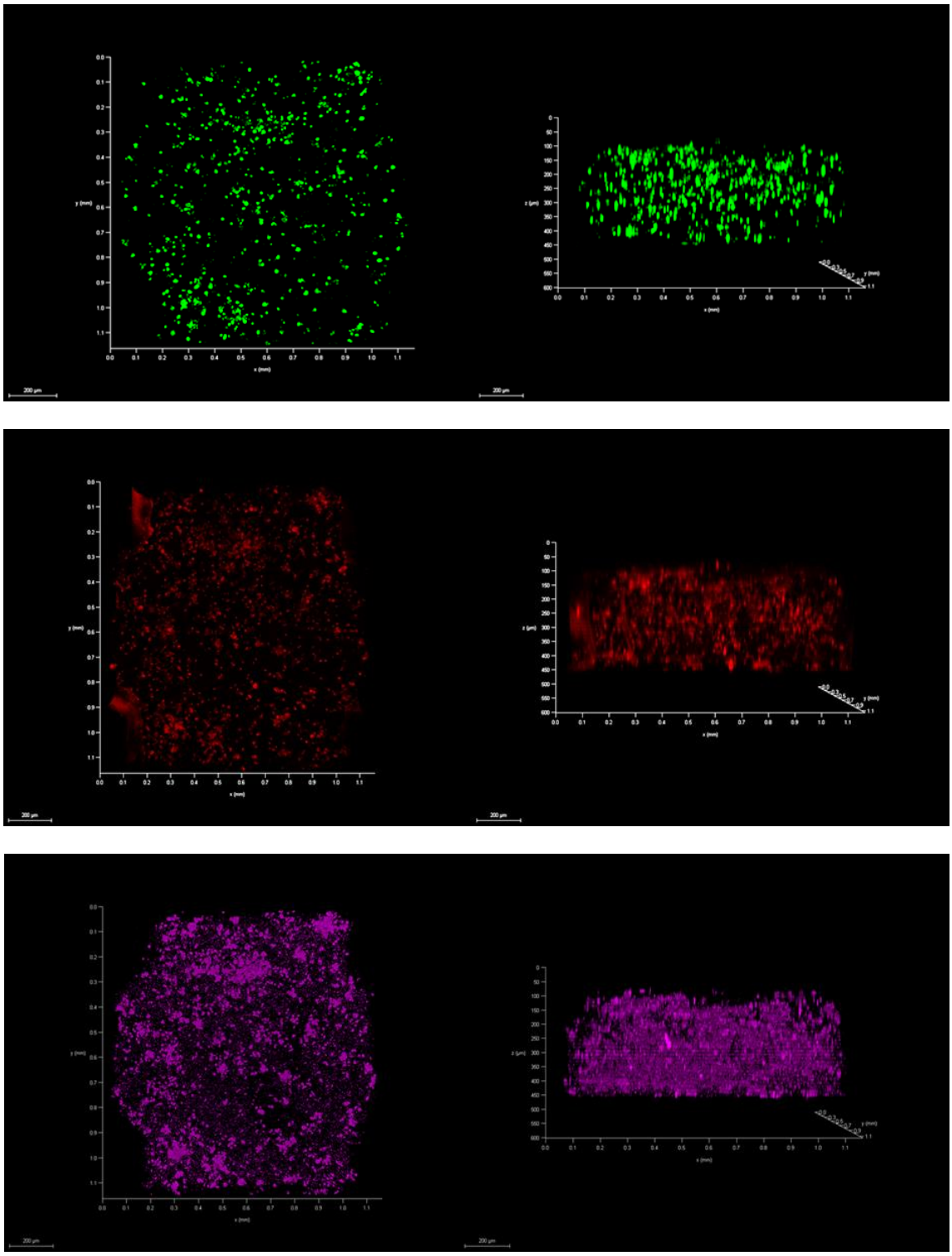

Figure 3.23. MDA-MB-231 cells (green) were treated with 10 uM Doxorubicin at 48 hours. Then NucRed Dead 647 reagent was applied to determine cell viability.

In figure 3.23., there was nat observed fluorescent color at the PDMS edges as in Figure 3.18-3.19.

Figure 3.24 shows MDA-MB-231 cells were stained green tracker and were in 3D environment. Cells had homogeneous distribution due to slides. All cells stained with green tracker. Amongst some cells, minor clusturing was observed. Not all cells were the same size. A narrow distribution was exhibited.

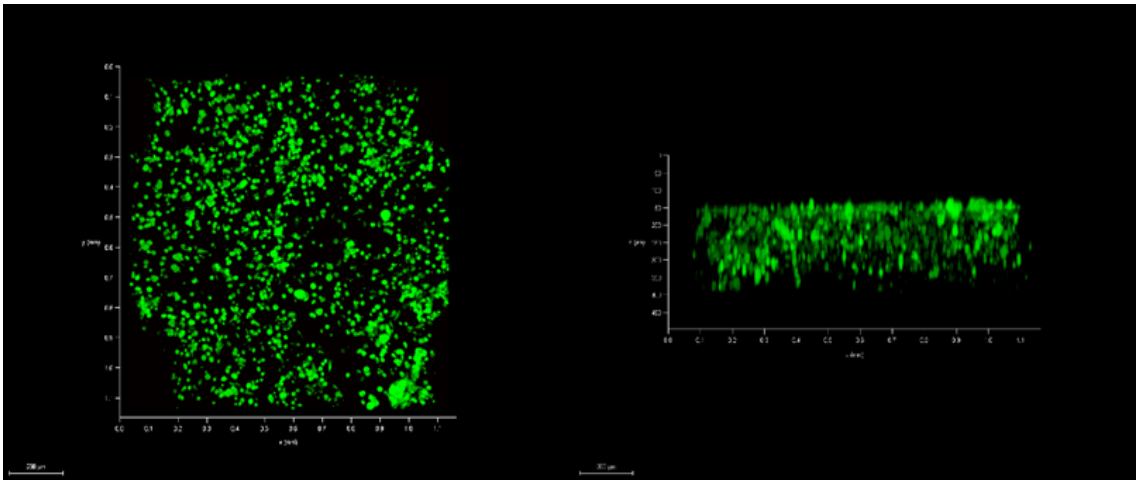

Figure 3.24. Mono-culture. MDA-MB-231 cells were stained with green tracker as a control group. MDA-MB-231 cells were mixed with matrigel at a 1:1 volume ratio.

Figure 3.25 shows a 3D confocal microscope image of MDA-MB-231 cells treated with klavuzon and applied Dead647 reagent to detect dead cells.

After cells were mixed with matrigel, they were loaded into the chip. Drug candidate klavuzon was applied to cells. After 48 hours, cell viability was observed with NucRed Dead 647 reagent. It was observed that some of the cells were concentrated at the PDMS side while waiting for the polymerization at the PDMS side. 3D structure was provided even though MDA-MB-231 cells were appear to be PDMS side. Intercellular clusters and voids have been observed.

Individual z-stack images for 3D images in Figure 3.26-3.27 were shown each section of 3D images detailed view in independent at z-position. Figure 3.2 shows individual z-stack images for MDA-MB-231cells. Figure 3.27 shows individual z-stack

images for dead cells which stain NucRed Dead 647 reagent. As expected, Dead 647 signals were observed in klavuzon-treated cells.

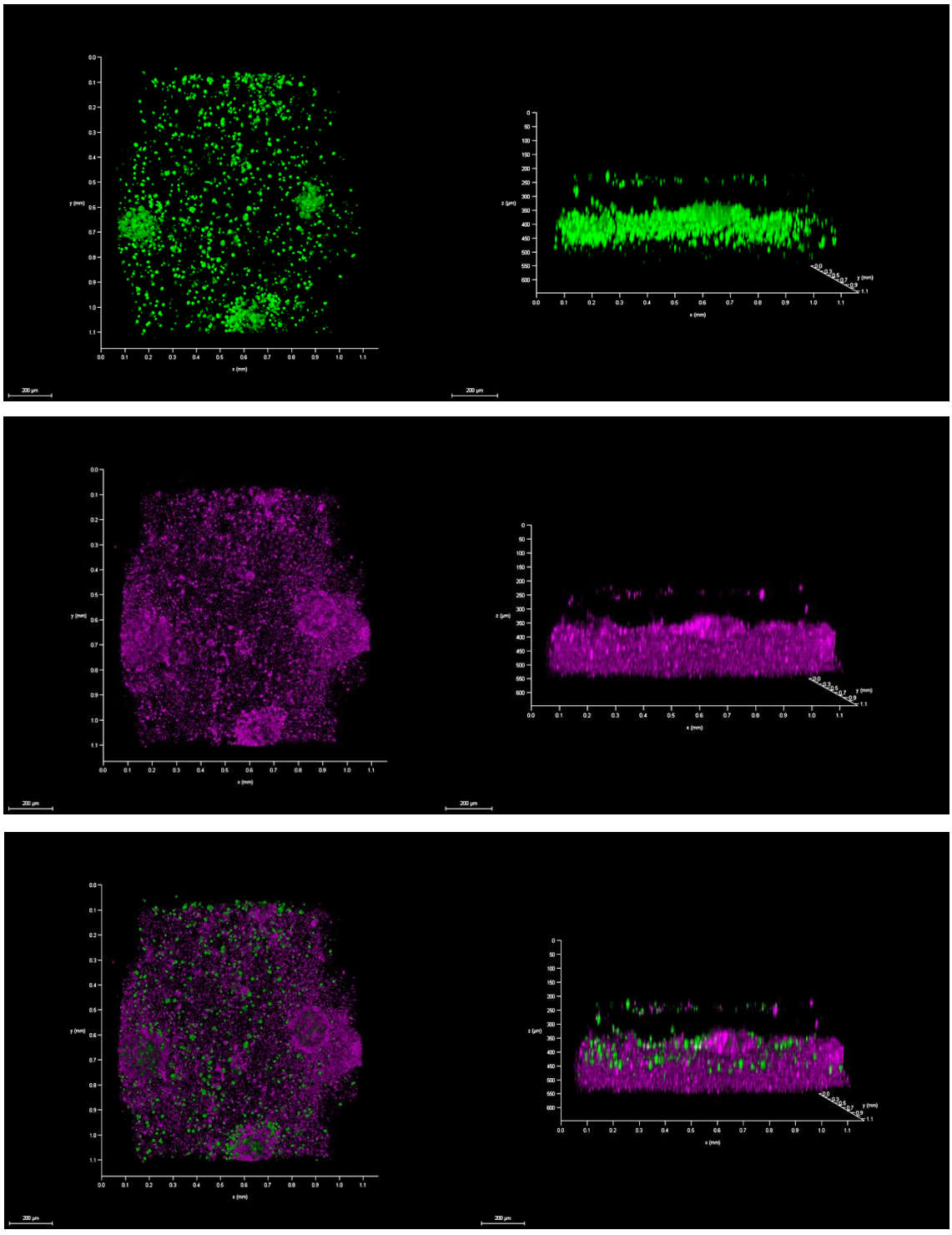

Figure 3.25. MDA-MB-231 cells were treated with 100 uM Klavuzon at 48 hours. After 48 hours, NucRed Dead 647 dye was used to measure cell viability.

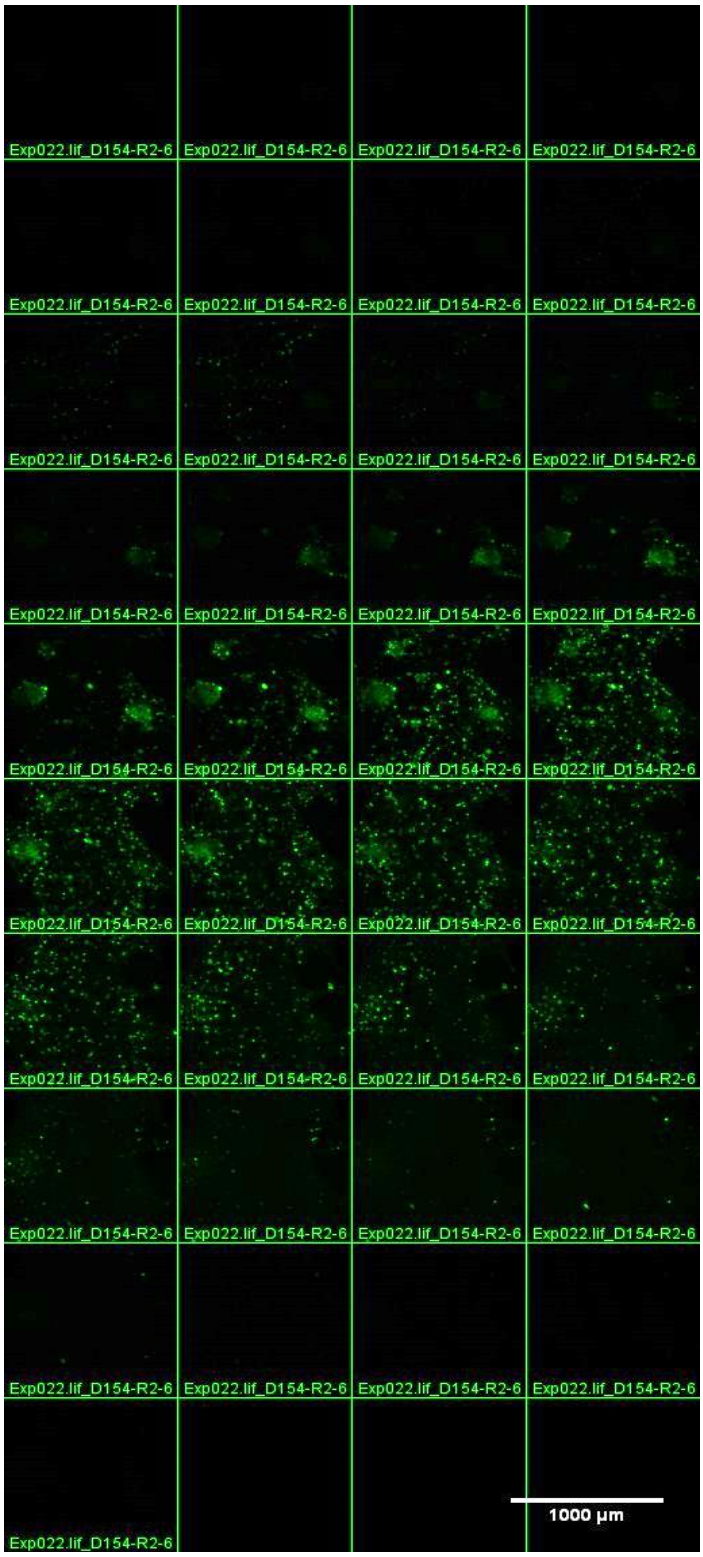

Figure 3.26. Individual z-stack images for MDA-MB-231cells.

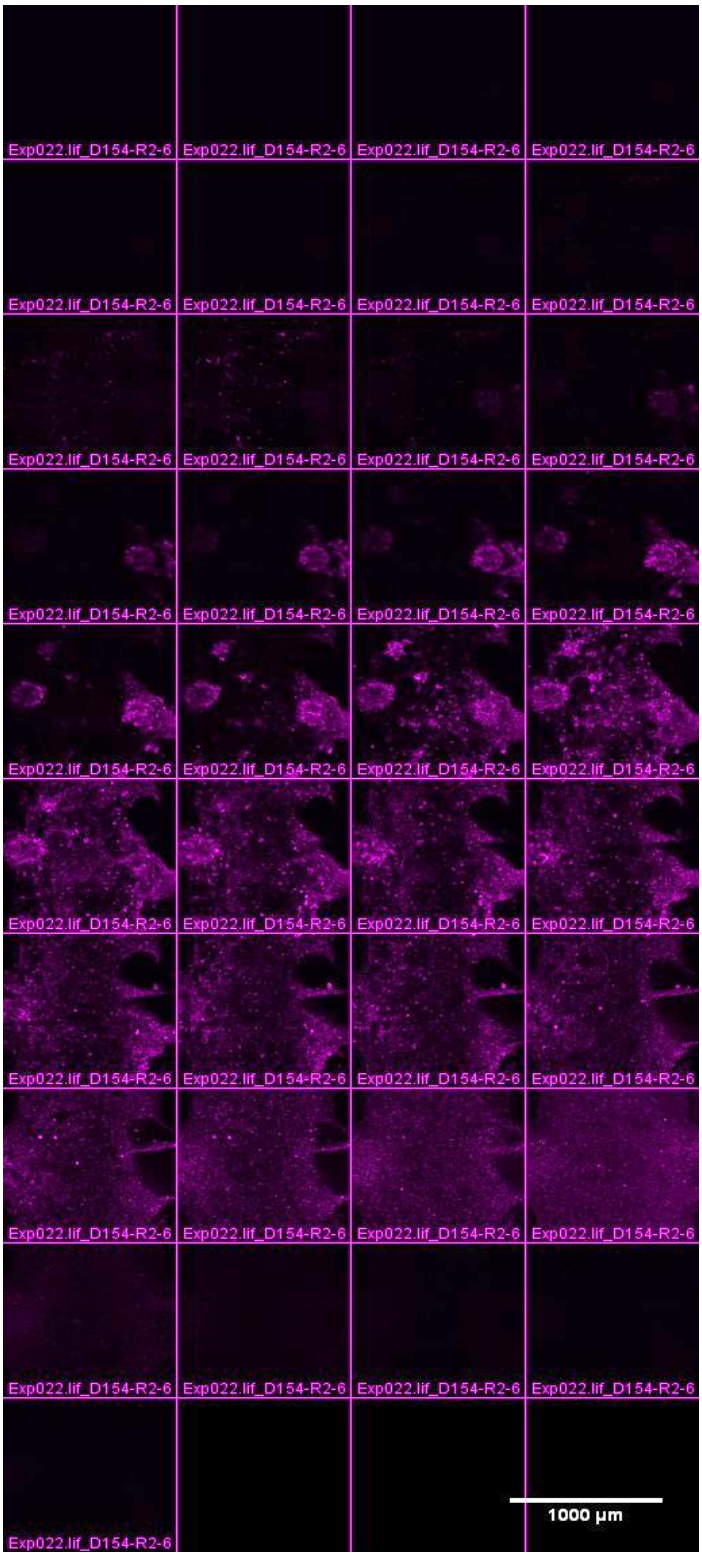

Figure 3.27. Individual z-stack images for dead cells which stain NucRed Dead 647 reagent.

MDA-M-231 cells were stained with green tracker and were in 3D environment. MCF-10A cells were stained with blue tracker. RAW 264.7 cells were not stained. Dead 647 signal was not observed in the untreated control group cells. Cells showed a homogenous distribution, but clusters were present amongst themselves.

As expected, no signal was observed in Dead647 channel for control group cells. Cells channels and the distribution of cells between stacks were shown in Figure 3.31-3.32.

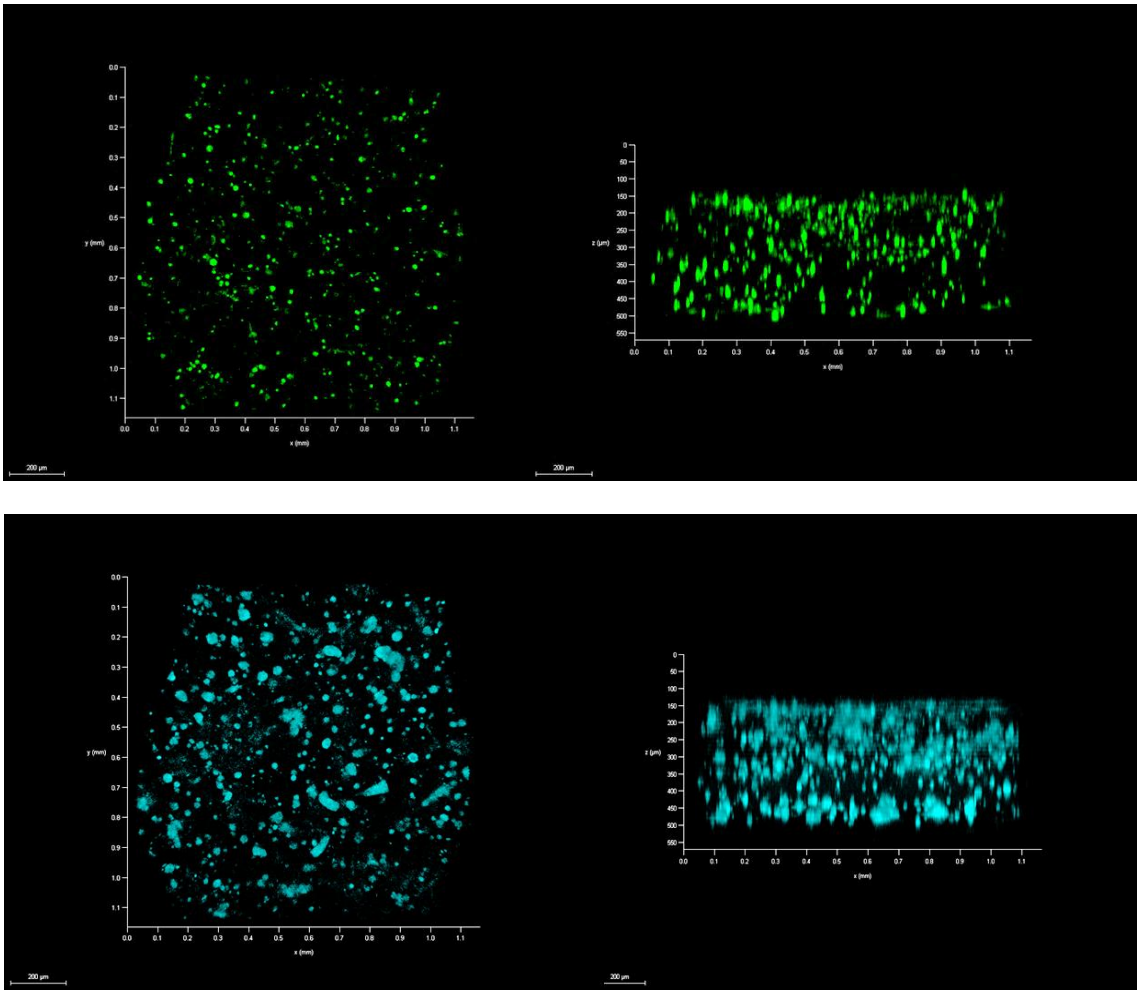

Figure 3.28. Tri-culture. MDA-MB-231 cells were stained with green tracker. MCF-10A cells were stained with blue tracker. RAW 264.7 cells were not stained.

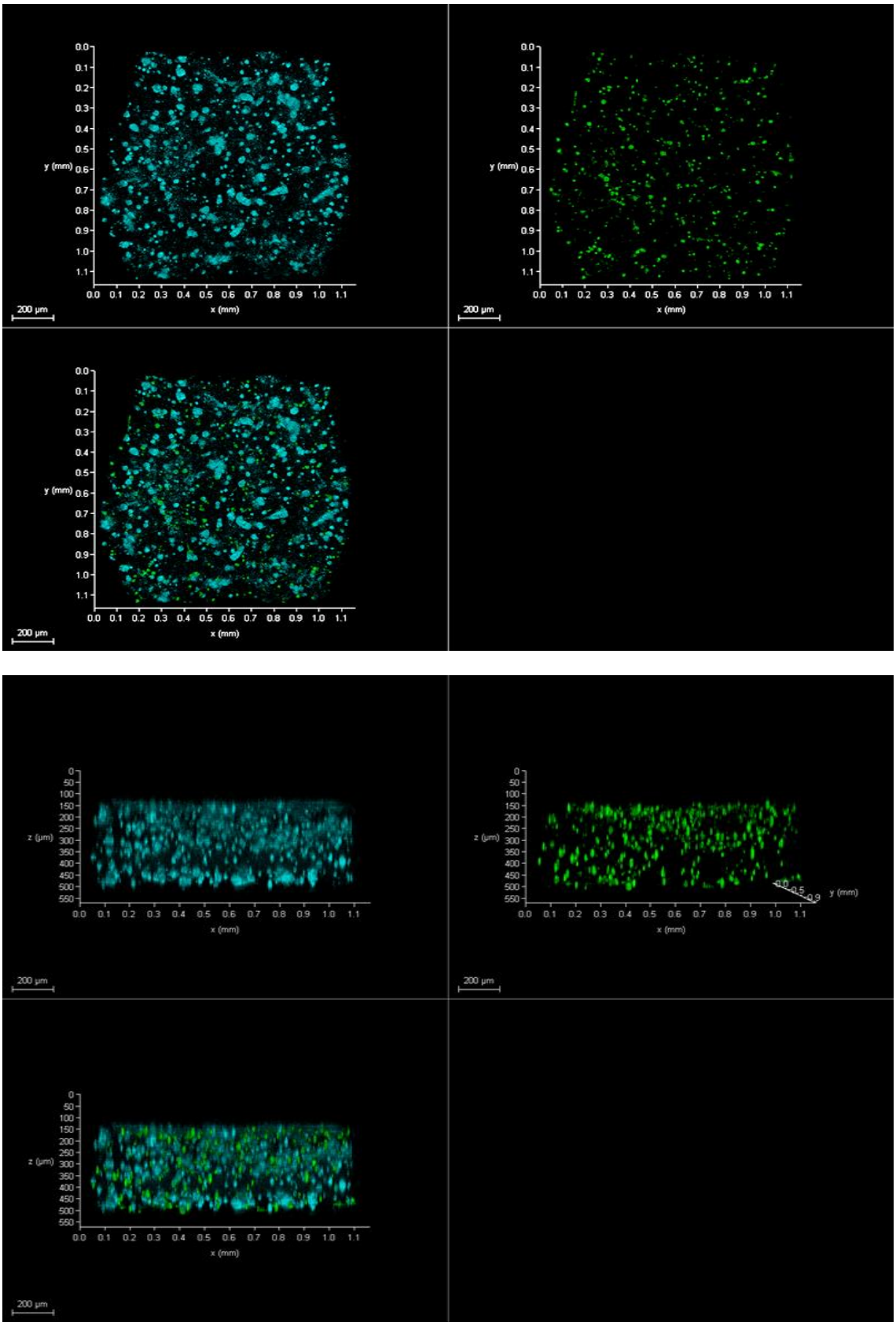

Figure 3.29. Tri-culture. MDA-MB-231 cells were stained with green tracker. MCF-10A cells were stained with blue tracker. RAW 264.7 cells were not stained.

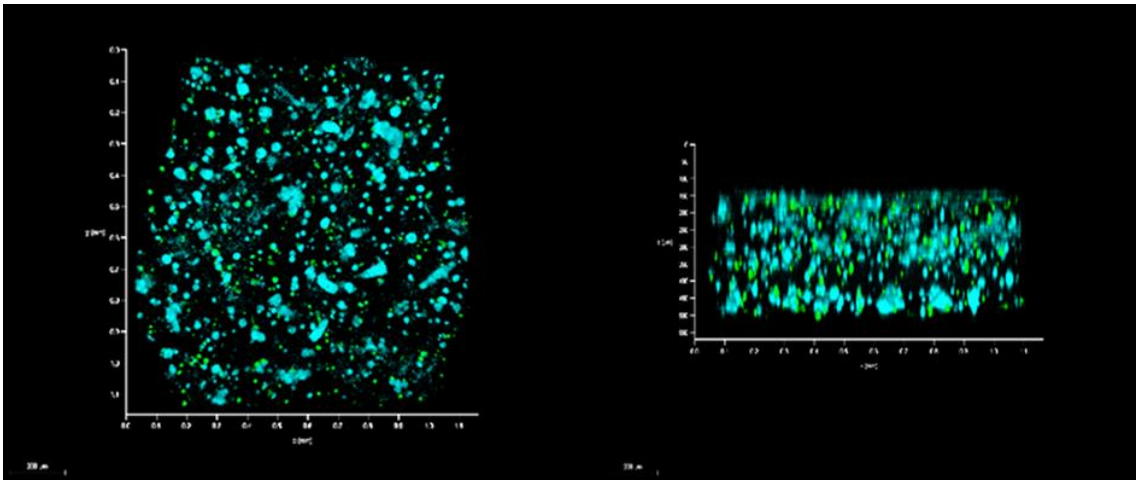

Figure 3.30. Tri-culture. MDA-MB-231 cells were stained with green tracker. MCF-10A cells were stained with blue tracker. RAW 264.7 cells were not stained. MDA-MB-231 (green), MCF-10A (cyan) and RAW 264.7 cells were mixed 1:1 volume ratio. Then cells were mixed with matrigel 1:1 volume ratio.

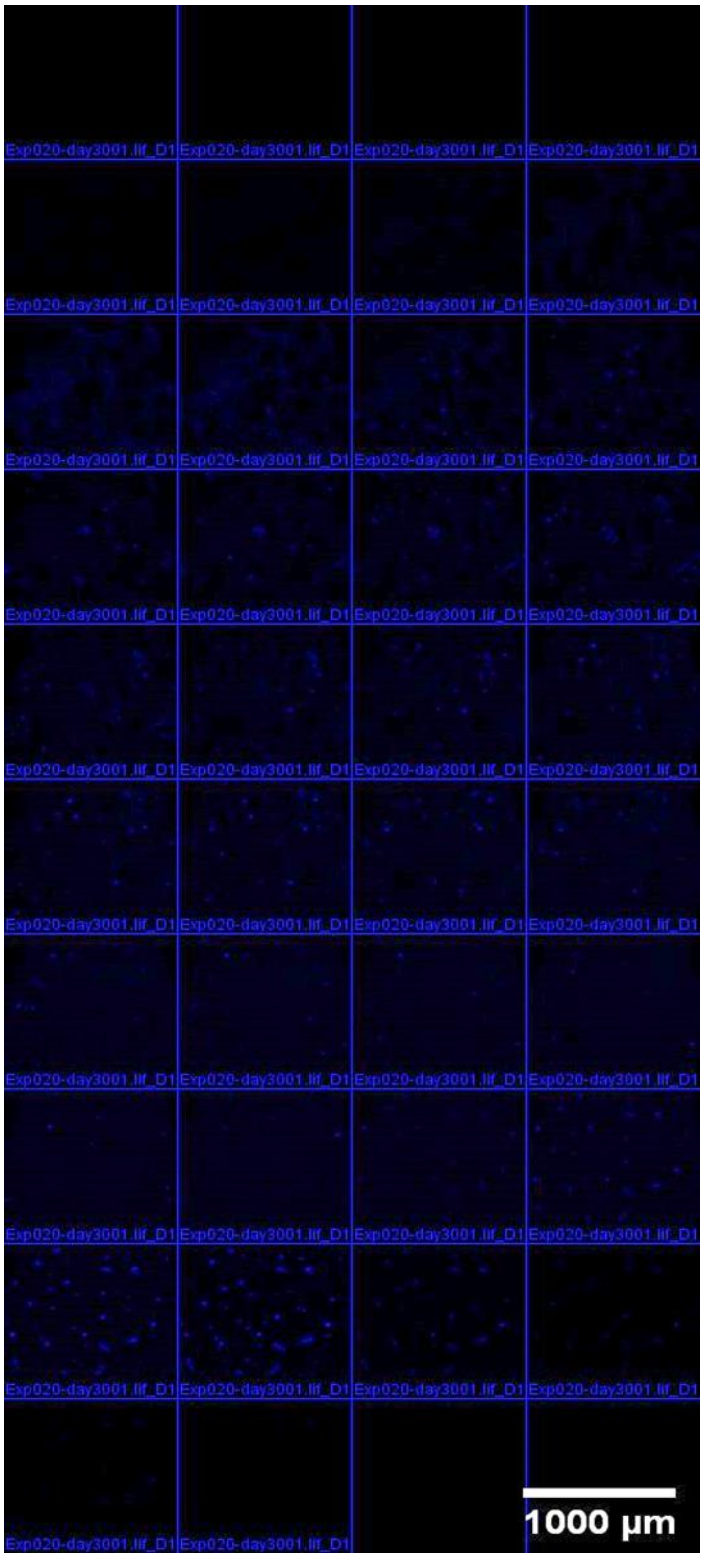

Figure 3.31. Individual z-stack images for MCF-10A cells.

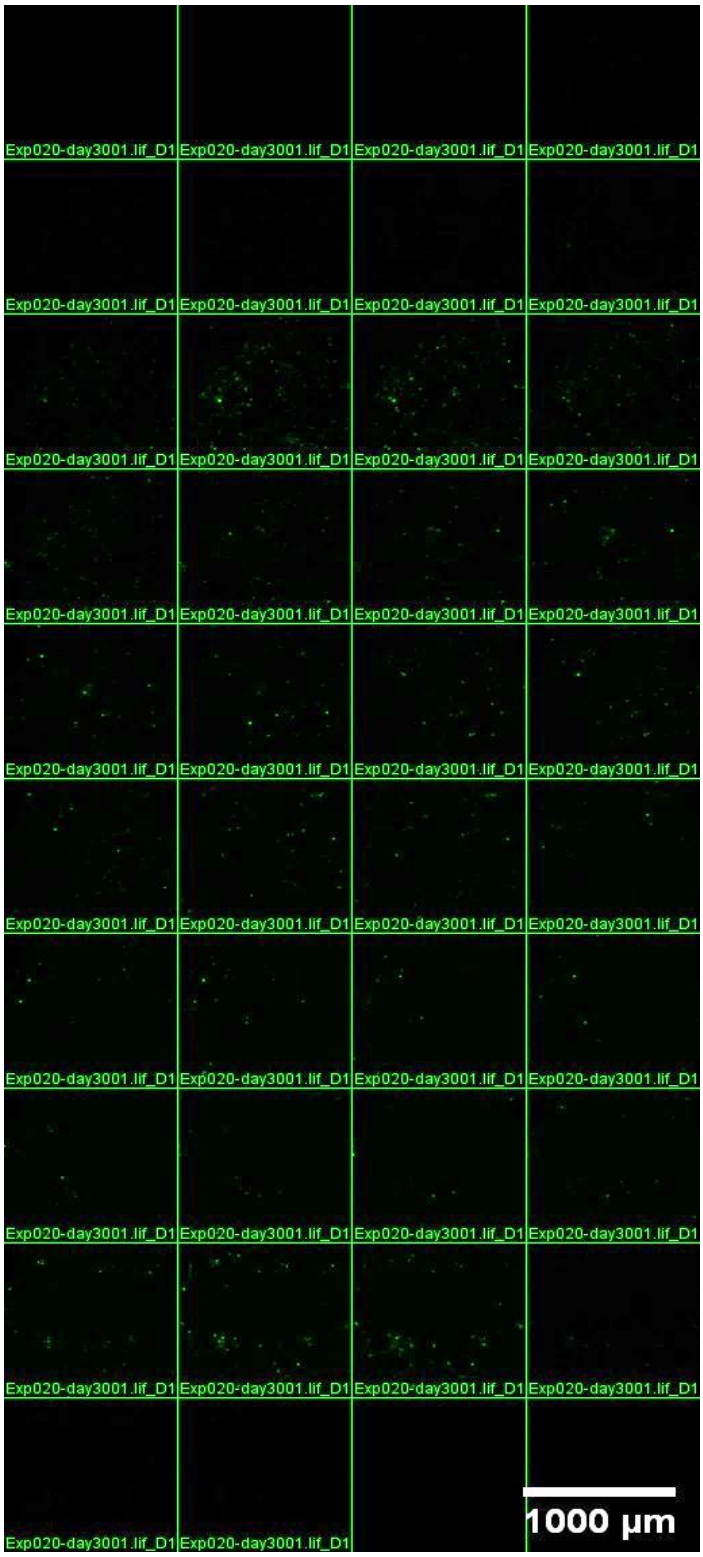

Figure 3.32. Individual z-stack images for MDA-MB-231 cells.

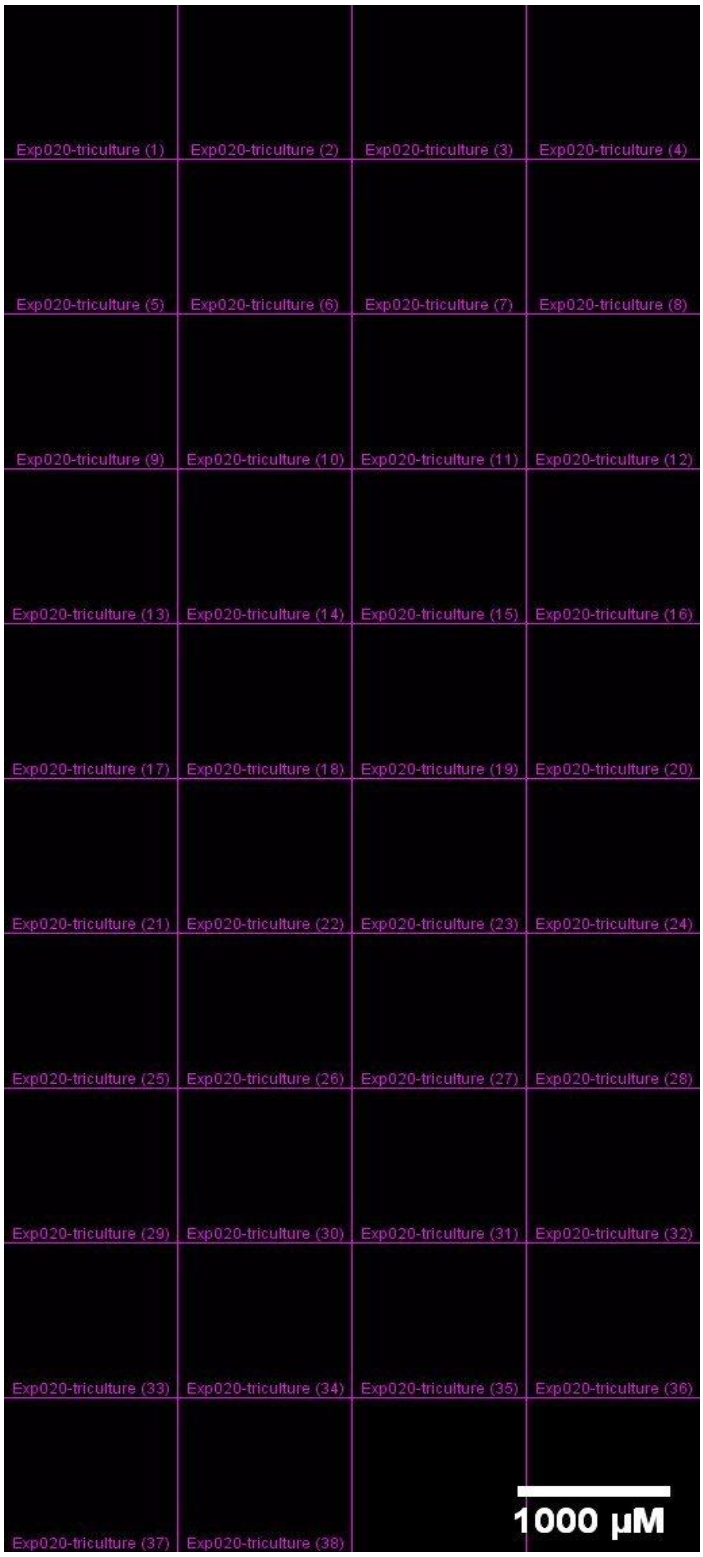

Figure 3.33. Individual z-stack images for dead cells which stain with NucRed Dead 647 reagent (Not observed dead cell).

Figure 3.34 shows MDA-MB-231 cells were stained green tracker, MCF-10A cells were stained with blue tracker and RAW 264.7 cells were not stained were in 3D environment. DMSO was applied to cells for 48 hours. Dead 647 signal was not observed in the DMSO-treated internal control group cells.

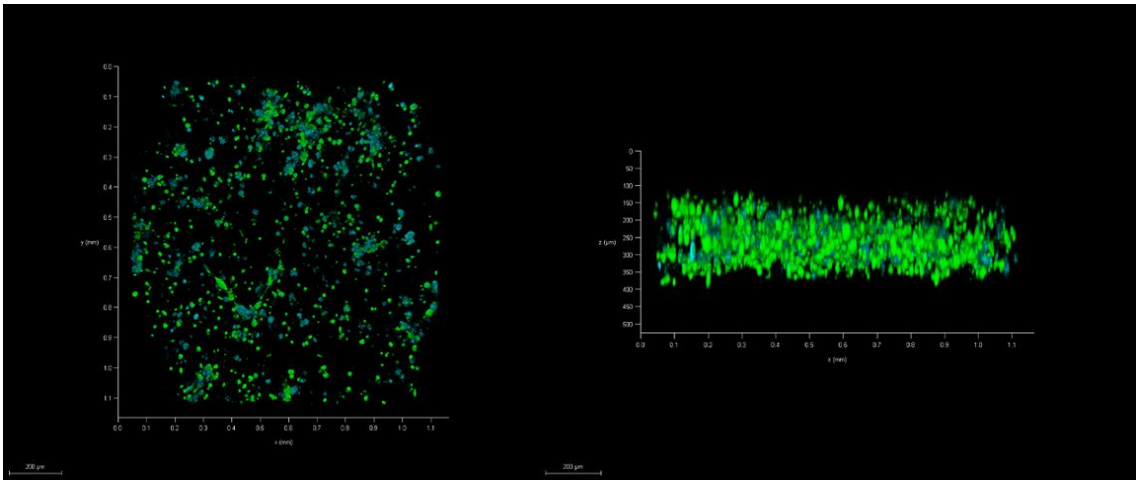

Figure 3.34. Tri-culture was treated with 100 uM DMSO at 48 hours.

Figure 3.35-3.36 show a 3D confocal microscope image of tri-culture treated with doxorubicin. MDA-M-231 cells were stained with green tracker and MCF-10A cells were stained with blue tracker. RAW 264.7 cells were not stained. Cells were in 3D environment. Cells were seen to accumulate on the one side, but they generally were distributed homogenously. Amongst some cells, minor clusturing was observed. Not all cells were the same size. MDA-MB-231 and MCF-10A cells were received doxorubicin.

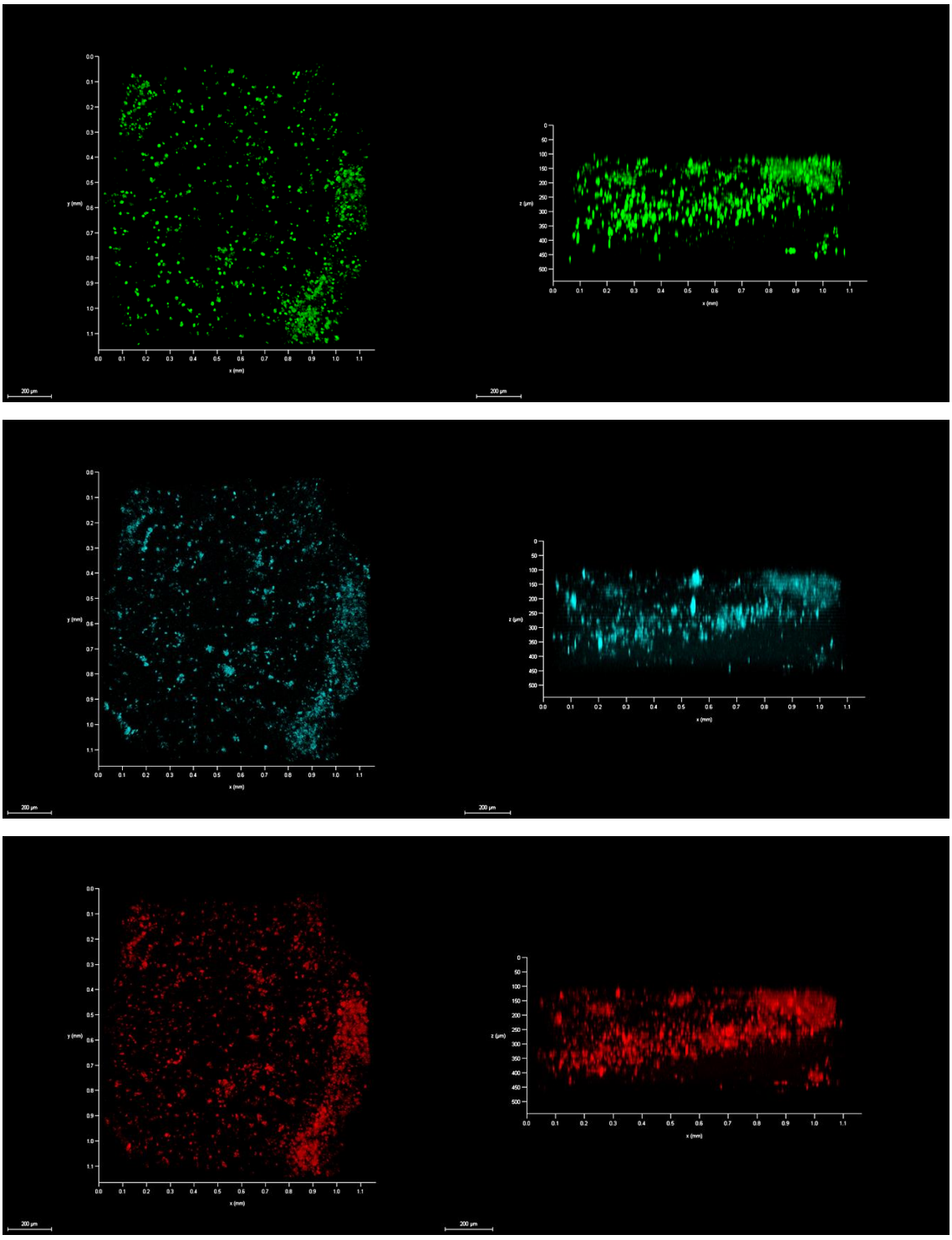

Figure 3.35. Tri-culture was treated with 10 µM Doxorubicin at 48 hours.

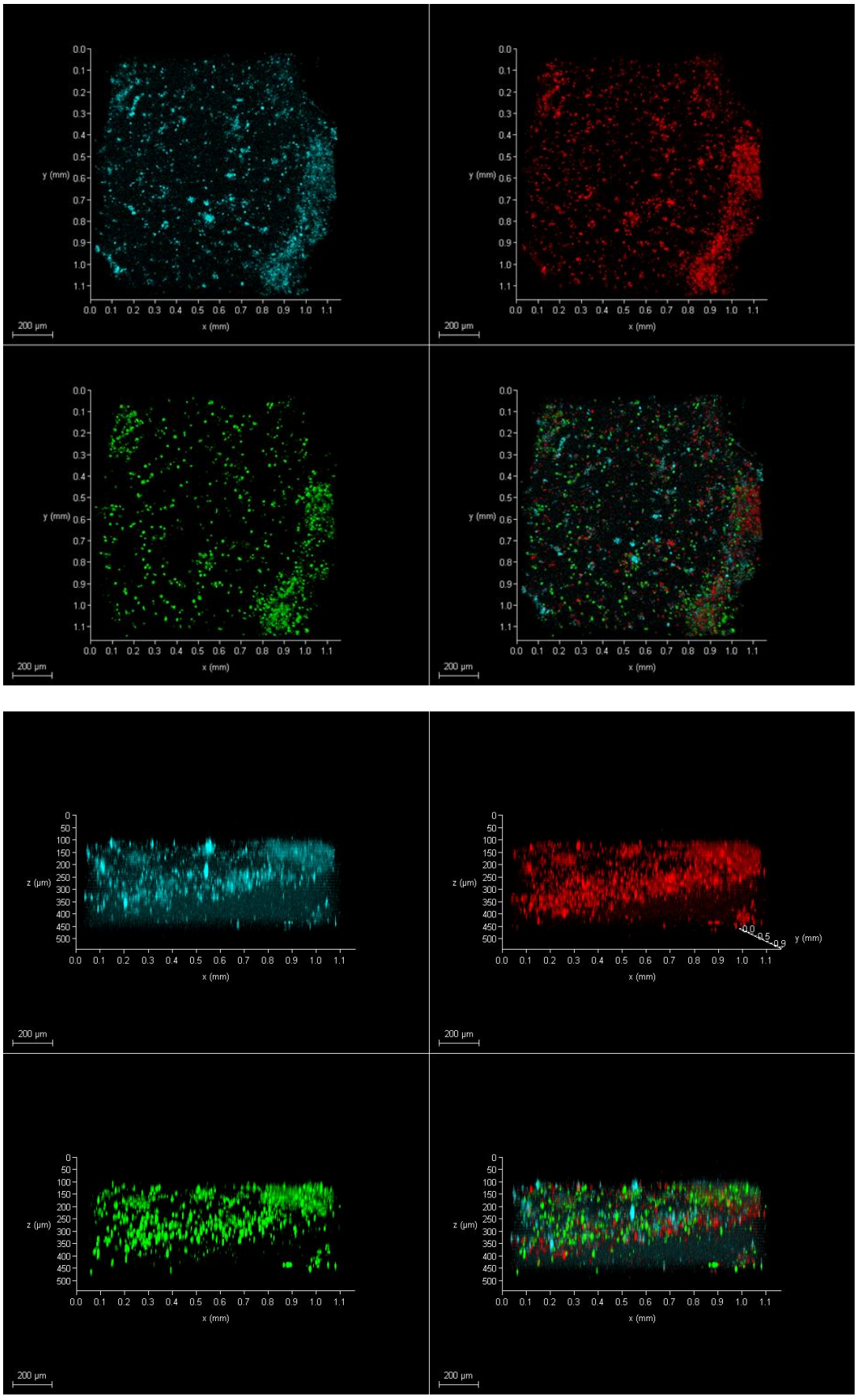

Figure 3.36. Tri-culture was treated with 10 uM Doxorubicin at 48 hours.

Dead 647 reagent was applied to cells which treated with doxorubicin for 48 hours in order to detect dead cells. All dead cells were stained with Dead 647 dye. Stack images show each section of 3D images detailed view. Dead 647 signals were observed in doxorubicin-treated cells in tri-culture.

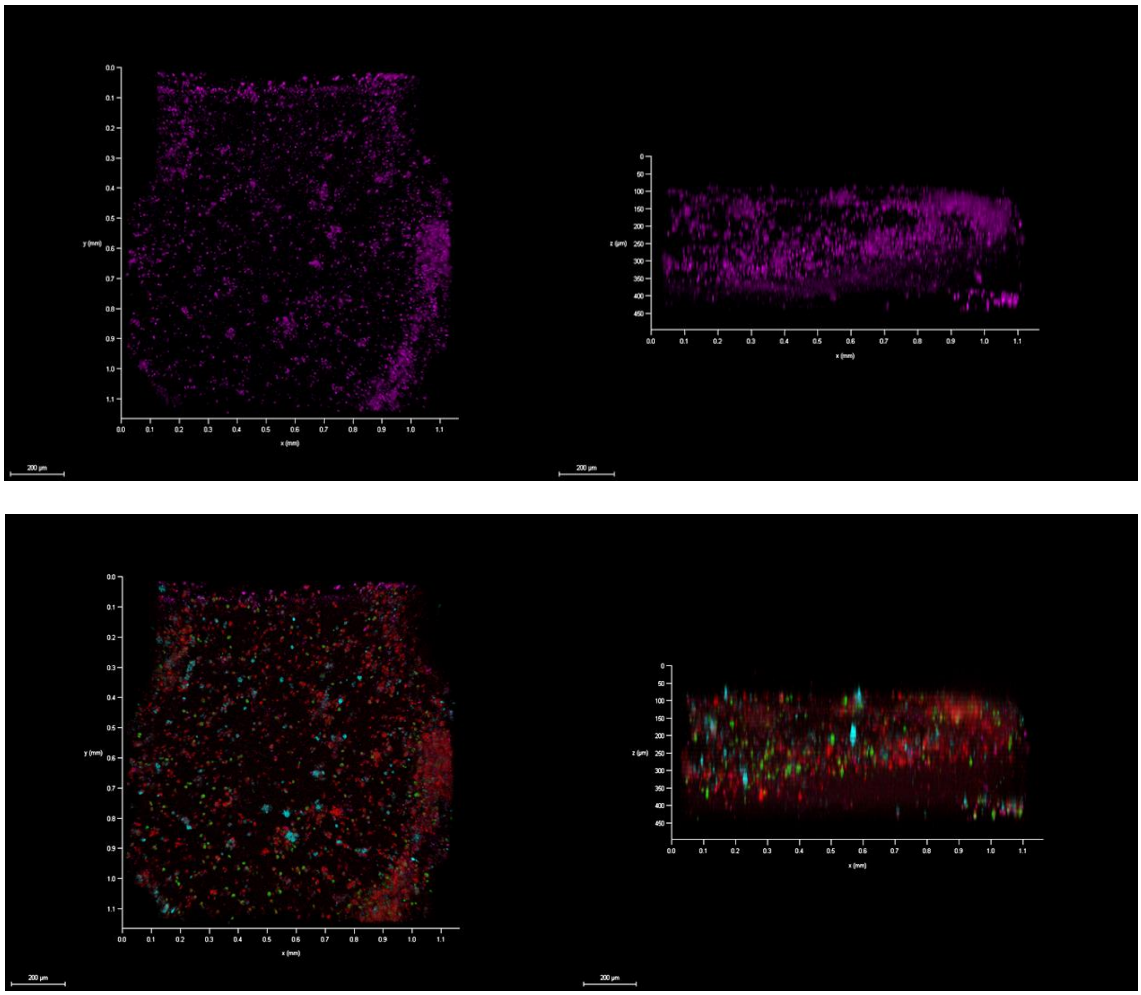

Figure 3.37. After 48 hours, NucRed Dead 647 dye was used to measure cell viability.

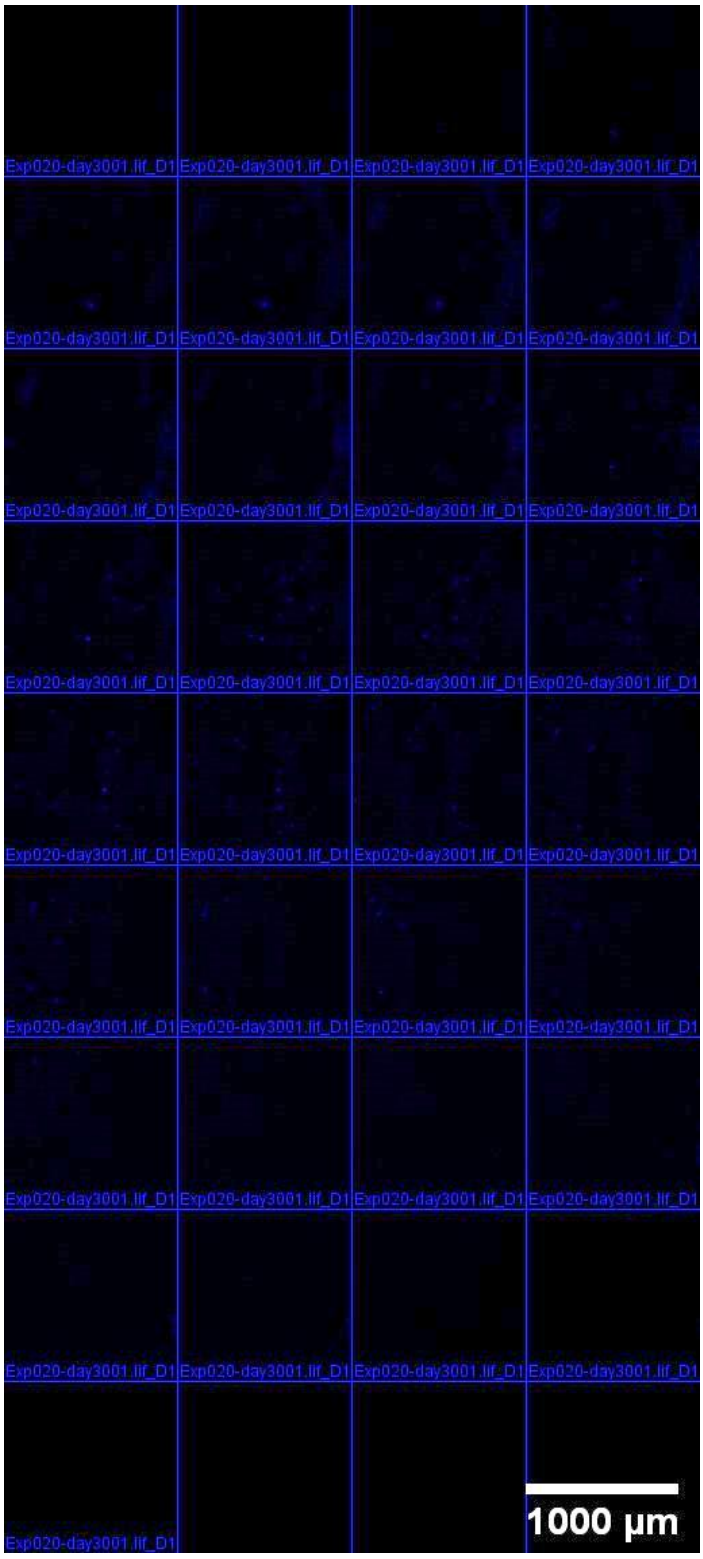

Figure 3.38. Individual z-stack images for MCF-10A cells.

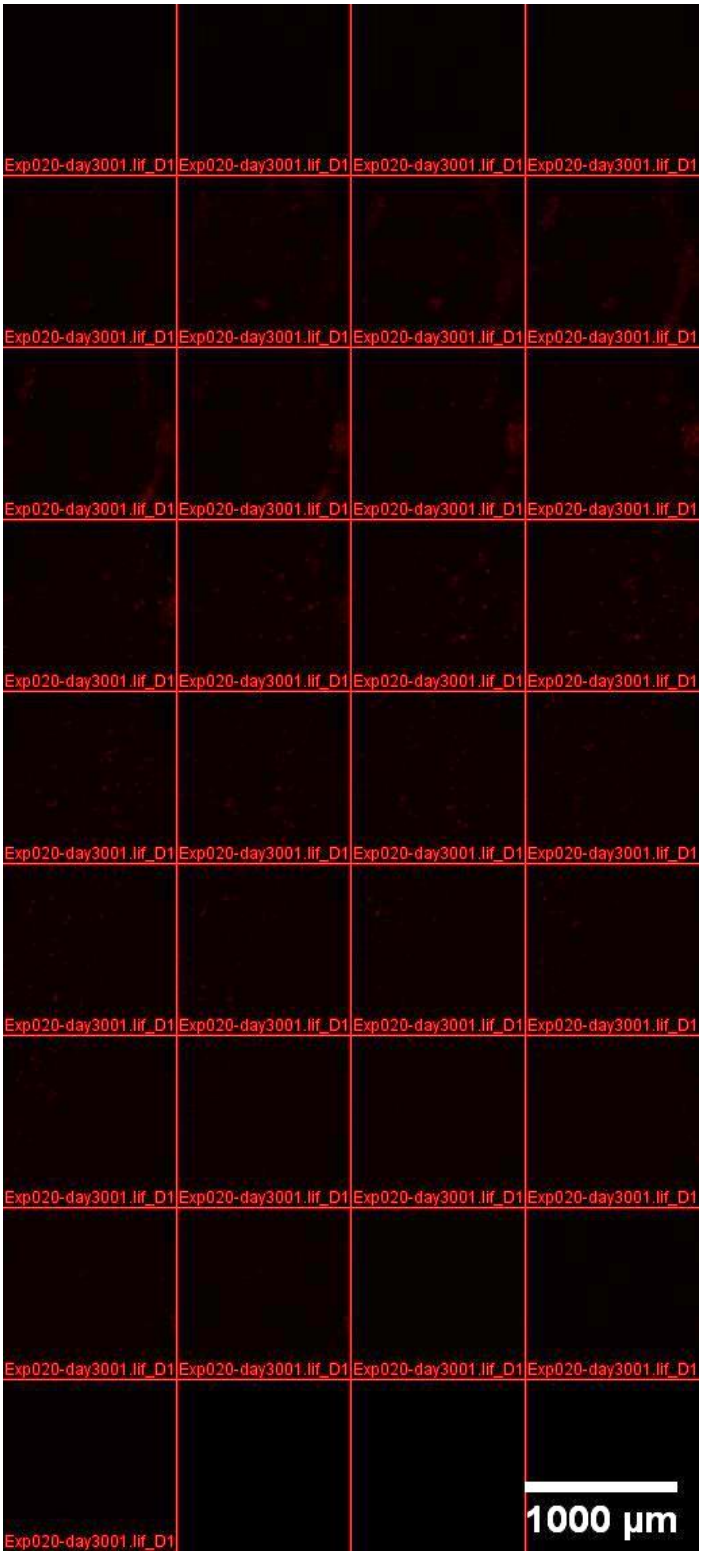

Figure 3.39. Individual z-stack images for cells which uptake doxorubicin.

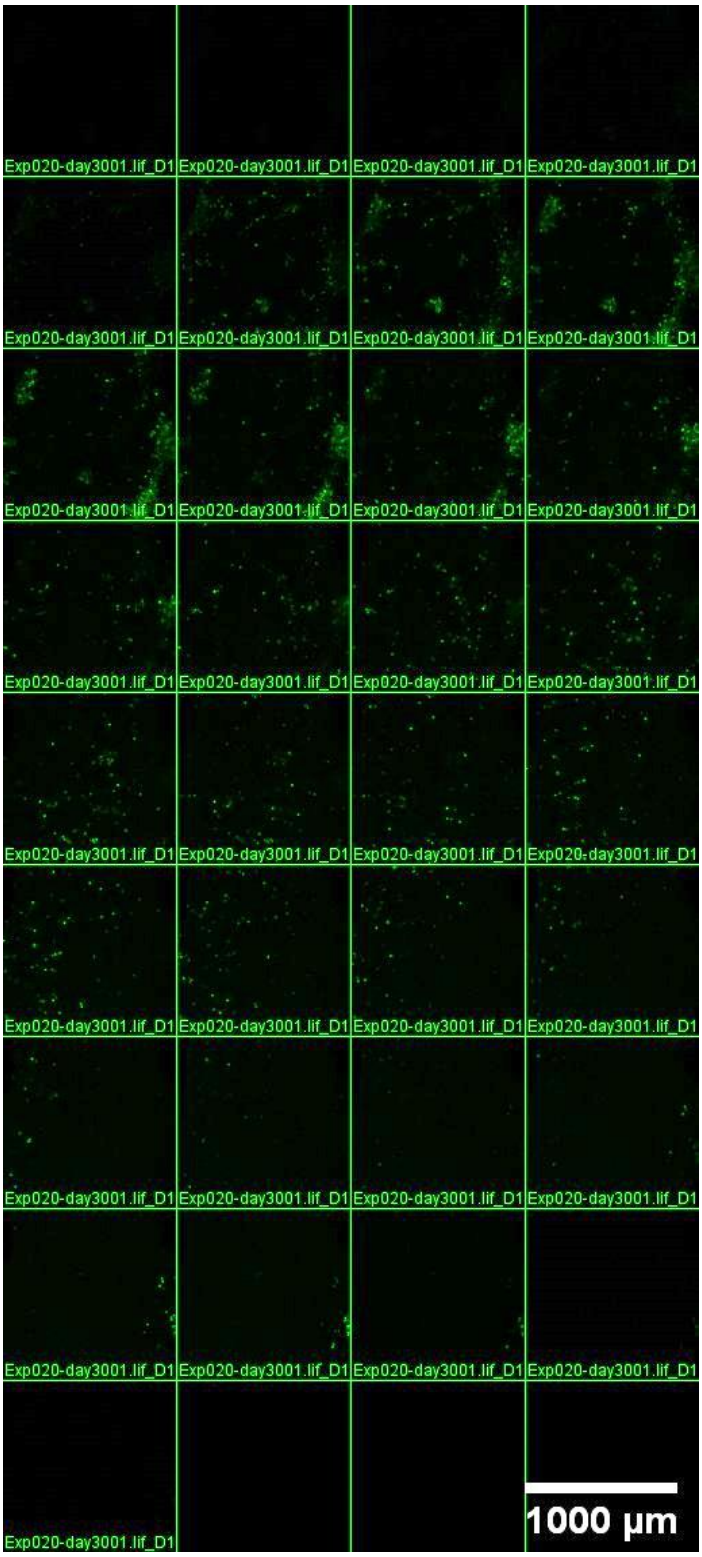

Figure 3.40. Individual z-stack images for MDA-MB-231 cells.

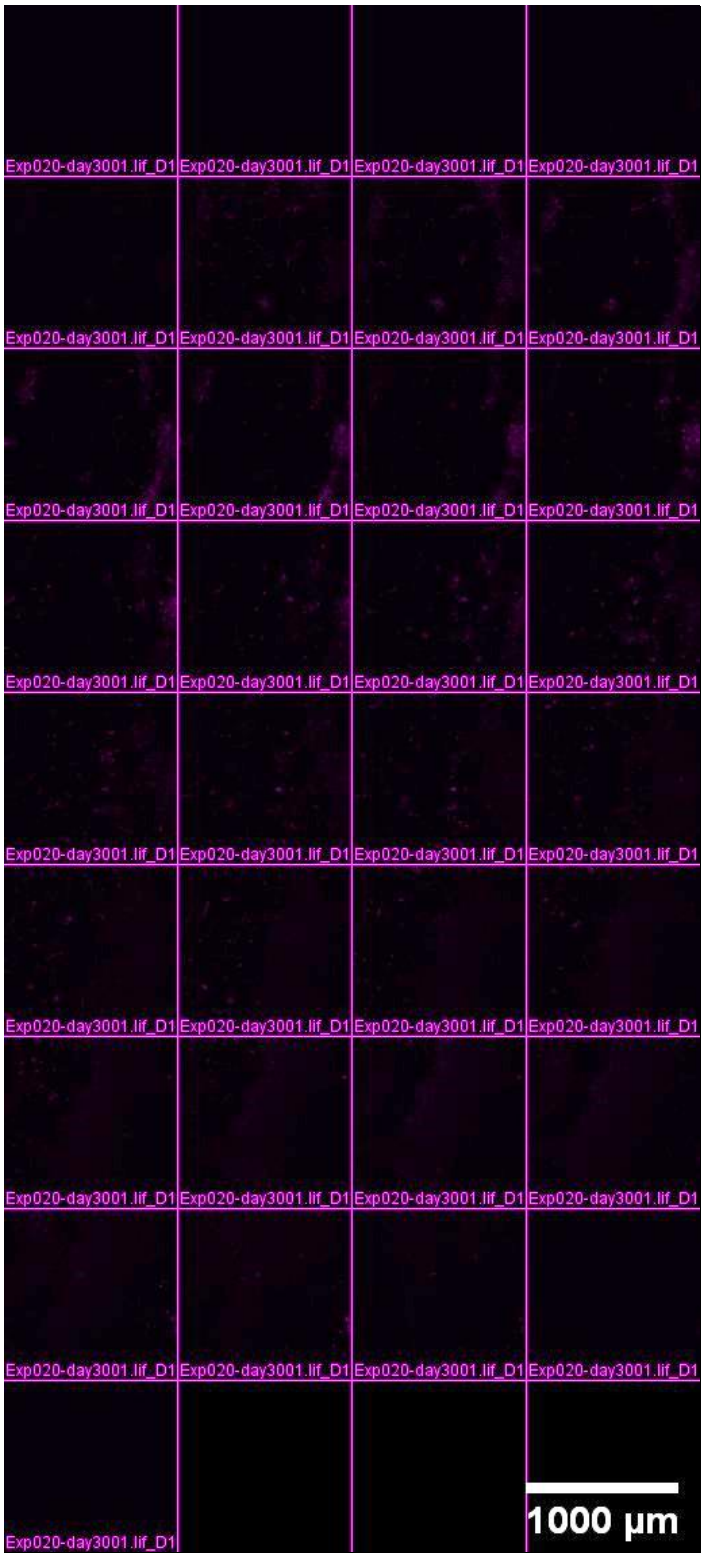

Figure 3.41. Individual z-stack images for dead cells which stain with NucRed Dead 647 reagent.

Cells had homogeneous distribution due to slides. All cells were stained with trackers. Amongst some cells, minor clusturing was observed. Not all cells were the same size. A narrow distribution was exhibited. 3D structure was provided between cells and cells distribution were homogeneously in stacks.

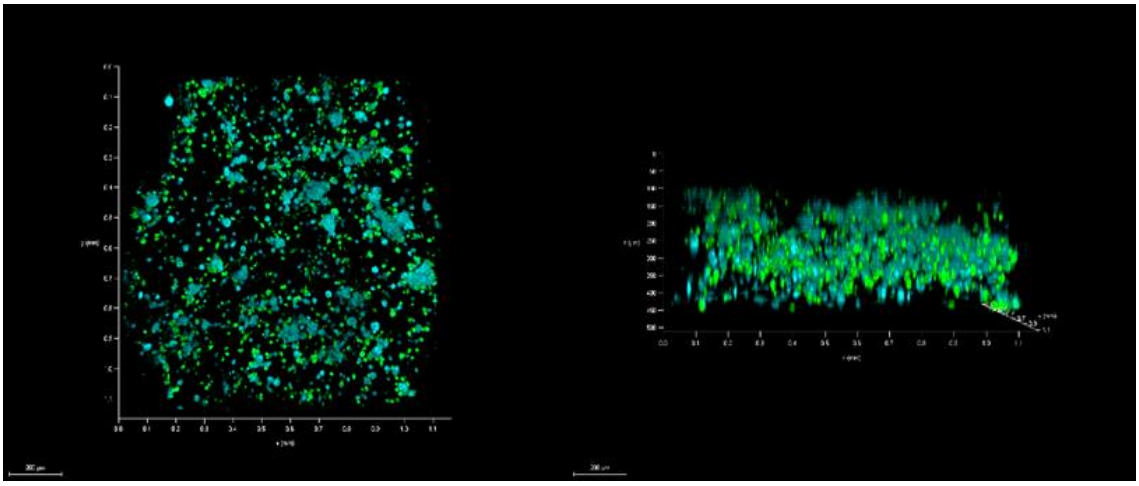

Figure 3.42. Tri-culture. MDA-MB-231 cells were stained with green tracker. MCF-10A cells were stained with blue tracker. RAW 264.7 cells were not stained. MDA-MB-231, MCF-10A and RAW 264.7 cells were mixed 1:1 volume ratio. Then cells were mixed with matrigel 1:1 volume ratio.

Dead 647 signals were observed in klavuzon-treated cells in tri-culture. It can be said that 3D structures are provided for all samples by looking at the 3D confocal images and the distribution of the cells in the stacks. Cells were tend to coexist more at the edges of PDMS, but they were homogeneously distributed. Some cells appeared to in groups among themselves such as minor clusturing. Not all cells were the same size. A narrow distribution was exhibited. Stack images show each section of 3D images detailed view in independent at z-position in Figure 3.46-3.47. Figure 3.46 shows MCF-10A channel, Figure 3.47 shows MDA-MB-231 channel and Figure 3.48 shows signal channel of Dead 647. As expected, Dead 647 signal was observed in klavuzon-treated group cells.

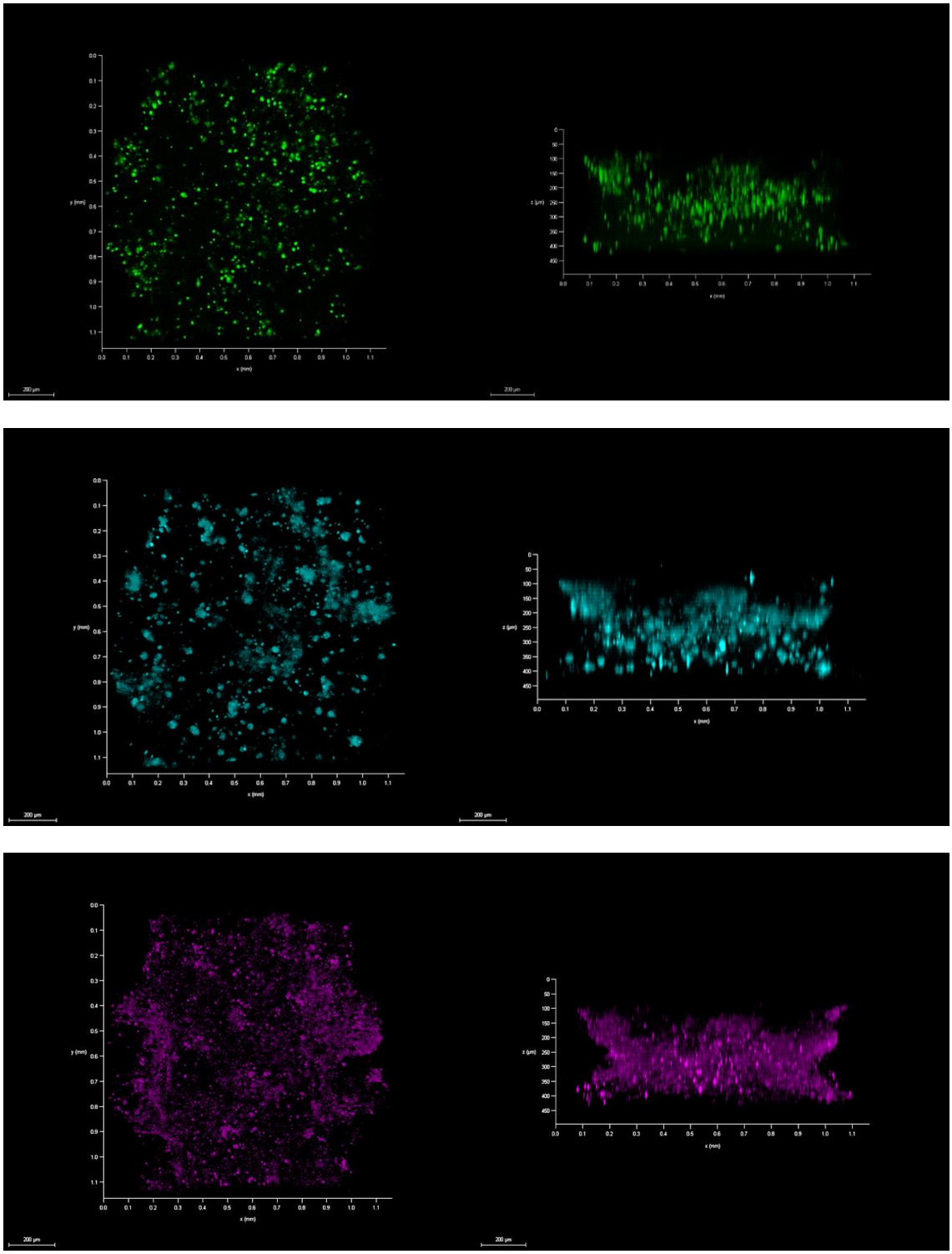

Figure 3.43. Tri-culture was treated with 100 uM Klavuzon at 48 hours. After 48 hours, NucRed Dead 647 dye was used to measure cell viability.

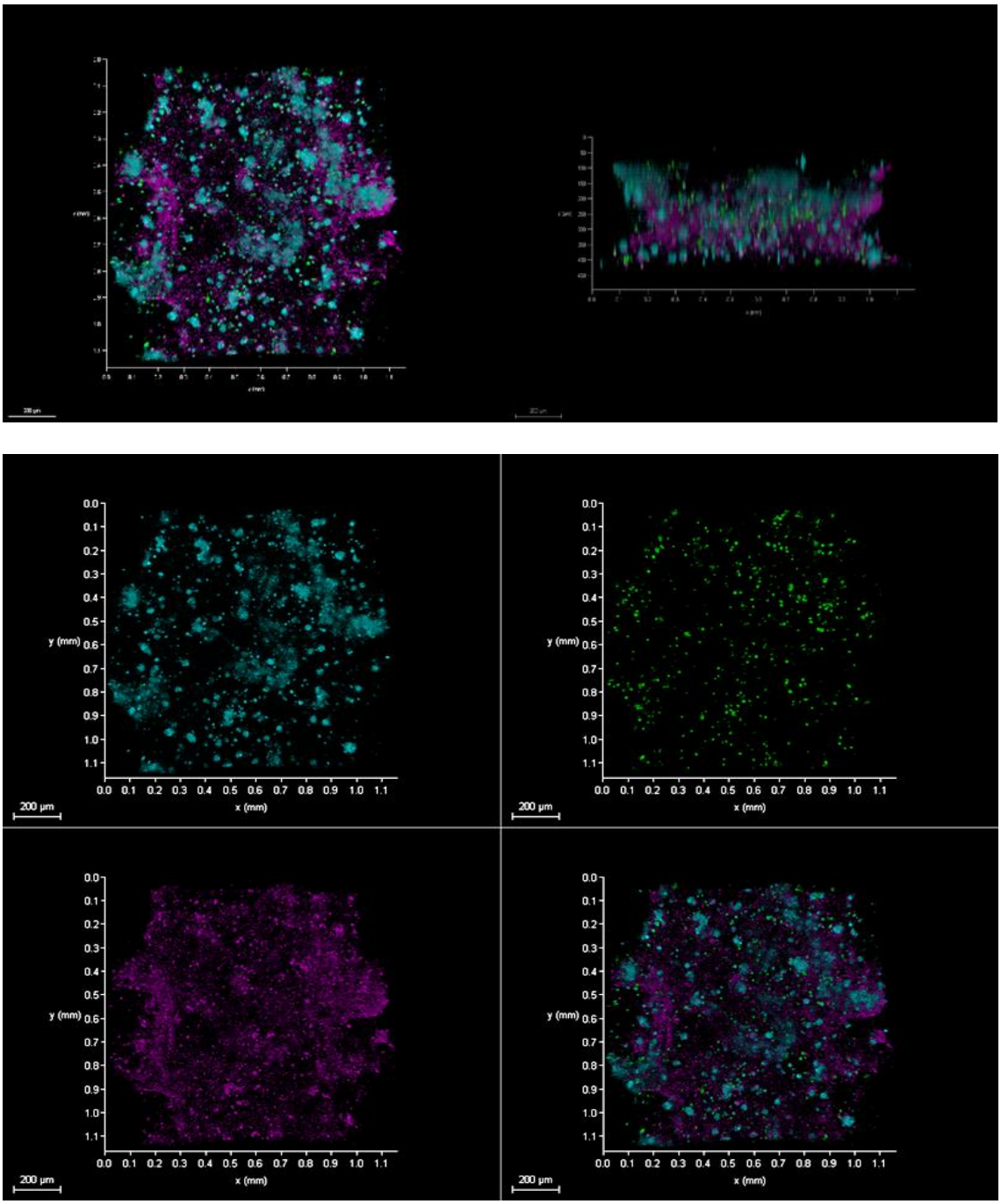

Figure 3.44. Tri-culture was treated with 100 uM Klavuzon at 48 hours. After 48 hours, NucRed Dead 647 dye was used to measure cell viability.

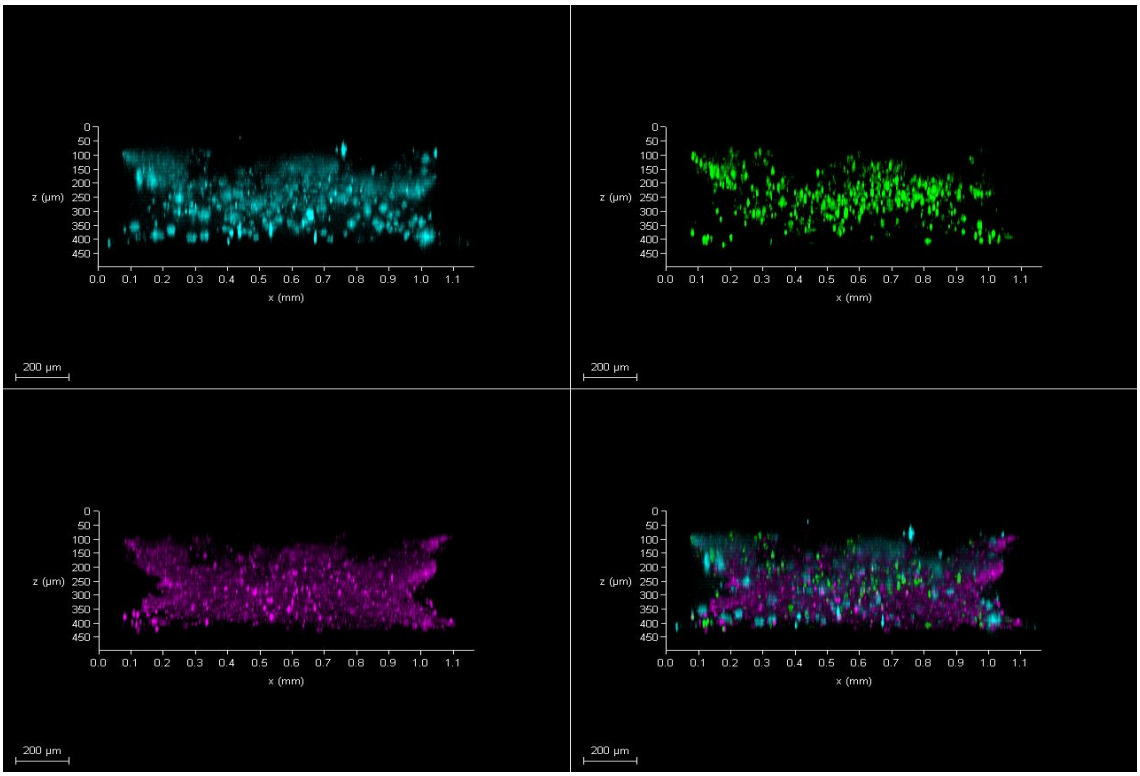

Figure 3.45. Tri-culture was treated with 100 uM Klavuzon at 48 hours. After 48 hours, NucRed Dead 647 dye was used to measure cell viability.

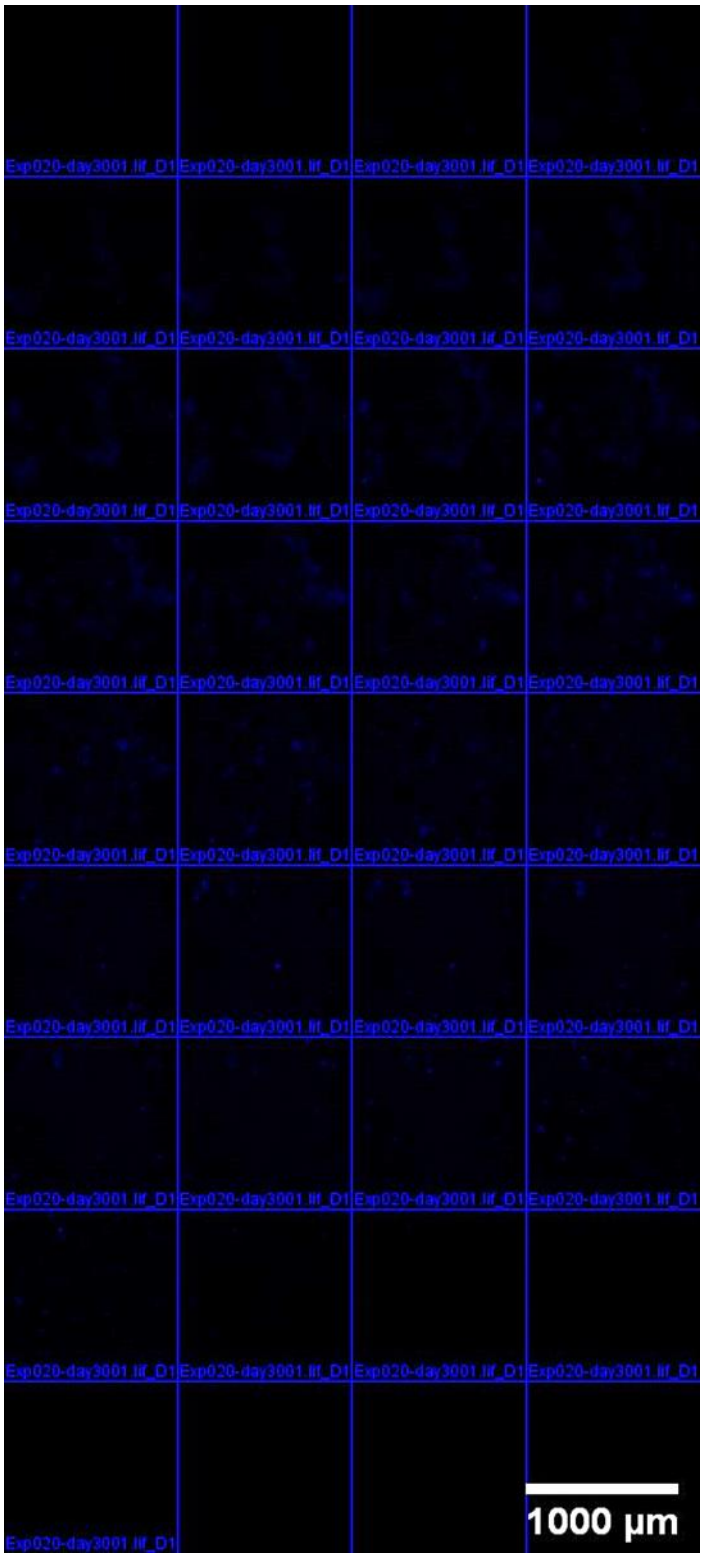

Figure 3.46. Individual z-stack images for MCF-10A cells.

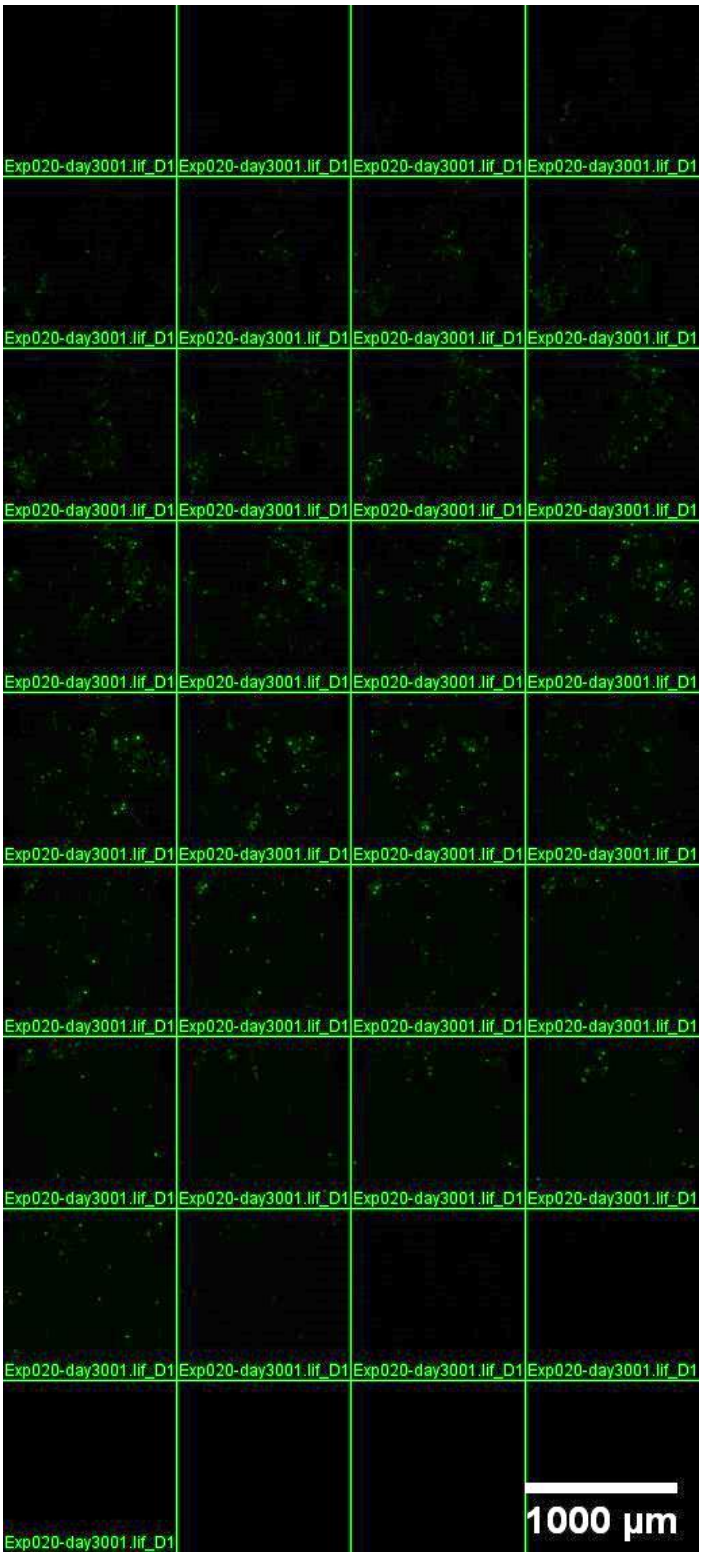

Figure 3.47. Individual z-stack images for MDA-MB-231 cells.

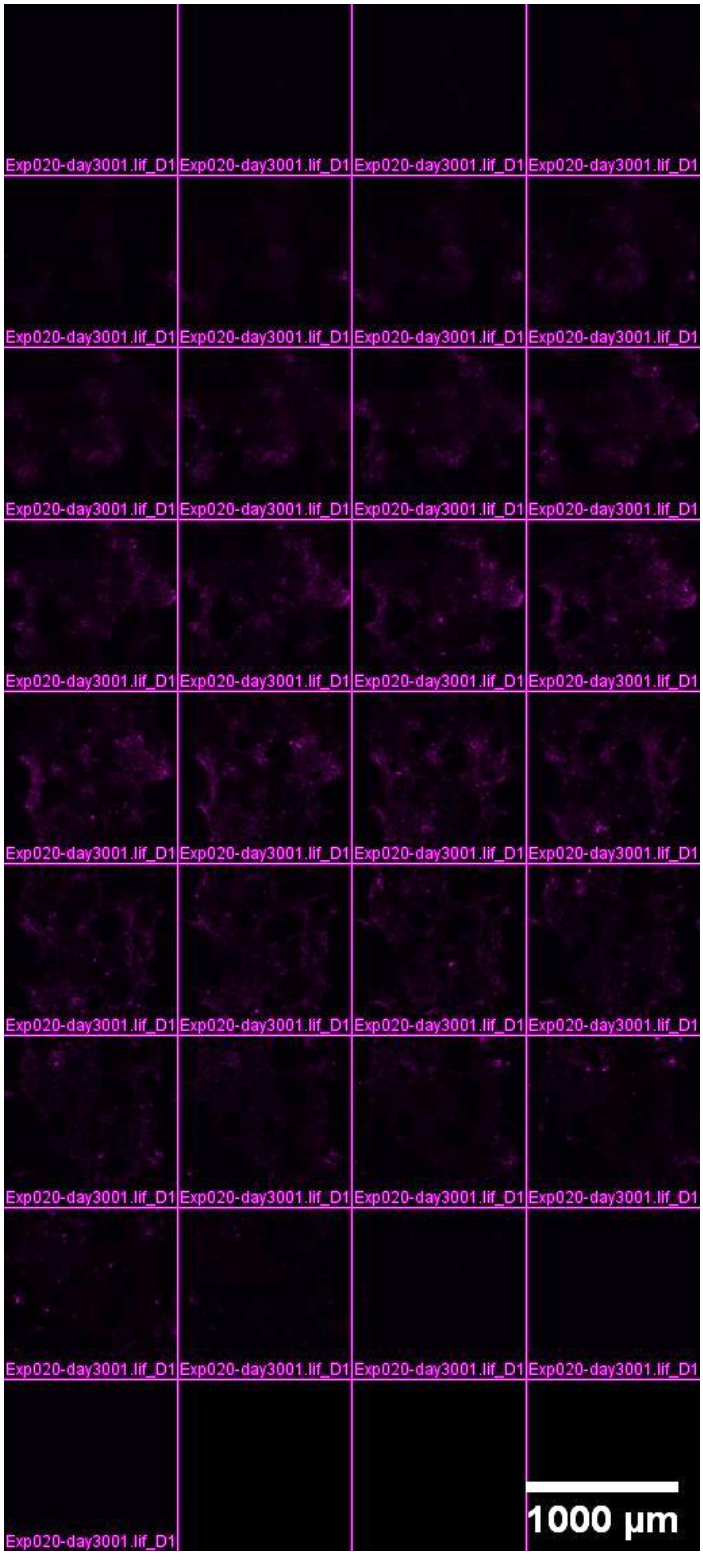

Figure 3.48. Individual z-stack images for dead cells which stain with NucRed Dead 647 reagent.

In order to determine the differences between the images, a macro was written in Fiji software and the results were analyzed and the excel tables were obtained. In first step, all images were converted to 8-bit and then ‘Gaussian Blur’ was applied as value sigma=10 using macro. Then in the second step, subtract operation was performed with GB filter and unfiltered images. The threshold (TH) value of the substract image was applied ‘auto TH’. Despeckle that is a median filter was applied. In third step, overlap was performed with the ‘AND’ operation between the channel where all the cells were located and the channel containing the dead647 probe. 512x512 pixels resize plugin was applied to result of this image. In the last step, all region was selected and multi measure was performed from analysis tools. Differences between the images were measured by taking RawIntDent1 data values.

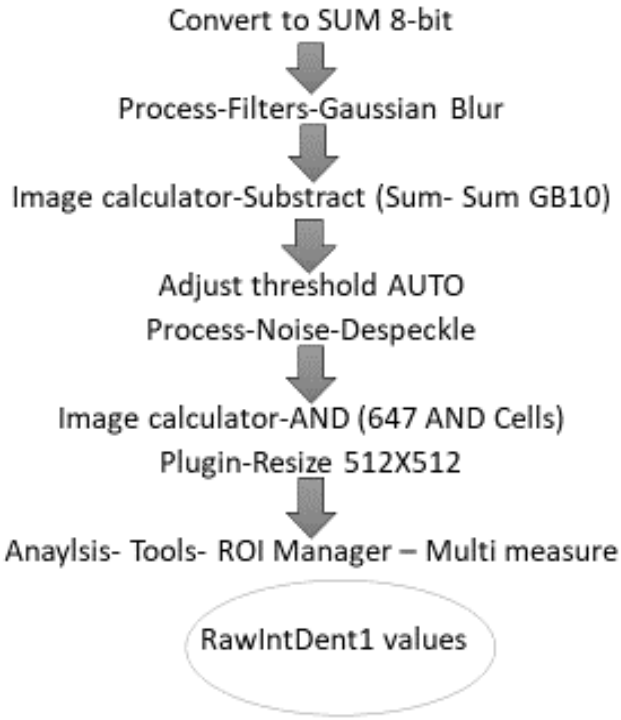

Figure 3.49. Abstract of step-by-step quantitative analysis.

As a result of image analysis, in the drug-free single culture, in the drug-free triple culture, in the single culture containing the drug and in the triple culture containing the drug MDA-MB-231 cell ratios were determined as A, B, C, D. When doxorubicin was used as the drug; A value was set to 2.19, B value was set to 7.39, C value was set to

22.45 and D value was set to 49.50. When klavuzon was used as the drug; A value was set to 2.19, B value was set to 7.39, C value was set to 27.64 and D value was set to 36.54.

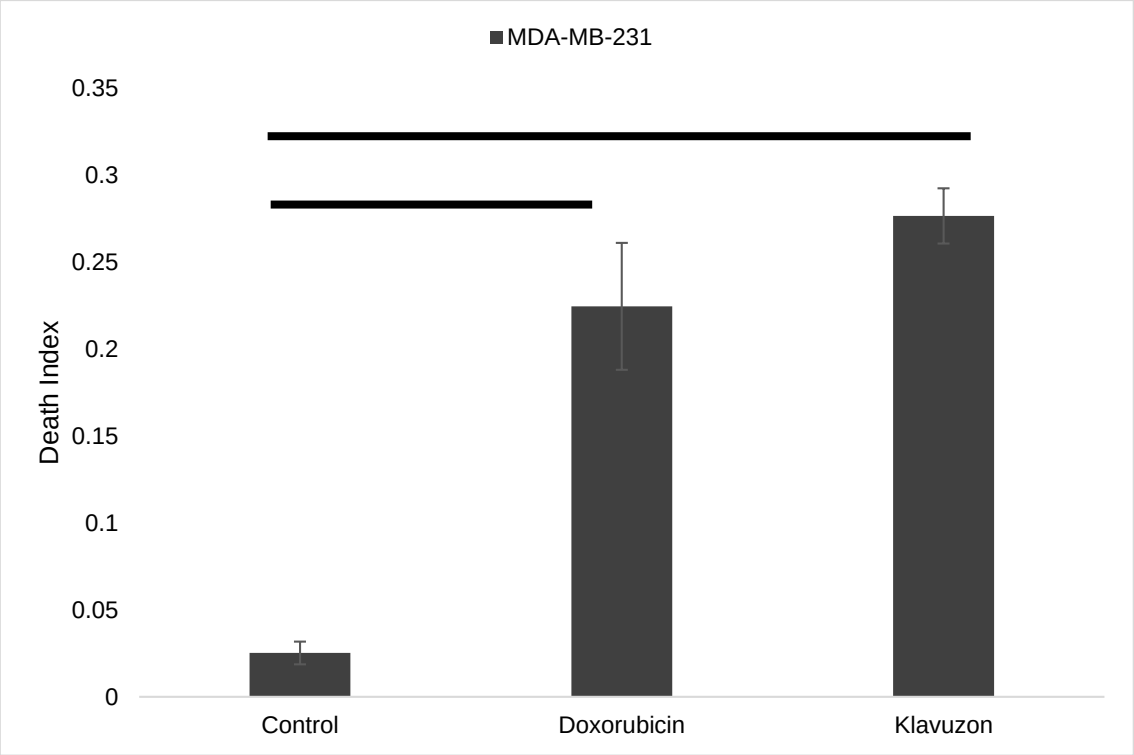

Figure 3.50. Death index of non-treated and treated cells in mono-culture.

Table 3.1. T-test values for MDA-MB-231 cells with doxorubicin and klavuzon in mono-culture ($p<0.05$ two-tail level).

	c231	*d231*		*c231*	*k231*		*d231*	*k231*
Mean	0.021941	0.22453	Mean	0.021941	0.276468	Mean	0.224529802	0.2764681
Variance	0.001248	0.018628	Variance	0.001248	0.006826	Variance	0.018628429	0.0068259
Observations	37	14	Observati	37	27	Observati	14	27
Hypothesized Mean	0		Hypothesi	0		Hypothesi	0	
df	14		df	33		df	18	
t Stat	-5.48475		t Stat	-15.0366		t Stat	-1.305240918	
P(T<=t) one-tail	4.02E-05		P(T<=t) on	1.26E-16		P(T<=t) on	0.104124986	
t Critical one-tail	1.76131		t Critical o	1.69236		t Critical o	1.734063607	
P(T<=t) two-tail	8.04E-05		P(T<=t) tw	2.51E-16		P(T<=t) tw	0.208249973	
t Critical two-tail	2.144787		t Critical t	2.034515		t Critical t	2.10092204	

According to T-test values, there was significant differences between non-treated and treated cells. In mono-culture, there was no significance between doxorubicin and

klavuzon (Table 3.1.). Both of drugs were killed MDA-MB-231 cancer cells in 3D mono-culture. Klavuzon inhibits topoisomerase-I enzyme[18] and doxorubicin inhibits topoisomerase-II enzyme[13]. They show their effects on cancer cells by these mechanisms.

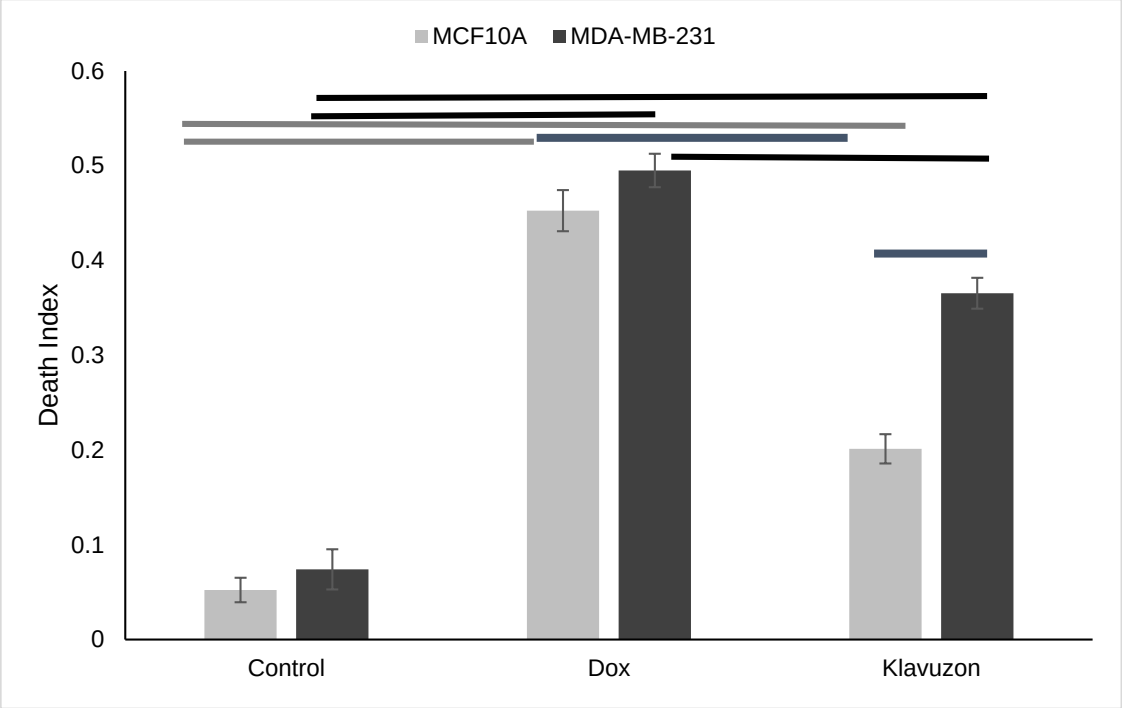

Figure 3.51. Death index of non-treated and treated cells in tri-culture.

It is known that the effects of drugs can differ in mono-culture even in co-culture[67]. As the cell type in the culture increases, the micro environment can be much better mimicked[68]. Doxorubicin uptake was less in tri-culture than mono-culture. Nevertheless, doxorubicin was killed more MDA-MB-231 cells in tri-culture than mono-culture. For MDA-MB-231 cells in the presence of doxorubicin, there was a significant difference between in the absence of doxorubicin. In the presence of klavuzon there was significant difference than in the absence of klavuzon. There was a significant difference between doxorubicin-treated cells and klavuzon-treated cells. For MCF-10A cells, there was a significant difference between doxorubicin-treated cells and non-treated cells. In the presence of klavuzon there was a significant difference between in the absence of klavuzon. There was a significant difference between doxorubicin and klavuzon. Also, there was a significant difference between klavuzon-treated MDA-MB-231 cells and klavuzon-treated MCF-10A cells. There was no significance between doxorubicin-treated

MDA-MB-231 cells and doxorubicin-treated MCF-10A cells. In the presence of drugs, cell death index has increased significantly.

Table 3.2. T-test values for MDA-MB-231 and MCF-10A cells with doxorubicin and klavuzon in mono-culture ($p < 0.05$ two-tail level).

	c10a	*d10a*		*c10a*	*k10a*
Mean	0.052243	0.452675	Mean	0.052243	0.201237
Variance	0.002851	0.006572	Variance	0.002851	0.005689
Observations	17	14	Observati	17	24
Hypothesized Mea	0		Hypothesi	0	
df	22		df	39	
t Stat	-15.864		t Stat	-7.40577	
P(T<=t) one-tail	7.92E-14		P(T<=t) on	2.99E-09	
t Critical one-tail	1.717144		t Critical o	1.684875	
P(T<=t) two-tail	1.58E-13		P(T<=t) tw	5.98E-09	
t Critical two-tail	2.073873		t Critical t	2.022691	

	c231	*d231*		*c231*	*k231*
Mean	0.07399	0.495078	Mean	0.07399	0.365422
Variance	0.007622	0.004349	Variance	0.007622	0.006394
Observations	17	14	Observati	17	24
Hypothesized Mea	0		Hypothesi	0	
df	29		df	33	
t Stat	-15.2843		t Stat	-10.9007	
P(T<=t) one-tail	1.03E-15		P(T<=t) on	8.94E-13	
t Critical one-tail	1.699127		t Critical o	1.69236	
P(T<=t) two-tail	2.07E-15		P(T<=t) tw	1.79E-12	
t Critical two-tail	2.04523		t Critical t	2.034515	

	d10a	*k10a*		*d231*	*k231*
Mean	0.452675	0.201237	Mean	0.495078	0.365422
Variance	0.006572	0.005689	Variance	0.004349	0.006394
Observations	14	24	Observati	14	24
Hypothesized Mean D	0		Hypothesi	0	
df	26		df	32	
t Stat	9.460029		t Stat	5.397297	
P(T<=t) one-tail	3.32E-10		P(T<=t) on	3.13E-06	
t Critical one-tail	1.705618		t Critical o	1.693889	
P(T<=t) two-tail	6.65E-10		P(T<=t) tw	6.25E-06	
t Critical two-tail	2.055529		t Critical t	2.036933	

In tri-culture, there was significant differences between non-treated and treated cells. There was also a significant difference between the two drugs according to the

T-test values (Table 3.2.). Doxorobicin was killed both MCF-10A non-tumorigenic cells and MDA-MB-231 cancers cells. Klavuzon was killed MCF-10A cells 20% less than MDA-MB-231 cells. In terms of minimizing the cytotoxic effect in cancer treatments, the fact that klavuzon was killed less healthy cells has been an important finding.

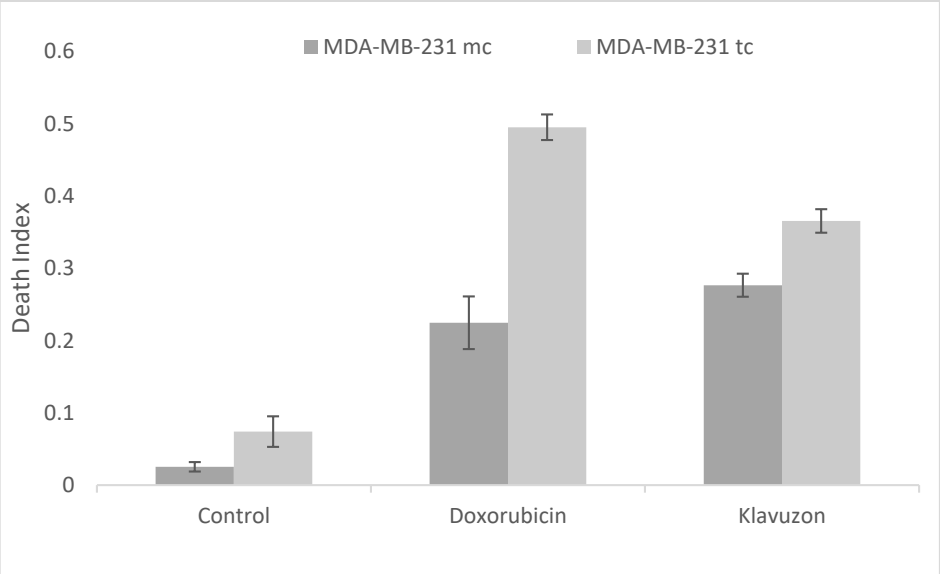

Figure 3.52. Comparison of death indexes of cells in mono- and tri-cultures. mc: mono-culture, tc: tri-culture

Table 3.3. T-test values for MDA-MB-231 cells with/without doxorubicin and klavuzon in mono- and tri-culture ($p < 0.05$ two-tail level).

	c231 tri	*c231 mono*		*d231 tri*	*d231 mono*		*k231 tri*	*k231 mono*
Mean	0.073990011	0.02194129	Mean	0.49507832	0.224529802	Mean	0.36542162	0.276468114
Variance	0.007621984	0.001247526	Variance	0.004349394	0.018628429	Variance	0.00639386	0.006825905
Observations	17	37	Observati	14	14	Observati	24	27
Hypothesized Mean Difference	0		Hypothesi	0		Hypothesi	0	
df	18		df	19		df	49	
t Stat	2.370584866		t Stat	6.678127991		t Stat	3.90379033	
P(T<=t) one-tail	0.01456514		P(T<=t) on	1.09631E-06		P(T<=t) on	0.00014472	
t Critical one-tail	1.734063607		t Critical o	1.729132812		t Critical o	1.67655089	
P(T<=t) two-tail	0.02913028		P(T<=t) tw	2.19261E-06		P(T<=t) tw	0.00028944	
t Critical two-tail	2.10092204		t Critical t	2.093024054		t Critical t	2.00957524	

According to T-test values, there was significant differences between tri-culture and mono-culture for MDA-MB-231 cells. For all conditions (with/without doxorubicin,

klavuzon), p value was less than 0.05. There was significance between doxorubicin-treated MDA-MB-231 cells in mono- and tri-culture (Table 3.3.).

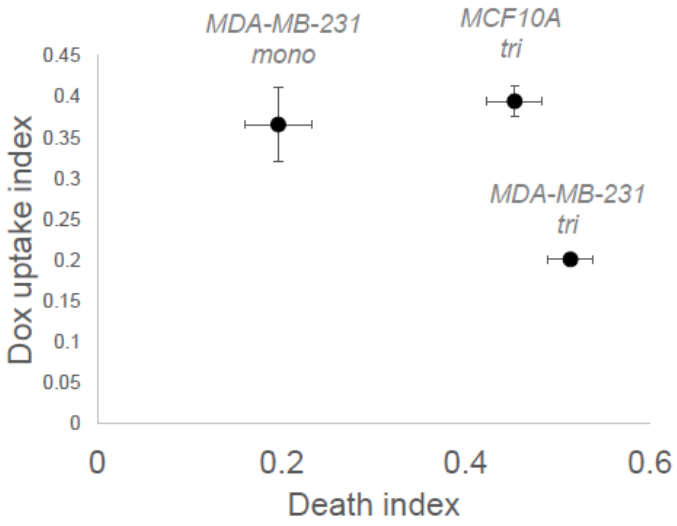

Figure 3.53. Drug uptake vs cell viability 3D cell culture lab-on-a-chip mono- vs. tri-culture.

According to analysis of doxorubicin uptake, cancer cells MDA-MB-231 uptake more doxorubicin in mono than tri-culture. Normal cells MCF-10A uptake more doxorubicin than cancer cells in tri-culture conditions.

CHAPTER 4

CONCLUSION

In this study, a drug-screening method was developed using 3D tri-cultures in LOC devices. Effects of drug doxorubicin and candidate drug klavuzon were observed in mono-culture and tri-culture conditions. Tumorigenic breast cancer cell line MDA-MB-231, non-tumorigenic epithelial cell line MCF-10A and macrophage cell line RAW 264.7 were used to test the effect of drug/drug candidate on cell viability. Klavuzon and doxorubicin were used to test LOC devices.

In the experiments, silicon wafer was used to form to mimic the micro environment. Different cell densities were tested to determine the optimal density of cells over a period of five days and the ideal cell density was found to be $10x10^6$ cells/ml. Matrigel was used as the extracellular matrix element to form a 3D micro environment and was mixed with the cells at a 1:1 volume ratio. MDA-MB-231 medium was chosen as the ideal medium for tri-culture.

For tri-culture conditions, cancer cells were marked with green-emitting cell-tracing dyes, epithelial cells were marked with blue-emitting cell-tracing dyes and macrophage cells were not marked. In mono-culture cancer cells were marked with green-emitting cell-tracing dyes. Doxorubicin and klavuzon were used for drug treatment. Cell viabilities were determined with NucRed Dead 647 ReadyProbes^{TM} Reagent on a confocal fluorescence microscope.

Cells were loaded with matrigel into the chip. The following day, drug treatment was carried out for 48 hours. After treatment, ead 647 signals were determined. 3D (z-stack) images were taken on at least three different sites in LOC devices for viability determinations, live and dead cell counts and percentages were determined for all cells stained. Numerical studies of the cells were performed with ImageJ / Fiji software.

As a result of the uptake analysis of doxorubicin, cancer cells uptake more doxorubicin in 3D mono-culture than in 3D tri-culture. Normal cells uptake more doxorubicin than cancer cells in 3D tri-culture.

Effectiveness of drugs was higher in tri than mono-culture condtions. The effect of klavuzon on cell viability in mono-culture was higher than doxorubicin.

Doxorubicin killed both cancer cells and normal cells at a similar rate in tri-culture. Klavuzon killed cancer cells 20% and normal cells 60% less than doxorubicin in 3D tri-culture.

In conclusion, tri-culture is more physiologically relevant than mono-culture. 3D cell culture in lab-on-a-chip devices can provide physiologically relevant data. Traditional drug screening study approaches are time-consuming and costly because more than 90% of scanned drug candidates fail after clinical trials. Drug screening is a promising and compherensive approach in 3D multi-culture. A much more efficient drug discovery can be achieved with 3D and multi-cultures to be applied in microfluidic systems that significantly reduce the sample volume required. In terms of identifying potential candidates for cancer treatment, these platforms provide valuable information in minimal sample volume and in less time in order to observe the effects of various drugs on cancer cells.

For this reason, we will expect that 3D cultures reflect the patient profile better than 2D cell cultures. Hence, 3D microfluidic devices and HTS studies are getting more and more important.

LOC devices have great importance to quickly predict the effects of drugs on the body. In this study, drug screening platform was created by forming 3D micro environment with different cell lines. Due to this platform, it is aimed to estimate the effects of various chemicals and drugs in the most likely way. Although effects have been studied in terms of viability, studies can be conducted at the level of protein expression in future studies. At the same time, different cell lines can be tried. The oxidative stress level in DNA can be tested. The drug screening platform can be improved to screen different molecules simultaneously. Platform will be used in future studies that will be able to perform more comprehensive screens that will include not-yet-characterized new molecules. As a result of the automation of the platform, improvements can be made in a way that cell viability can be measured more quickly by luminescence.

REFERENCES

1. Alberts, B. M., Cell biology: recipes for replication. *Nature* **1990,** *346* (6284), 514-5.

2. Hanahan, D.; Weinberg, R. A., The hallmarks of cancer. *Cell* **2000,** *100* (1), 57-70.

3. Hanahan, D.; Weinberg, R. A., Hallmarks of cancer: the next generation. *Cell* **2011,** *144* (5), 646-74.

4. Parkin, D. M.; Bray, F.; Ferlay, J.; Pisani, P., Global cancer statistics, 2002. *CA: a cancer journal for clinicians* **2005,** *55* (2), 74-108.

5. Siegel, R. L.; Miller, K. D.; Jemal, A., Cancer statistics, 2018. *CA: a cancer journal for clinicians* **2018,** *68* (1), 7-30.

6. Sliwoski, G.; Kothiwale, S.; Meiler, J.; Lowe, E. W., Jr., Computational methods in drug discovery. *Pharmacological reviews* **2014,** *66* (1), 334-95.

7. Qu, Y.; Han, B.; Yu, Y.; Yao, W.; Bose, S.; Karlan, B. Y.; Giuliano, A. E.; Cui, X., Evaluation of MCF10A as a Reliable Model for Normal Human Mammary Epithelial Cells. *PloS one* **2015,** *10* (7), e0131285.

8. Tung, Y. C.; Hsiao, A. Y.; Allen, S. G.; Torisawa, Y. S.; Ho, M.; Takayama, S., High-throughput 3D spheroid culture and drug testing using a 384 hanging drop array. *The Analyst* **2011,** *136* (3), 473-8.

9. Middleman, E.; Luce, J.; Frei, E., 3rd, Clinical trials with adriamycin. *Cancer* **1971,** *28* (4), 844-50.

10. Arcamone, F.; Cassinelli, G., Biosynthetic anthracyclines. *Current medicinal chemistry* **1998,** *5* (5), 391-419.

11. Arcamone, F.; Cassinelli, G.; D'Amico, G.; Orezzi, P., Mannosidohydroxystreptomycin from Streptomyces sp. *Experientia* **1968,** *24* (5), 441-2.

12. Fornari, F. A.; Randolph, J. K.; Yalowich, J. C.; Ritke, M. K.; Gewirtz, D. A., Interference by doxorubicin with DNA unwinding in MCF-7 breast tumor cells. *Molecular pharmacology* **1994,** *45* (4), 649-56.

13. Tacar, O.; Indumathy, S.; Tan, M. L.; Baindur-Hudson, S.; Friedhuber, A. M.; Dass, C. R., Cardiomyocyte apoptosis vs autophagy with prolonged doxorubicin treatment: comparison with osteosarcoma cells. *The Journal of pharmacy and pharmacology* **2015,** *67* (2), 231-43.

14. Tewey, K. M.; Rowe, T. C.; Yang, L.; Halligan, B. D.; Liu, L. F., Adriamycin-induced DNA damage mediated by mammalian DNA topoisomerase II. *Science* **1984,** *226* (4673), 466-8.

15. Agudelo, D.; Bourassa, P.; Berube, G.; Tajmir-Riahi, H. A., Intercalation of antitumor drug doxorubicin and its analogue by DNA duplex: structural features and biological implications. *International journal of biological macromolecules* **2014,** *66*, 144-50.

16. Kasaplar, P.; Yilmazer, O.; Cagir, A., 6-Bicycloaryl substituted (S)- and (R)-5,6-dihydro-2H-pyran-2-ones: asymmetric synthesis, and anti-proliferative properties. *Bioorganic & medicinal chemistry* **2009,** *17* (1), 311-8.

17. Kanbur, T.; Kara, M.; Kutluer, M.; Sen, A.; Delman, M.; Alkan, A.; Otas, H. O.; Akcok, I.; Cagir, A., CRM1 inhibitory and antiproliferative activities of novel 4'-alkyl substituted klavuzon derivatives. *Bioorganic & medicinal chemistry* **2017,** *25* (16), 4444-4451.

18. Akcok, I.; Mete, D.; Sen, A.; Kasaplar, P.; Korkmaz, K. S.; Cagir, A., Synthesis and Topoisomerase I inhibitory properties of klavuzon derivatives. *Bioorganic chemistry* **2017,** *71*, 275-284.

19. Bissell, M. J.; Kenny, P. A.; Radisky, D. C., Microenvironmental regulators of tissue structure and function also regulate tumor induction and progression: the role of extracellular matrix and its degrading enzymes. *Cold Spring Harbor symposia on quantitative biology* **2005,** *70*, 343-56.

20. Lee, G. Y.; Kenny, P. A.; Lee, E. H.; Bissell, M. J., Three-dimensional culture models of normal and malignant breast epithelial cells. *Nature methods* **2007,** *4* (4), 359-65.

21. Edmondson, R.; Broglie, J. J.; Adcock, A. F.; Yang, L., Three-dimensional cell culture systems and their applications in drug discovery and cell-based biosensors. *Assay and drug development technologies* **2014,** *12* (4), 207-18.

22. Breslin, S.; O'Driscoll, L., The relevance of using 3D cell cultures, in addition to 2D monolayer cultures, when evaluating breast cancer drug sensitivity and resistance. *Oncotarget* **2016,** *7* (29), 45745-45756.

23. Ravi, M.; Paramesh, V.; Kaviya, S. R.; Anuradha, E.; Solomon, F. D., 3D cell culture systems: advantages and applications. *Journal of cellular physiology* **2015,** *230* (1), 16-26.

24. Kim, J. B., Three-dimensional tissue culture models in cancer biology. *Seminars in cancer biology* **2005,** *15* (5), 365-77.

25. Huang, H.; Ding, Y.; Sun, X. S.; Nguyen, T. A., Peptide hydrogelation and cell encapsulation for 3D culture of MCF-7 breast cancer cells. *PloS one* **2013,** *8* (3), e59482.

26. Baker, B. M.; Chen, C. S., Deconstructing the third dimension: how 3D culture microenvironments alter cellular cues. *Journal of cell science* **2012,** *125* (Pt 13), 3015-24.

27. Xu, X.; Gurski, L. A.; Zhang, C.; Harrington, D. A.; Farach-Carson, M. C.; Jia, X., Recreating the tumor microenvironment in a bilayer, hyaluronic acid hydrogel construct for the growth of prostate cancer spheroids. *Biomaterials* **2012,** *33* (35), 9049-60.

28. Yip, D.; Cho, C. H., A multicellular 3D heterospheroid model of liver tumor and stromal cells in collagen gel for anti-cancer drug testing. *Biochemical and biophysical research communications* **2013,** *433* (3), 327-32.

29. Hongisto, V.; Jernstrom, S.; Fey, V.; Mpindi, J. P.; Kleivi Sahlberg, K.; Kallioniemi, O.; Perala, M., High-throughput 3D screening reveals differences in drug sensitivities between culture models of JIMT1 breast cancer cells. *PloS one* **2013,** *8* (10), e77232.

30. Tibbitt, M. W.; Anseth, K. S., Hydrogels as extracellular matrix mimics for 3D cell culture. *Biotechnology and bioengineering* **2009,** *103* (4), 655-63.

31. Tredan, O.; Galmarini, C. M.; Patel, K.; Tannock, I. F., Drug resistance and the solid tumor microenvironment. *Journal of the National Cancer Institute* **2007,** *99* (19), 1441-54.

32. Price, K. J.; Tsykin, A.; Giles, K. M.; Sladic, R. T.; Epis, M. R.; Ganss, R.; Goodall, G. J.; Leedman, P. J., Matrigel basement membrane matrix influences expression of microRNAs in cancer cell lines. *Biochemical and biophysical research communications* **2012,** *427* (2), 343-8.

33. Zhang, M.; Chen, X.; Ying, M.; Gao, J.; Zhan, C.; Lu, W., Glioma-Targeted Drug Delivery Enabled by a Multifunctional Peptide. *Bioconjugate chemistry* **2017,** *28* (3), 775-781.

34. Nelson, C. M.; Bissell, M. J., Modeling dynamic reciprocity: engineering three-dimensional culture models of breast architecture, function, and neoplastic transformation. *Seminars in cancer biology* **2005,** *15* (5), 342-52.

35. Shield, K.; Ackland, M. L.; Ahmed, N.; Rice, G. E., Multicellular spheroids in ovarian cancer metastases: Biology and pathology. *Gynecologic oncology* **2009,** *113* (1), 143-8.

36. Wu, M. H.; Huang, S. B.; Lee, G. B., Microfluidic cell culture systems for drug research. *Lab on a chip* **2010,** *10* (8), 939-56.

37. Amelian, A.; Wasilewska, K.; Megias, D.; Winnicka, K., Application of standard cell cultures and 3D in vitro tissue models as an effective tool in drug design and development. *Pharmacological reports : PR* **2017,** *69* (5), 861-870.

38. Paget, S., The distribution of secondary growths in cancer of the breast. 1889. *Cancer metastasis reviews* **1989,** *8* (2), 98-101.

39. Ma, H.; Liu, T.; Qin, J.; Lin, B., Characterization of the interaction between fibroblasts and tumor cells on a microfluidic co-culture device. *Electrophoresis* **2010,** *31* (10), 1599-605.

40. Miki, Y.; Ono, K.; Hata, S.; Suzuki, T.; Kumamoto, H.; Sasano, H., The advantages of co-culture over mono cell culture in simulating in vivo environment. *The Journal of steroid biochemistry and molecular biology* **2012,** *131* (3-5), 68-75.

41. De Wever, O.; Mareel, M., Role of tissue stroma in cancer cell invasion. *The Journal of pathology* **2003,** *200* (4), 429-47.

42. Oliveira, N. M.; Vilabril, S.; Oliveira, M. B.; Reis, R. L.; Mano, J. F., Recent advances on open fluidic systems for biomedical applications: A review. *Materials science & engineering. C, Materials for biological applications* **2019,** *97*, 851-863.

43. Volpatti, L. R.; Yetisen, A. K., Commercialization of microfluidic devices. *Trends in biotechnology* **2014,** *32* (7), 347-50.

44. Lee, N. Y., Recent Progress in Lab-on-a-Chip Technology and Its Potential Application to Clinical Diagnoses. *International neurourology journal* **2013,** *17* (1), 2-10.

45. Bsoul, A.; Pan, S.; Cretu, E.; Stoeber, B.; Walus, K., Design, microfabrication, and characterization of a moulded PDMS/SU-8 inkjet dispenser for a Lab-on-a-Printer platform technology with disposable microfluidic chip. *Lab on a chip* **2016,** *16* (17), 3351-61.

46. Sin, M. L.; Gao, J.; Liao, J. C.; Wong, P. K., System Integration - A Major Step toward Lab on a Chip. *Journal of biological engineering* **2011,** *5*, 6.

47. Popova, A. A.; Schillo, S. M.; Demir, K.; Ueda, E.; Nesterov-Mueller, A.; Levkin, P. A., Droplet-Array (DA) Sandwich Chip: A Versatile Platform for High-Throughput Cell Screening Based on Superhydrophobic-Superhydrophilic Micropatterning. *Advanced materials* **2015,** *27* (35), 5217-22.

48. Chin, C. D.; Linder, V.; Sia, S. K., Lab-on-a-chip devices for global health: past studies and future opportunities. *Lab on a chip* **2007,** *7* (1), 41-57.

49. Barata, D.; van Blitterswijk, C.; Habibovic, P., High-throughput screening approaches and combinatorial development of biomaterials using microfluidics. *Acta biomaterialia* **2016,** *34*, 1-20.

50. Berndt, E. R.; National Bureau of Economic Research., Assessing the impacts of the Prescription Drug User Fee Acts (PDUFA) on the FDA approval process. In

NBER working paper series working paper 10822 [Online] National Bureau of Economic Research,: Cambridge, MA, 2004. http://papers.nber.org/papers/W10822.

51. Saribasak, H.; Arakawa, H., Basic cell culture conditions. *Sub-cellular biochemistry* **2006,** *40*, 345-6.

52. Hartwell, L. H.; Hopfield, J. J.; Leibler, S.; Murray, A. W., From molecular to modular cell biology. *Nature* **1999,** *402* (6761 Suppl), C47-52.

53. Saglam, Murat; Design and fabrication of microfluidic device that allows investigation of distance dependent interactions of two different cell types. *Master Thesis, Izmır Institute of Technology* **2004.**

54. Lin, E. Y.; Gouon-Evans, V.; Nguyen, A. V.; Pollard, J. W., The macrophage growth factor CSF-1 in mammary gland development and tumor progression. *Journal of mammary gland biology and neoplasia* **2002,** *7* (2), 147-62.

55. Ivers, L. P.; Cummings, B.; Owolabi, F.; Welzel, K.; Klinger, R.; Saitoh, S.; O'Connor, D.; Fujita, Y.; Scholz, D.; Itasaki, N., Dynamic and influential interaction of cancer cells with normal epithelial cells in 3D culture. *Cancer cell international* **2014,** *14* (1), 108.

56. Nikkhah, M.; Strobl, J. S.; Schmelz, E. M.; Roberts, P. C.; Zhou, H.; Agah, M., MCF10A and MDA-MB-231 human breast basal epithelial cell co-culture in silicon micro-arrays. *Biomaterials* **2011,** *32* (30), 7625-32.

57. Mi, S.; Du, Z.; Xu, Y.; Wu, Z.; Qian, X.; Zhang, M.; Sun, W., Microfluidic co-culture system for cancer migratory analysis and anti-metastatic drugs screening. *Scientific reports* **2016,** *6*, 35544.

58. Lanz, H. L.; Saleh, A.; Kramer, B.; Cairns, J.; Ng, C. P.; Yu, J.; Trietsch, S. J.; Hankemeier, T.; Joore, J.; Vulto, P.; Weinshilboum, R.; Wang, L., Therapy response testing of breast cancer in a 3D high-throughput perfused microfluidic platform. *BMC cancer* **2017,** *17* (1), 709.

59. Kievit, F. M.; Wang, F. Y.; Fang, C.; Mok, H.; Wang, K.; Silber, J. R.; Ellenbogen, R. G.; Zhang, M., Doxorubicin loaded iron oxide nanoparticles overcome multidrug resistance in cancer in vitro. *Journal of controlled release : official journal of the Controlled Release Society* **2011,** *152* (1), 76-83.

60. Rampersad, S. N., Multiple applications of Alamar Blue as an indicator of metabolic function and cellular health in cell viability bioassays. *Sensors* **2012,** *12* (9), 12347-60.

61. Yildiz-Ozturk, E.; Gulce-Iz, S.; Anil, M.; Yesil-Celiktas, O., Cytotoxic responses of carnosic acid and doxorubicin on breast cancer cells in butterfly-shaped microchips in comparison to 2D and 3D culture. *Cytotechnology* **2017,** *69* (2), 337-347.

62. Huan, M. L.; Zhou, S. Y.; Teng, Z. H.; Zhang, B. L.; Liu, X. Y.; Wang, J. P.; Mei, Q. B., Conjugation with alpha-linolenic acid improves cancer cell uptake and cytotoxicity of doxorubicin. *Bioorganic & medicinal chemistry letters* **2009,** *19* (9), 2579-84.

63. Glynn, L. E.; Holborow, E. J.; Johnson, G. D., The relationship of polymer size and sulphation to the haptenic specificity of dextrans. *The Journal of pathology and bacteriology* **1954,** *68* (1), 205-20.

64. Laurent, T. C.; Sundelof, L. O.; Wik, K. O.; Warmegard, B., Diffusion of dextran in concentrated solutions. *European journal of biochemistry* **1976,** *68* (1), 95-102.

65. Lebrun, L.; Junter, G. A., Diffusion of sucrose and dextran through agar gel membranes. *Enzyme and microbial technology* **1993,** *15* (12), 1057-62.

66. Rincon, E.; Rocha-Gregg, B. L.; Collins, S. R., A map of gene expression in neutrophil-like cell lines. *BMC genomics* **2018,** *19* (1), 573.

67. Goers, L.; Freemont, P.; Polizzi, K. M., Co-culture systems and technologies: taking synthetic biology to the next level. *Journal of the Royal Society, Interface* **2014,** *11* (96).

68. Kasurinen, S.; Happo, M. S.; Ronkko, T. J.; Orasche, J.; Jokiniemi, J.; Kortelainen, M.; Tissari, J.; Zimmermann, R.; Hirvonen, M. R.; Jalava, P. I., Differences between co-cultures and monocultures in testing the toxicity of particulate matter derived from log wood and pellet combustion. *PloS one* **2018,** *13* (2), e0192453.